PB88-131297

Performance and Modeling of a Hot Potassium Carbonate Acid Gas Removal System in Treating Coal Gas

North Carolina State Univ., Raleigh

Prepared for

Environmental Protection Agency
Research Triangle Park, NC

Nov 87

U.S. Department of Commerce
National Technical Information Service
NTIS

PB88-131297
EPA/600/7-87/023
November 1987

PERFORMANCE AND MODELING OF A HOT POTASSIUM CARBONATE ACID GAS REMOVAL SYSTEM IN TREATING COAL GAS

by

J. K. Ferrell, J. S. Staton, and R. W. Rousseau

North Carolina State University
Department of Chemical Engineering
Raleigh, North Carolina 27695-7905

Cooperative Agreement No. CR-809317

EPA Project Officer: N. Dean Smith

Air and Energy Engineering Research Laboratory
Office of Environmental Engineering and Technology Demonstration
Research Triangle Park, NC 27711

REPRODUCED BY
U.S. DEPARTMENT OF COMMERCE
NATIONAL TECHNICAL
INFORMATION SERVICE
SPRINGFIELD, VA. 22161

AIR AND ENERGY ENGINEERING RESEARCH LABORATORY
OFFICE OF RESEARCH AND DEVELOPMENT
U.S. ENVIRONMENTAL PROTECTION AGENCY
RESEARCH TRIANGLE PARK, NC 27711

TECHNICAL REPORT DATA

(Please read Instructions on the reverse before completing)

1. REPORT NO. EPA/600/7-87/023	2.	3. RECIPIENT'S ACCESSION NO. PB88 131297/AS
4. TITLE AND SUBTITLE Performance and Modeling of a Hot Potassium Carbonate Acid Gas Removal System in Treating Coal Gas		5. REPORT DATE November 1987 6. PERFORMING ORGANIZATION CODE
7. AUTHOR(S) J.S. Staton, R.W. Rousseau, and J.K. Ferrell		8. PERFORMING ORGANIZATION REPORT NO.
9. PERFORMING ORGANIZATION NAME AND ADDRESS North Carolina State University Department of Chemical Engineering Raleigh, North Carolina 27695-7905		10. PROGRAM ELEMENT NO. 11. CONTRACT/GRANT NO. CR809317
12. SPONSORING AGENCY NAME AND ADDRESS EPA, Office of Research and Development Air and Energy Engineering Research Laboratory Research Triangle Park, NC 27711		13. TYPE OF REPORT AND PERIOD COVERED Final; 6/84 - 10/85 14. SPONSORING AGENCY CODE EPA/600/13

15. SUPPLEMENTARY NOTES AEERL project officer is N. Dean Smith, Mail Drop 62B, 919/541-2708.

16. ABSTRACT The report discusses the performance and modeling of a hot potassium carbonate (K_2CO_3) acid gas removal system (AGRS) in treating coal gas. Aqueous solutions of K_2CO_3, with and without amine additive, were used as the acid gas removal solvent in the Coal Gasification/Gas Cleaning Test Facility at North Carolina State University. The AGRS consisted of a packed absorption column, one or more flash tanks for intermediate pressure reduction, and a packed stripping column operated with a reboiler. The removal of CO_2, H_2S, COS, and other species from the crude coal gas was studied, and data on the distribution of these gases in regeneration exit streams were obtained. Operating conditions for the selective removal of sulfur species were also examined. A system model for chemical solvents was developed and incorporated in a simulation program. The model was based on the mass transfer rate of a key component, CO_2, with the assumption that non-key reactive components affect the equilibrium of the key component, but not its mass transfer rate. The absorption and stripping of non-key components were assumed to be controlled by equilibrium between the gas and liquid phases in these columns. An isothermal flash model for chemical solvents was also developed and included in the program. Agreement between program predictions and pilot plant data was good.

17. KEY WORDS AND DOCUMENT ANALYSIS

a. DESCRIPTORS		b. IDENTIFIERS/OPEN ENDED TERMS	c. COSATI Field/Group	
Pollution	Amines	Pollution Control	13B	07C
Coal Gasification	Solvents	Stationary Sources	13H	11K
Coal Gas		Acid Gas Removal	21D	
Treatment			14G	
Potassium Carbonates			07B	
Mathematical Models			12A	

18. DISTRIBUTION STATEMENT Release to Public	19. SECURITY CLASS *(This Report)* Unclassified	21. NO. OF PAGES 164
	20. SECURITY CLASS *(This page)* Unclassified	22. PRICE PC 19.95 / MF 6.95

EPA Form 2220-1 (9-73)

NOTICE

This document has been reviewed in accordance with U.S. Environmental Protection Agency policy and approved for publication. Mention of trade names or commercial products does not constitute endorsement or recommendation for use.

ABSTRACT

Aqueous solutions of potassium carbonate, with and without an amine additive, were used as the acid gas removal solvent in the Coal Gasification/Gas Cleaning Test Facility at North Carolina State University. The acid gas removal system consisted of a packed absorption column, one or more flash tanks for intermediate pressure reduction, and a packed stripping column operated with a reboiler. The removal of CO_2, H_2S, COS, and other species from the crude coal gas was studied and data on the distribution of these gases in regeneration exit streams were obtained. Operating conditions for the selective removal of sulfur species were also examined.

A system model for chemical solvents was developed and incorporated into a simulation program. The model was based on the mass transfer rate of a key component, CO_2, with the assumption that non-key reactive components affect the equilibrium of the key component, but not its mass transfer rate. The absorption and stripping of non-key components were assumed controlled by equilibrium between the gas and liquid phases in these columns. An isothermal flash model for chemical solvents was also developed and included in the program.

The agreement between program predictions and pilot plant data was quite good, supporting the the validity of the model. Program simulations are shown to provide insights into the effects of changes in process variables on system operation.

TABLE OF CONTENTS

Page

ABSTRACT iii

FIGURES viii

TABLES x

1. INTRODUCTION 1

2. BACKGROUND 3

COAL GASIFICATION 3
ACID GAS REMOVAL SYSTEMS 5
HOT POTASSIUM CARBONATE PROCESSES 9
THERMODYNAMICS OF ACID GASES AND CHEMICAL SOLVENTS 12
MASS TRANSFER WITH CHEMICAL REACTION 20
PROMOTION OF MASS TRANSFER IN CARBONATE SOLUTIONS 38
MODELING OF PACKED COLUMNS WITH CHEMICAL SOLVENTS 41

3. FACILITY DESCRIPTION 46

4. EXPERIMENTAL RESULTS AND DISCUSSION 50
Test Run Numbers

ACIL-23 52
ACIL-24 52
ACIL-25 52
ACIL-26 59
ACIL-27 61
ACIL-28 61
ACIL-29 63
ACIL-30 63
ACIL-31 64
ACIL-32 64
ACIL-33 64

ACIL-35 65
ACIL-36 65
ACIL-38 65
ACIN-1 66
ACIN-2 66
ACIN-3 66
ACIN-5 67
ACIN-6 67
ACIN-7 66
ACIN-8 68
ACIN-9 68

5. DEVELOPMENT OF SIMULATION MODEL 74

DIFFERENTIAL ELEMENT 78
ABSORBER MODEL 80
FLASH TANK MODEL 85
STRIPPER MODEL 87

6. THERMODYNAMIC AND TRANSPORT PROPERTIES 90

DENSITY 90
VISCOSITY 90
VAPOR PRESSURE OF SOLVENT 91
LATENT HEAT OF VAPORIZATION 91
SURFACE TENSION 91
DIFFUSIVITY 92
EQUILIBRIUM RELATIONSHIPS 92
  Henry's Law Constants 92
  Reaction Equilibrium Constants 93
MASS TRANSFER COEFFICIENTS 94
  Gas Phase Mass Transfer Coefficients 94
  Liquid Phase Mass Transfer Coefficients 94
  Interfacial Area for Mass Transfer 95

7. DESCRIPTION OF COMPUTER PROGRAMS 96

- MAIN PROGRAM AND SUBROUTINES 96
- CONVERGENCE 106
- COMPUTATIONAL REQUIREMENTS 106

8. COMPARISON OF MODEL PREDICTIONS AND EXPERIMENTAL DATA 108

9. APPLICATIONS 123

- PARAMETRIC STUDIES 123
- SELECTIVITY 140

10. CONCLUSIONS 142

11. REFERENCES 144

12. LIST OF SYMBOLS 151

LIST OF FIGURES

Page

1. Basic Scheme for an Acid Gas Removal System 6
2. Film Theory Concentration Profile 22
3. Asymptotic Behavior of the Enhancement Factor 24
4. Gasifier/PCS System 47
5. Acid Gas Removal System 48
6. Sweet Gas Analyses for Run ACIL-26 60
7. Sweet Gas Analyses for Run ACIL-27 62
8. Experimental CO_2 Removal 69
9. Experimental H_2S Removal 70
10. Experimental COS Removal 71
11. Experimental Selectivity 72
12. Absorption with Physical Solvents 76
13. Differential Element of Packing 79
14. Bottom Pinch of Key Component 81
15. Absorption with High Liquid-to-Gas Ratio 83
16. Top Pinch of Key Component 84
17. Stripper Column Schematic 88
18. Stream Array Sequence 99
19. Absorber Calculative Scheme 100
20. Flash Calculative Scheme 101
21. Stripper Calculative Scheme 102
22. AGRS Calculative Scheme 103
23. DSEC Calculative Scheme 104
24. Measured and Predicted Sweet Gas Flow Rates 111
25. Measured and Predicted Flash Gas Flow Rates 112
26. Measured and Predicted Acid Gas Flow Rates 113
27. Measured and Predicted Removals of CO_2 114
28. Measured and Predicted Removals of CO_2 Greater Than 90% 115
29. Measured and Predicted Removals of H_2S 116

30. Fractional Conversion of COS 117
31. Predicted Removals of COS with Equation 175 118
32. Predicted Removals of COS with Equation 176 121
33. Effect of Absorber Pressure on Absorption of CO_2 124
34. Effect of Absorber Temperature on Absorption of CO_2 125
35. Effect of Absorber Temperature on Enhancement Factor 127
36. Effect of Absorber Temperature on Overall Mass Transfer Coefficient of CO_2 128
37. Effect of Absorber Temperature on Equilibrium Gas Phase Mole Fraction of CO_2 129
38. Effect of Absorber Gas Flow Rate on Absorption of CO_2 130
39. Effect of Absorber Packing Height on Absorption of CO_2 131
40. Effect of Stripper Packing Height on Absorption of CO_2 133
41. Effect of Reboiler Steam Flow Rate on Absorption of CO_2 134
42. Effect of Solvent Composition on Absorption of CO_2 135
43. Absorption of CO_2 with Bottom Pinch 137
44. Absorption of CO_2 with Top Pinch 138
45. Effect of Solvent Circulation Rate on Absorption of CO_2 139

LIST OF TABLES

Page

1. Composition of Gas from NCSU Fluidized Bed Gasifier Texas Lignite Coal 4
2. Acid Gas Removal Processes 8
3. Commercial Acid Gas Removal Systems 9
4. Analyses and Mass Balances for ACIL-23 51
5. Acid Gas Removal System Operating Conditions 53
6. Summary of Sour and Sweet Gas Compositions 58
7. Removal of CO_2, H_2S and COS 59
8. Program Formats 97
9. Levels of Program Output 97
10. Coal Gas Species Included in CARB 98
11. Main Program and Subroutines 105
12. Program Convergence Parameters 107
13. Model Predictions and Experimental Data for ACIL-24 109

INTRODUCTION

Synthetic fuels may be defined as those obtained by converting a carbonaceous material to another form (Probstein and Hicks, 1982). This conversion is typically a process of hydrogenation since most synthetic fuels have a higher hydrogen content than the raw materials from which they are produced. Most processes currently in use convert a solid fuel into a gaseous or liquid form.

The most abundant carbonaceous material is coal, which represents approximately 80% of the proven energy reserve of the world; about one fourth of this reserve lies in the United States (Probstein and Hicks, 1982). Consequently, it is likely that the first synthetic fuels used in large quantities in the United States will be derived from coal.

A number of processes have been developed for the gasification of coal and several of these are now available for commercial use. All of these processes produce the desired product gases such as CO, H_2, and CH_4, and all produce some undesirable products. Depending on the gasification process, these may include a large number of sulfur and nitrogen compounds, aliphatic and aromatic hydrocarbons, and trace elements such as mercury and lead, in addition to CO_2. To produce a clean gas, the primary compounds to be removed are CO_2, H_2S, and COS. Removal of the remaining trace contaminants may also be essential to the success of a synfuels production operation.

As gasification processes have developed in the United States, it has become apparent that improved technology in gas cleaning is needed to meet current environmental standards. As part of a program to develop this technology, the U. S. Environmental Protection Agency sponsored a Coal Gasification/Gas Cleaning Test Facility at North Carolina State University. The final gas clean-up in this facility is accomplished by an acid gas removal system (AGRS) in which a solvent is circulated through a packed absorption column, for removal of acid gases from the coal gas. Several flash tanks and a packed stripping column are used for regeneration of the solvent. A process that removes CO_2 and H_2S from a gas stream is referred to as an acid gas removal system due to the acidic nature of these species.

Most gas cleaning processes were developed for the natural gas and petroleum refining industries to treat gas streams having low acid gas content, few trace contaminants, and a high ratio of H_2S to CO_2 (Auyang et al., 1985). Acid gas removal systems are used extensively in the natural gas and petroleum industries to "sweeten" gas streams; however, little work has been done to evaluate their performance in treating coal gas. The primary objectives of the project at North Carolina State University are to demonstrate the performance of various acid gas removal solvents in treating coal gas, and to provide information on the fate of environmentally significant compounds produced in the gasification process.

All previous work at the facility has employed refrigerated methanol as the acid gas removal solvent. The effect of absorber operating conditions on system performance is described by Kelly (1981) and that of solvent regeneration by Staton et al. (1985). Models for the design of packed absorption and stripping columns in an acid gas removal system using refrigerated methanol to treat coal gas have also been developed (Kelly, 1981; Kelly et al., 1983; Staton, 1983).

The experimental work described in this report employed an aqueous solution of potassium carbonate, K_2CO_3, as the AGRS solvent. This process is referred to as the hot potassium carbonate process since both absorption and regeneration units are typically operated at elevated temperatures. The primary difference between this solvent and methanol is that potassium carbonate removes the acid gases by a chemical reaction, and is thus classified as a chemical solvent. while methanol physically absorbs the acid gases, and is thus termed a physical solvent. Another important difference is the solubility of organic compounds in the two solvents. Hydrocarbons such as methane, benzene, and large cyclic compounds are essentially insoluble in the aqueous solution of potassium carbonate, and thus remain in the product gas stream. Such compounds are, however, highly soluble in methanol, and they are absorbed and ultimately distributed in all gas streams leaving the regeneration units. These hydrocarbons are important for their energy value, and many are also considered environmentally hazardous.

The primary goals of the work described in this report are to:

1. Evaluate the hot potassium carbonate process as an acid gas removal solvent in treating crude coal gas.
2. Identify key operating variables that determine system performance for both the absorption and regeneration portions of the AGRS.
3. Provide information on the distribution of environmentally significant compounds in process exit streams at both optimal and non-optimal operating conditions.
4. Develop a model that simulates the absorption, flash, and stripping operations; devise an algorithm that incorporates the model into a simulation program; and test the model and simulation algorithm against operating data.

BACKGROUND

COAL GASIFICATION

The technology to produce gas from coal has existed since the early 1800's when gas lamps were used to light streets in the world's major cities (Lom and Williams, 1976). Interest in such processes in the United States, however, declined with the discovery of large reserves of natural gas and petroleum, and has since changed with the world oil situation. One prediction made recently by the U. S. Synthetic Fuel Task Force estimates "it is highly probable that we will need commercial-scale synthetic fuel production by the year 2000; there are genuine chances of an abrupt earlier need" (Forman, 1984).

Coal is a complex chemical mixture formed by the anaerobic decomposition of vegetable matter under high temperature and pressure. The chemical composition of coal varies greatly, and gas produced from coal is neither well-defined nor of constant composition. The reactions that occur when coal is gasified may be divided into four catagories: pyrolysis or devolatilization, gasification, oxidation, and inorganic reactions (Purdy, 1983). Pyrolysis is the thermal decomposition of coal to yield volatile hydrocarbons, tars, and liquids. Gasification involves reaction of carbon with steam or H_2 to form CO or CH_4. Oxidation of carbon to form CO and CO_2 is the reaction used to provide heat for the endothermic gasification reactions. Inorganic reactions include the reactions of nitrogen, sulfur and volatile trace metals such as lead, mercury and arsenic; they are important primarily for environmental considerations. The complex nature of coal, and the variety of reactions possible means that the composition of the gas produced will vary over a wide range.

The composition of the crude coal gas to be cleaned is also determined by the type of reactor used in gasification and the reactor operating conditions. Coal gasification reactors are often divided into three classes: fixed or moving bed, fluidized bed, and entrained bed. Fixed or moving bed reactors employ a slowly moving bed with solids fed from the top and residue removed from the bottom. An example is the Lurgi gasifier. With entrained bed gasifiers, the solids are suspended completely in a high velocity cocurrent gas stream at a high temperature. Examples of this type of reactor are the Texaco and Shell gasifiers. Fluidized bed gasifiers, such as the Winkler gasifier, operate between the regimes of moving bed and entrained bed gasifiers.

The gasifier used for this study was a fluidized bed reactor with the coal fed into the freeboard zone above the bed. The gas produced during pyrolysis was thus an important part of the reactor product gas. A typical composition of the gas from the fluidized bed gasifier is given in Table 1.

TABLE 1
COMPOSITION OF GAS FROM NCSU FLUIDIZED BED GASIFIER
TEXAS LIGNITE COAL

Compound	Mole % Dry Basis or ppm
H_2	34.28 %
CO	13.58
CO_2	26.87
N_2	19.42
CH_4	4.99
H_2S	1608 ppm
COS	35
Methyl Mercaptan	31
Thiophene	17
C_2H_4	1612
C_2H_6	2909
C_3H_6	777
C_3H_8	390
C_4H_8	359
Benzene	566
Toluene	179
o-Xylene	15
m-Xylene	30
p-Xylene	6
Ethylbenzene	13

ACID GAS REMOVAL SYSTEMS

A process that removes CO_2 and H_2S from a gas stream is referred to as an acid gas removal system due to the acidic nature of these species. This removal is carried out primarily to achieve the following (Ghassemi et al., 1978):

1. Removal of H_2S and other sulfur compounds to produce clean fuels, to protect downstream gas processing catalysts, and to avoid corrosion.
2. Removal of CO_2 to produce a high BTU gas stream suitable for long-distance pipeline transportation.

Major industrial processes that require gas treating include the production of hydrogen and ammonia, natural gas purification, oil desulfurization and coal gasification (Astarita, et al., 1983). An acid gas removal system used in a coal gasification process must often be able to handle a wide range of compounds that includes carbonyl sulfide, mercaptans, thiophene, aromatic hydrocarbons, and others. For this reason, many of the available acid gas removal processes are not considered directly applicable in coal gas purification.

The first step in purification of a crude coal gas stream usually involves cooling, quenching, or washing to condense tars and oils, and to remove dust and water-soluble materials (such as phenols, chlorides, ammonia, cyanides, thiocyanates, and perhaps some H_2S (Fleming and Primack, 1976). After the initial cleaning, the ratio of H_2 to CO in the gas may be adjusted, depending on the intended use of the product gas. The gas is then fed to an acid gas removal system.

Most acid gas removal systems employ a liquid solvent process involving a combination of gas absorption and regeneration operations. These processes use variations of the basic process shown in Figure 1, although in actual design multiple absorption and regeneration columns are often used, and more than one flash operation may be used for staged pressure reduction.

The removal of CO_2 and H_2S may be nonselective (removed simultaneously) or selective (removed separately) (Ghassemi et al., 1978). The type of removal may be fixed by the downstream sulfur-recovery process. Selective processes produce an acid gas stream with high concentrations of H_2S that can be treated in a Claus sulfur-recovery plant. Nonselective processes produce an acid gas stream with approximately the same CO_2 to H_2S ratio contained in the feed to the acid gas removal system. Gas produced from coal gasification has a high CO_2 to H_2S ratio which means the acid gas stream from a nonselective acid gas removal system, used in conjuction with coal gasification, would require treatment by some other process that could handle low concentrations of H_2S. The Stretford or Selectox processes are examples of such treatments

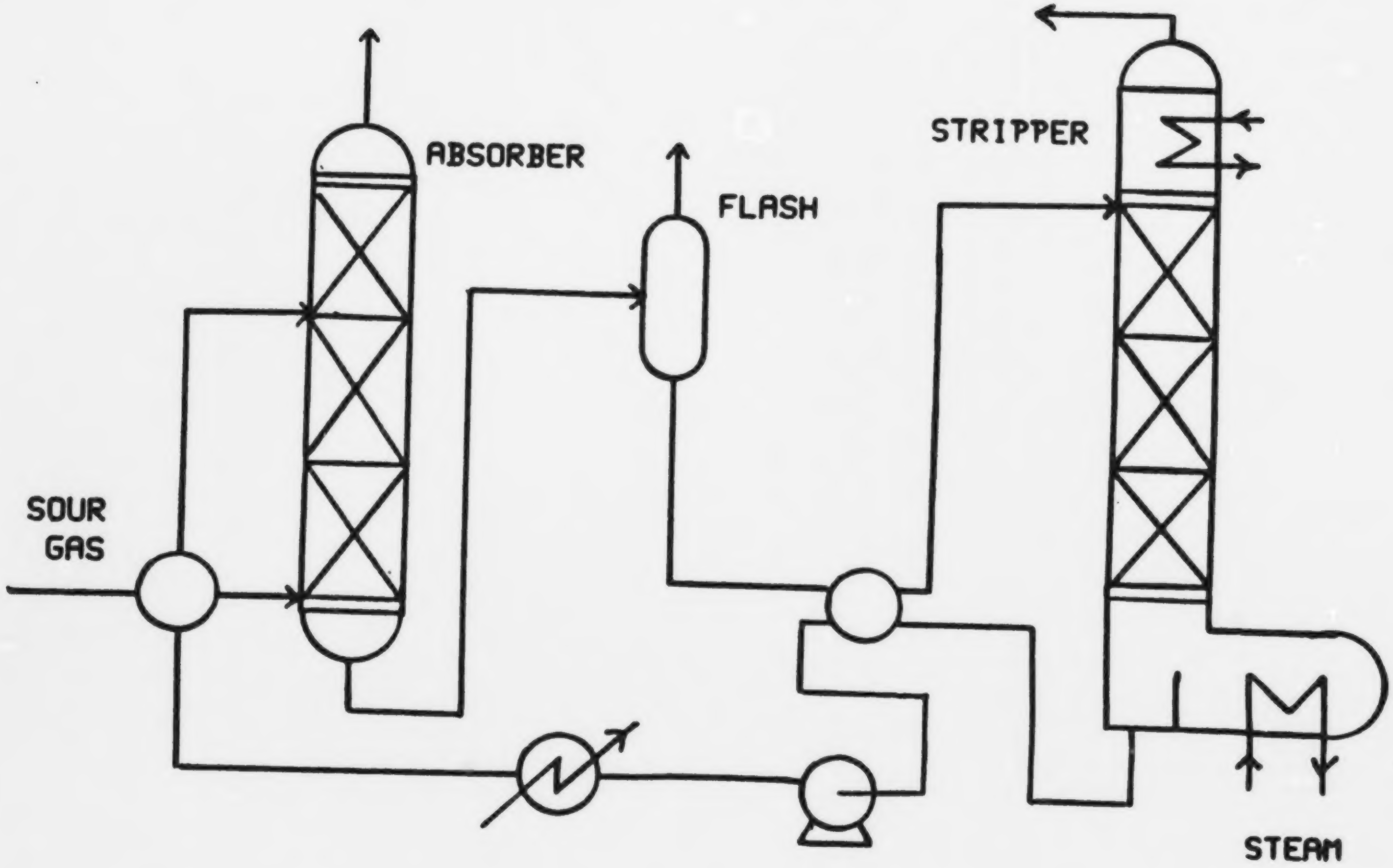
SOUR
GAS
ABSORBER
FLASH
STRIPPER
STEAM

Figure 1 Basic Scheme for an Acid Gas Removal System

(Ghassemi et al., 1978; Goar, 1982).

Acid gas removal solvents may be classified as physical solvents, chemical solvents, or mixtures of physical and chemical solvents. Physical solvent processes use organic solvents that absorb acid gases without chemical reactions between solutes and the solvent. The solubilities of acid gases in physical solvents increase with increasing partial pressure and decreasing temperature and become infinite at the dew point of the gas. Generally, physical solvents are considered better for cleaning gas streams with high partial pressures of acid gases. Physical solvent processes, in general, have two major disadvantages: affinity of the solvent for heavy hydrocarbons, and a relatively high cost (Goar, 1978).

With chemical solvents, a chemical reaction takes place between the active component(s) in the solvent and the acid gases, taking advantage of the acidic nature of the latter. These reactions must, however, be reversible to allow solvent regeneration. Since most chemical solvents are solutions of active components in water, their capacity is fixed by the amount of active component(s) in solution. Some chemical solvents also contain rate promoters that catalyze reactions of the acid gases with the solvent. Chemical solvents are usually considered preferable for applications in which the gas to be conditioned has low partial pressures of acid gases. The major disadvantages of chemical solvents are that some reactive components may experience irreversible degradation with CO, COS, CS_2, and other species, and some solvents are highly corrosive.

Table 2 lists major examples of each type of solvent (Wall, 1982; Kelly, 1982), and given in Table 3 are the approximate number of commercial installations of more common solvents (Wall, 1982; Astarita et al., 1983). The choice of an acid gas removal solvent in a coal gasification process presents a complex problem. This decision will be based not only on the properties of the solvent but also on how the acid gas removal system is integrated into the overall process. Key factors affecting this choice include (Ghassemi et al., 1978; Dunlop, 1982):

1. Temperature, pressure, and composition of the sour gas (determined by composition of the coal, gasifier type, and gasifier conditions)
2. Processes used for tail gas treating CO_2 and/or sulfur recovery
3. Utility requirements and the availability of waste heat
4. Intended use of the product gas
5. Environmental regulations
6. Economics

TABLE 2
ACID GAS REMOVAL PROCESSES

Process	Physical Solvent
Rectisol	Methanol or Methanol Mixture
Selexol	Dimethyl Ether of Polyethylene Glycol
Purisol	n-Methyl-Pyrrolidone (NMP)
Process	**Chemical Solvent**
MEA	Monoethanolamine
DEA	Diethanolamine
TEA	Triethanolamine
DIPA	Diisopropanolamine
MDEA	Methyldiethanolamine
DGA	Diglycolamine
Alkazid "M"	Aqueous Solution of Potassium Salt of Methyl Amino Propionic Acid
Alkazid "DIK"	Aqueous Solution of Potassium Salt of Dimethyl Amino Acetic Acid
Benfield	Hot Potassium Carbonate Solution With Additives
Catacarb	Hot Potassium Carbonate Solution With Amine Borates
Hindered Amine	Proprietary Amine Solution
Process	**Mixture of Physical and Chemical Solvents**
Amisol	Mixture of MEA or DEA and Methanol
Sulfinol	Mixture of DIPA, Sulfolane, and Water

TABLE 3
COMMERCIAL ACID GAS REMOVAL SYSTEMS

Chemical Solvents	Approximate Number
Aqueous Alkanolamines	1000
Promoted Potassium Carbonate	
Benfield	500
Catacarb	100
Giammarco-Vetrocoke	200
Physical Solvents	
Rectisol	35
Selexol	30
Purisol	10
Mixtures of Physical and Chemical Solvents	
Sulfinol	140
Amisol	3

HOT POTASSIUM CARBONATE PROCESSES

Due to the acidic nature of CO_2 and H_2S, alkaline solutions react with these gases. However, for solvent regeneration and good process economics, these reactions must be reversible to be used in an acid gas removal process. This precludes the use of strong alkalies, but the salts of these compounds with weak acids may be used. Aqueous solutions of such salts, being alkaline in nature, will absorb CO_2 and H_2S and, due to the buffering effect, these reactions may be reversed. Salts that have been proposed include sodium and potassium carbonate, phosphate, borate and arsenite (Kohl and Riesenfeld, 1979).

Aqueous potassium carbonate solutions are used extensively in gas conditioning processes. These processes may be divided into two groups: those in which absorption takes place at ambient temperatures and those in which absorption takes place at elevated temperatures approximating those at which the solvent is regenerated (Kohl and Riesenfeld, 1979). The latter type, referred to as hot potassium carbonate processes, were originally developed by Benson and coworkers at the U. S. Bureau of Mines as part of a program to produce liquid fuels from coal (Benson et al., 1954).

The overall reaction of CO_2 in aqueous carbonate solutions is

$$CO_2 + H_2O + CO_3^{=} \longrightarrow 2HCO_3^{-} \qquad (1)$$

and takes place through the following mechanism:

$$CO_3^{=} + H_2O \longleftrightarrow HCO_3^{-} + OH^{-} \qquad (2)$$

$$CO_2 + OH^{-} \longleftrightarrow HCO_3^{-} \qquad (3)$$

There is no direct reaction between CO_2 and the carbonate ion, which acts only as a source of OH^-. The reaction of CO_2 with water is referred to as the acidic mechanism (Wall, 1966)

$$CO_2 + H_2O \longleftrightarrow H_2CO_3 \qquad (4)$$

The reaction in Equation 1 predominates at pH values greater than 8, and industrial processes typically operate in the pH range 9 to 11 (Astarita et al., 1983).

The primary reaction of H_2S in carbonate solutions is the proton transfer reaction with the hydroxide ion to form the hydrosulfide ion and water

$$H_2S + OH^{-} \longleftrightarrow HS^{-} + H_2O \qquad (5)$$

The reactions of Equations 3 and 5 may be combined to form a shift reaction (Astarita et al., 1983)

$$H_2S + HCO_3^{-} \longleftrightarrow HS^{-} + CO_2 + H_2O \qquad (6)$$

that illustrates that the equilibria of CO_2 and H_2S are not independent.

Another important contaminant, COS, is also absorbed by potassium carbonate solutions and undergoes hydrolysis to form CO_2 and H_2S:

$$COS + H_2O \longrightarrow CO_2 + H_2S \qquad (7)$$

This conversion is enhanced by absorption at elevated temperatures (Rib et al., 1982).

Since all proton transfer reactions are extremely rapid, the reaction of H_2S may be considered instantaneous in comparison with diffusion phenomena (Savage et al., 1980). The absorption of CO_2 is, however, much slower than that of H_2S and it is thought to be limited by the kinetics of the reaction of Equation 3. This difference in rates of absorption allows selective separation of H_2S in some situations, and it has led to the use of additives in other situations that increase the rate of CO_2 absorption by increasing the rate of the reaction in Equation 3. These additives, called rate promoters, are used in all hot potassium carbonate processes and distinguish such processes from one another.

The Benfield Process, licensed by Union Carbide Corporation, is used in over 520 commercial installations (Bartoo, 1984), and typically employs an amine promoter. Recent work at Union Carbide has led to the development of an undisclosed inorganic catalyst (for certain applications) and effective corrosion inhibitors (Bartoo, 1984). The Giammarco-Vetrocoke Process, licensed by Davy McKee Corporation, uses arsenic trioxide, As_2O_3, as a rate promoter. This process has, however, found little acceptance in the United States due to the hazardous nature of its promoter. Development of a new and safer catalyst for this process has received recent attention since an accident in Italy in 1976 (Giavarini and Moresi, 1982).

The Catacarb Process, licensed by Eickmeyer and Associates, is another hot potassium carbonate process and it is used in approximately 200 locations (Eickmeyer and Gangriwala, 1981). This process employs an undisclosed catalyst, which also acts as a corrosion inhibitor and is claimed to be nontoxic and nonpoisonous to methanation catalysts (Kohl and Riesenfeld, 1979). Research by Exxon Inc. has led to the development of a promoted hot potassium carbonate process that employs an undisclosed sterically hindered amine as a rate promoter (Say et al., 1984).

The Benfield Process has been used at the General Electric Integrated Gasifier Combined Cycle Power Plant Simulation Facility (Rib et al., 1983) and at a coal gasification research facility in Westfield, Scotland, operated by British Gas Corporation. However, due to the proprietary nature of these processes, few data are available.

THERMODYNAMICS OF ACID GASES AND CHEMICAL SOLVENTS

The simultaneous physical and chemical equilibria of gases in solutions of reactive components is an area overlooked in most chemical engineering texts. The prediction of equilibrium compositions in such a system is essential to the simulation of an acid gas removal system employing a chemical solvent. In this section, a general methodology is presented and applied to the equilibrium of CO_2, H_2S, and COS in aqueous solutions of K_2CO_3. This methodology is based on principles presented by Astarita et al. (1983).

There are two thermodynamic problems to address. The first is to determine the equilibrium concentrations of the dissolved volatile components in the bulk of the liquid corresponding to a given concentration of the non-volatile components. The second is to determine the partial pressures of the volatile components that equilibrate with liquids having known concentrations of these components.

First consider the case of a single volatile component A that may react in the solution. There are two useful concepts to which the composition of the liquid phase may be related. The first is molarity of the solvent, m, which is defined here as the actual concentration of reactive species that could be obtained in the chemical solvent if all chemically combined A could be stripped from the solvent (Astarita et al., 1983). In a carbonate solution, the molarity of the solvent is simply the total K_2CO_3 concentration or the molarity of the solution. The second concept is the degree of saturation, y, defined such that ym is the total concentration of chemically combined A in the liquid phase. The total concentration of A in the solution, $[A]_t$, may then be represented as

$$[A]_t = [A] + ym \tag{8}$$

where $[A]$ is the concentration of physically dissolved A. If the molarity of the solvent has been defined correctly for the given reaction stoichiometry, the values of y can range from 0 to 1 (Astarita et al., 1983).

Both m and ym may be expressed as linear combinations of the concentrations of the non-volatile components:

$$m = \sum_j q_j'[B_j] \tag{9}$$

where $[B_j]$ is the concentration of non-volatile component B_j and q_j' is the number of atoms in B_j of some element not present in component A. Similarly

$$ym = \sum_j z_j[B_j] \tag{10}$$

where z_j are the number of moles of component A chemically combined in component B_j (Astarita et al., 1983).

The concentrations of the non-volatile species may be first addressed by writing each independent reaction involving only non-volatile species in the form

$$\sum_j \nu_{jk} B_j = 0 \quad (k = 1,2,.....N) \tag{11}$$

where ν_{jk} is the stochiometric coefficient for non-volatile component B_j in reaction k and N is the total number of independent reactions involving only non-volatile species. Selection of a set of $[B_j]^o$ allows one to express the $[B_j]$ as

$$[B_j] = [B_j]^o - \sum_j \nu_{jk} Z_k \tag{12}$$

where Z_k is the extent of reaction k. The $[B_j]^o$ are selected by finding a simple set of values that satisfy Equations 9 and 10 for any given values of m and y. Substitution of Equation 12 into the definition of the concentration-based equilibrium constant for reaction k:

$$K_k = \prod_j [B_j]^{-\nu_{jk}} = \prod_j \left[[B_j]^o - \sum_k \nu_{jk} Z_k \right]^{-\nu_{jk}} \quad (k = 1,2,.....N) \tag{13}$$

yields a set of N polynomial equations that may be solved for the one set of Z_k values that are all real, and when substituted into Equation 12 give non-negative values for each $[B_j]$ (Astarita et al., 1983).

Once the liquid-phase concentrations of the non-volatile components have been determined, they may then be related to the concentration of the volatile component physically dissolved in the liquid phase. Writing the reaction of the volatile component A in the form

$$A + \sum_j \nu_j B_j = 0 \tag{14}$$

the concentration of physically dissolved A may be obtained from K , the equilibrium constant for this reaction:

$$[A] = \frac{\prod [B_j]^{-\nu_j}}{K} \tag{15}$$

The partial pressure of A, P_A, may then be calculated using the Henry's law constant:

$$P_A = H_A\,[A] \tag{16}$$

To apply this methodo[illegible]o the K_2CO_3 system, first consider the equilibrium of CO_2 as the single volatile [illegible]nent that can react in the liquid. The overall reaction of CO_2 is

$$CO_2 + H_2O + CO_3^{=} \longleftrightarrow 2HCO_3^{-} \tag{17}$$

Since the concentration of H_2O is essentially constant and K^+ may be considered inert, the only two non-volatile components to consider are $CO_3^{=}$ and HCO_3^{-}. The concentrations of OH^- and H^+ are always much smaller than those of $CO_3^{=}$ and HCO_3^{-} and may be considered negligible from a thermodynamic view (Astarita et al., 1983).

From Equation 9 the molarity of the solvent may be expressed as

$$m = [CO_3^{=}] + \frac{1}{2}\,[HCO_3^{-}] \tag{18}$$

From Equation 10 the degree of saturation may be expressed by

$$ym = \frac{1}{2}\,[HCO_3^{-}] \tag{19}$$

since 1/2 mole of CO_2 may be considered chemically combined in each mole of HCO_3^{-}. The degree of saturation of CO_2 corresponds to the degree of conversion of carbonate to bicarbonate, when CO_2 is the only volatile component that may react with the carbonate.

Since there are no significant independent reactions involving only non-volatile species, the definitions of m and ym are adequate to express the concentrations of $CO_3^=$ and HCO_3^-. Combining Equations 18 and 19 yields

$$[CO_3^=] = m(1 - y) \tag{20}$$

while rearranging Equation 19 gives

$$[HCO_3^-] = 2ym \tag{21}$$

Now that the concentrations of the non-volatile components have been expressed in terms of molarity and degree of saturation, the concentration of physically dissolved CO_2 may be expressed. Using the concentation-based equilibrium constant of the reaction of Equation 17

$$K = \frac{[HCO_3^-]^2}{[CO_2][CO_3^=]} \tag{22}$$

or

$$[CO_2] = \frac{(2ym)^2}{Km\ (1 - y)} = \frac{4m\ y^2}{K\ (1 - y)} \tag{23}$$

The total concentration of CO_2 in solution may then be expressed as

$$[CO_2]_t = [CO_2] + ym = \frac{4my^2}{K\ (1 - y)} + ym = ym \left[1 + \frac{4y}{K\ (1 - y)} \right] \tag{24}$$

Finally, the equilibrium partial pressure of CO_2 may be expressed in terms of the Henry's law constant

$$P_{CO_2} = H\ [CO_2] = \frac{4Hmy^2}{K\ (1 - y)} \tag{25}$$

Given the partial pressure of CO_2 in the gas phase and the molarity of the solvent, the degree of saturation at equilibrium can be calculated and used to evaluate the equilibrium composition of the liquid. Alternatively, given the composition of the liquid phase, the degree of saturation may be evaluated and used to evaluate the corresponding equilibrium partial pressure of CO_2. Equation 25 has been shown to correlate very well with experimentally measured partial pressures of CO_2 at temperatures and liquid molarities of industrial interest (Joshi, 1980).

The concentration of OH^- may be evaluated from the equilibrium constant of the reaction

$$CO_3^{=} + H_2O \longleftrightarrow HCO_3^- + OH^- \tag{26}$$

once $[CO_3^{=}]$ and $[HCO_3^-]$ have been evaluated. The concentration of H^+ may be evaluated from the equilibrium constant of the reaction (Astarita et al., 1983).

$$H_2O \longleftrightarrow H^+ + OH^- \tag{27}$$

Now consider the equilibrium of three volatile reactive components, CO_2, H_2S, and COS in K_2CO_3 solutions. Since COS undergoes hydrolysis only

$$COS + H_2O \longleftrightarrow H_2S + CO_2 \tag{28}$$

the equilibrium concentration of COS in the liquid phase may be evaluated once the concentrations of CO_2 and H_2S have been found. Using the concentration-based equilibrium constant of the reaction of Equation 28

$$K'' = \frac{[H_2S]\,[CO_2]}{[COS]\,[H_2O]} \tag{29}$$

$$[COS] = \frac{[H_2S]\,[CO_2]}{K''[H_2O]} \tag{30}$$

The equilibrium partial pressure of COS may then be calulated using the Henry's law constant

$$P_{COS} = H''\,[COS] \tag{31}$$

The overall reaction of H_2S is

$$H_2S + CO_3^{=} \longleftrightarrow HS^{-} + HCO_3^{-} \qquad (32)$$

The second dissociation constant of H_2S is so low in the pH range of interest that essentially no $S^{=}$ is formed, and all chemically combined H_2S is in the form HS^{-} (Astarita et al., 1983).

As was done when only CO_2 was present, a degree of saturation of H_2S, y', may be defined and the total concentration of H_2S in solution represented as

$$[H_2S]_t = [H_2S] + y'm \qquad (33)$$

From Equation 10, the degree of saturation of H_2S is given by

$$y'm = [HS^{-}] \qquad (34)$$

With H_2S present, however, Equations 18 and 19 do not correctly represent the molarity of the solvent and the degree of saturation of CO_2.

To derive expressions for these terms, first consider a solution containing CO_2 but no H_2S. As H_2S is added, the reaction in Equation 32 takes place. Although this will change the concentrations of $CO_3^{=}$ and HCO_3^{-}, it will not change their sum. From Equations 20 and 21.

$$[CO_2^{=}] + [HCO_3^{-}] = m(1 - y) + 2my = m(1 + y) \qquad (35)$$

From Equation 9, an expression for the molarity may be obtained

$$m = [CO_3^{=}] + \frac{1}{2}[HCO_3^{-}] + \frac{1}{2}[HS^{-}] \qquad (36)$$

The concentrations of the non-volatile components may now be expressed in terms of m, y and y'. Combining Equations 34, 35, and 36

$$[CO_3^{=}] = m(1 - y - y') \qquad (37)$$

$$[HCO_3^{-}] = m(2y + y') \qquad (38)$$

$$[HS^-] = my' \tag{39}$$

Using the concentration based equilibrium constant of the reaction of Equation 17

$$[CO_2] = \frac{[HCO_3^-]^2}{K\,[CO_3^=]} = \frac{m(2y + y')^2}{K(1 - y - y')} \tag{40}$$

and that of the reaction of Equation 32

$$[H_2S] = \frac{[HS^-]\,[HCO_3^-]}{K'\,[CO_3^=]} = \frac{my'(2y + y')}{K'(1 - y - y')} \tag{41}$$

Expressing the vapor pressures of CO_2 and H_2S in terms of the Henry's law constants:

$$P_{CO_2} = \frac{Hm(2y + y')^2}{K(1 - y - y')} \tag{42}$$

$$P_{H_2S} = \frac{H'my'(2y + y')}{K'(1 - y - y')} \tag{43}$$

Given the partial pressures of CO_2 and H_2S in the gas phase and the molarity of the solvent, these equations may be solved simultaneously to yield values for y and y'. These values may then be used to calculate the composition of the liquid phase. It is interesting to note that the partial pressure of CO_2 depends on the amount of H_2S in the liquid phase, and vice-versa. This may be considered similar to non-ideal behavior in a physical solvent.

In physical solvents, the Henry's law constant may be obtained from an experimentally determined equilibrium plot of P_A vs $[A]_T$; the constant being the slope near the origin. With a chemical solvent, the partial pressure of the gas is proportional to the ratio of the Henry's law constant and a reaction equilibrium constant. Thus, the Henry's law constant can be obtained from the vapor liquid equilibrium data only when the corresponding value of the reaction equilibrium constant is known (Astarita et al., 1983).

Henry's law constants for reactive and non-reactive gases in electrolyte solutions may be estimated by the method of Van Krevelen and Hoftijzer (1948). In a K_2CO_3 solution, this method relates the Henry's law constant to that in water by the expression

$$\log\left(\frac{H}{H^o}\right) = h\ I_i \qquad (44)$$

where H^o is the Henry's law constant for that gas in water and I_i is the ionic contribution of the solution, defined as

$$I_i = \frac{1}{2}\sum_i C_i Z_i^2 \qquad (45)$$

and C_i is the concentration of ion i with charge Z_i.

Joshi (1980) correlated experimental data to obtain a value of 0.065 for h in Equation 44. He also correlated his own and literature data with the equation

$$\log\left(\frac{H}{H^o}\right) = 0.125\ m \qquad (46)$$

where m is the molarity of the solution. This method was considered better than Equation 44 for estimating H since experimentally measured values of H/K were found to be independent of the fractional conversion, y. The molarity is independent of the fractional conversion while the ionic strength, I_i, is not (Joshi, 1980).

The effect of an amine rate promoter on vapor liquid equilibrium will be discussed in a later section.

MASS TRANSFER WITH CHEMICAL REACTION

Chemical reactions have two primary effects on the behavior of systems that are used to condition gases with chemical solvents. The first is a large increase in the capacity of the liquid by allowing the dissolved gas to react (Sherwood et al., 1975). In absorption, the reaction of the dissolved gas keeps the concentration of the gas in the liquid at a low level, and thus maintains a higher driving force for mass transfer than would be the case with no reaction. In desorption, the reaction is reversed and continually produces the component to be desorbed, thereby providing a driving force for desorption that is larger than would be the case with no reaction (Astarita et al., 1983). The second effect of the reaction is that, at a given driving force, if the rate of reaction is fast enough to occur appreciably near the gas-liquid interface, it increases the rate of mass transfer (Sherwood et al., 1975). This increase in mass transfer rate is usually expressed in terms of a rate enhancement factor.

The latter point can be illustrated by considering absorption of component A from a gas into a liquid. The mass transfer flux in the liquid phase may be expressed in the form

$$N_A = k_L \left([A]_i - [A]_o \right) \tag{47}$$

where k_L is the mass transfer coefficient in the liquid phase, $[A]_i$ is the concentration of A at the interface and $[A]_o$ is the bulk concentration of A in the liquid. If the gas undergoes a chemical reaction in the liquid, the flux may be expressed similarly as

$$N_A = k_L^* \left([A]_i - [A]_o \right) \tag{48}$$

where k_L^* is the liquid-phase mass transfer coefficient that takes into account the increase in mass transfer rate due to the chemical reaction. The enhancement factor, I, is defined by the relationship

$$I = \frac{k_L^*}{k_L} \tag{49}$$

and the expression for the mass transfer flux with chemical reaction in the liquid phase becomes

$$N_A = I\ k_L\ \left([A]_i - [A]_o \right) \tag{50}$$

Since values of k_L may be predicted from existing correlations, the problem of evaluating flux then becomes one of developing an expression for the enhancement factor.

There are three primary models of the hydrodynamics at a gas-liquid interface: the film theory, the penetration theory and the surface renewal theory. An expression for the mass transfer coefficient may be obtained from each of these theories; however, each expression contains a quantity that can not be calculated by theory alone. In the case of the film theory, this quantity is the film thickness, in the penetration theory, the interphase exposure time, and in the surface renewal theory, the surface element mean lifetime. These theories cannot be used to predict a numerical value for the mass transfer coefficient, but they can be used to develop a theoretical expression for the enhancement factor (Sherwood et al., 1975). Although the expressions for k_L and k_L^* are dependent on the theory used in their derivation, their ratio (I) is almost independent of theory (Astarita et al., 1983). In the following discussion, a brief description of the film theory is presented and used to obtain expressions for the enhancement factor.

In the film theory, which is the simplest of the three models introduced above, a stagnant film of thickness δ is assumed to exist near the gas-liquid interface. Mass transfer through the film can take place by molecular diffusion only, and the concentrations of all species at a distance δ from the interface are equal to the bulk liquid concentrations. Transport in the film theory is shown schematically in Figure 2.

In the presence of chemical reaction, the film theory equations for the diffusion of A become

$$D\ \frac{d^2[A]}{dx^2} = r \tag{51}$$

where r is a function of $[A]$ and $[B_j]$. Accordingly, the rate of chemical reaction is not constant through the liquid but depends on the local composition. Thus, Equation 51 must be solved simultaneously with the equation

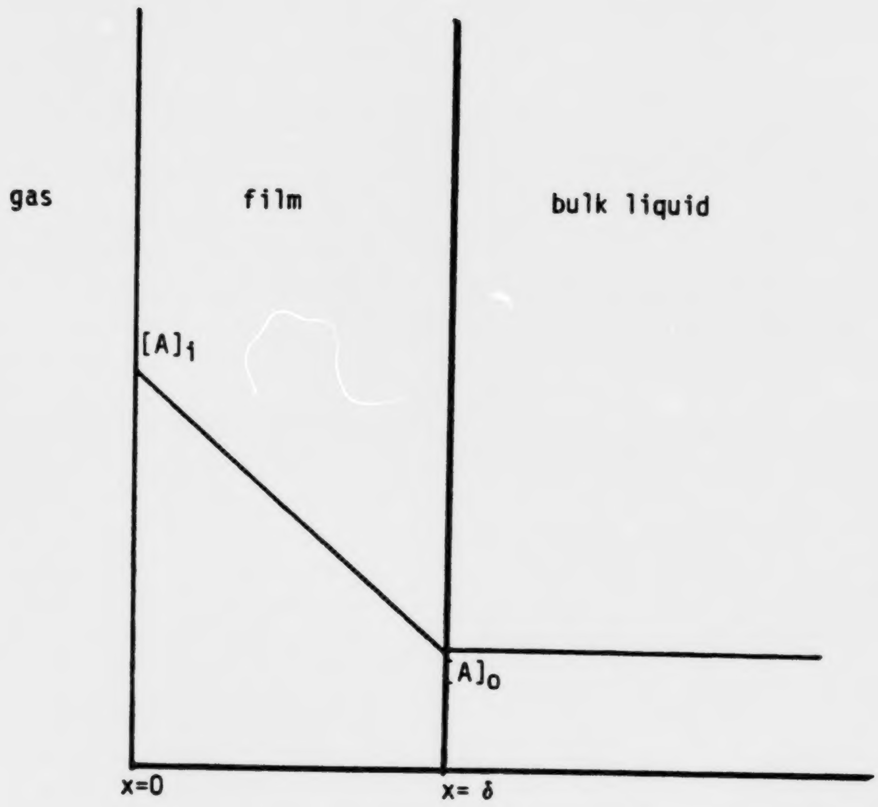
gas
film
bulk liquid
[A]i
[A]o
x=0
x= δ

Figure 2 Film Theory Concentration Profile

$$D \frac{d^2[B_j]}{dx^2} = \nu B_j r \qquad (52)$$

and the boundary conditions

$$\text{at } x = 0 \quad [A] = [A]_i \text{ and } [B_j] = [B_j]_i$$
$$\text{at } x = \delta \quad [A] = [A]_o \text{ and } [B_j] = [B_j]_o$$

Equations 51 and 52 represent, in general, a series of coupled non-linear differential equations that cannot be solved analytically. Certain limiting conditions may, however, be introduced that simplify considerably the mathematical problem and allow asymptotic solutions referred to as the slow, fast and instantaneous reaction regimes. The enhancement factor obtained from these asymptotic solutions is shown in Figure 3 as a function of the relative rate of reaction to that of diffusion (Astarita et al., 1983).

The enhancement factor is in general a complicated function of the compositions of the gas and liquid phases. As noted by Secor and Southworth (1961), there is often a large change in stream compositions and driving forces along the axis of a packed tower. Hence, an expression for the enhancement factor must approach the proper asymptotes of slow, fast, and infinite reaction regimes if it is to be used in the simulation of a packed absorption or stripping column.

In the **slow reaction regime,** it is assumed that the chemical reaction is so slow that it takes place only in the bulk of the liquid. In this case, the chemical reaction increases the driving force for mass transfer by its effect on the bulk concentration $[A]_o$, but it is not rapid enough to affect the diffusion of A in the film. In this case no rate enhancement is observed and

$$I_S = 1 \qquad (53)$$

Astarita and Savage (1982) have presented a methodology based on the film theory to predict enhancement factors in the case of reversible reactions for both absorption and stripping. This methodology is illustrated in the following discussion for the fast and instantaneous regime solutions. First, however, note that the film theory can be used to derive an expression for the flux of A across the gas-liquid interface in terms of the total concentration of both physically dissolved and chemically combined A in the liquid interface, $[A]_{t,i}$, and in the bulk liquid phase, $[A]_{t,o}$. This derivation leads to the expression

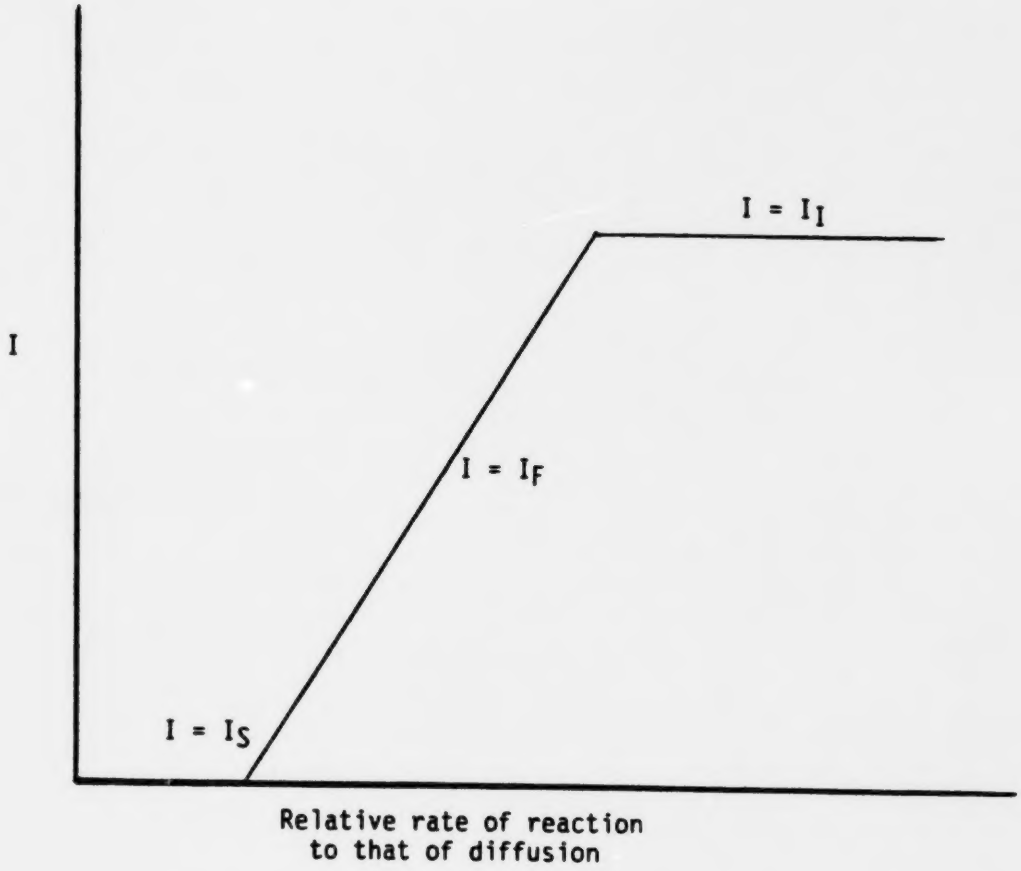

Figure 3 Asymptotic Behavior of the Enhancement Factor

$$N_A = k_L \Big([A]_{t,i} - [A]_{t,o} \Big) \tag{54}$$

where N_A is the flux with chemical reaction and k_L is the physical mass transfer coefficient. Recalling the flux with chemical reaction expressed in terms of a mass transfer coefficient that includes the effect of chemical reaction

$$N_A = k_L^* \Big([A]_i - [A]_o \Big) \tag{55}$$

the enhancement factor may be expressed as

$$I = \frac{k_L^*}{k_L} = \frac{[A]_{t,i} - [A]_{t,o}}{[A]_i - [A]_o} \tag{56}$$

which is positive in both absorption and stripping (Astarita and Savage, 1982).

The **instantaneous reaction regime** is the asymptotic limit of mass transfer enhancement as the rate of chemical reaction becomes very large. In this limit, chemical equilibrium is assumed to exist locally everywhere in the liquid phase with the chemical reaction taking place at whatever rate the reactants are brought together by diffusion (Astarita and Savage, 1982). Thus, Equation 56 becomes

$$I_I = \frac{[A]_{t,i}^* - [A]_{t,o}}{[A]_i - [A]_o} \tag{57}$$

where $[A]_{t,i}^*$ is the value of $[A]_t$ corresponding to chemical equilibrium with the interfacial partial pressure, P_{Ai}. An explicit expression for I_I may then be developed by considering the specific system.

An expression for I_I for the absorption and stripping of CO_2 with hot carbonate solutions has been developed by Savage et al. (1980). If Equations 18, 19, 22, and 24 are solved simultaneously and substituted into Equation 57, the result is

$$I_I = 1 + \frac{K(F_3^* - 1)(1 - y)}{4y \left(\dfrac{[CO_2]_i}{[CO_2]_o} - 1 \right)} \tag{58}$$

where

$$F_3^* = \frac{y\left(\dfrac{[CO_2]_i}{[CO_2]_o}\right)}{2(1-y)}\left[\left(1+\frac{4(1-y)}{\left(\dfrac{[CO_2]_i}{[CO_2]_o}\right)y^2}\right)^{1/2}-1\right]$$

Equation 56 holds for both absorption and stripping (Savage, et al., 1980).

The third asymptotic solution to mass transfer enhancement by chemical reaction lies between the previous two solutions (Figure 3) and is referred to as the **fast reaction regime.** Unlike the first two solutions, chemical kinetics cannot be avoided in this solution and to obtain a result applicable for stripping as well as absorption, reversibility must be accounted for. The method of Astarita and Savage (1982) includes such an approach and it is illustrated in the following discussion.

Consider the case where component A undergoes a single reaction with the kinetics of the forward reaction, r_F represented as

$$r_F = r_F\left([A],[B_j]\right) \qquad j = 1,2....N \tag{59}$$

Now assume that the dependence of the reaction rate on $[A]$ can be separated from the dependence of r_F on the concentrations of other species. Then r_F may also be expressed as

$$r_F = f\left([A]\right)\, g\left([B_j]\right) \qquad j = 1,2....N \tag{60}$$

At chemical equilibrium, the rates of the forward and reverse reactions are equal

$$r_F^* = r_R^* = f\left([A]^*\right)\, g\left([B_j]^*\right) \tag{61}$$

and the equilibrium concentrations are related by

$$K = \frac{\prod [B_j]^{*-\nu_j}}{[A]^*} \tag{62}$$

Solving Equation 62 for $[A]^*$ and substituting into Equation 61

$$r_R^* = f\left[\frac{\prod [B_j]^{*-\nu_j}}{K}\right] g\left([B_j]^*\right) \tag{63}$$

Assuming the form of Equation 63 also holds when chemical equilibrium does not prevail

$$r_R = f\left([A']\right) g\left([B_j]\right) \tag{64}$$

where

$$[A'] = \frac{\prod [B_j]^{-\nu_j}}{K}$$

The net rate of reaction then becomes

$$r = r_F - r_R = g\left([B_j]\right)\left[f\left([A]\right) - f\left([A']\right)\right] \tag{65}$$

In the fast reaction regime, an asymptotic solution is obtained by assuming the concentrations $[B_j]$ are equal to their bulk liquid values throughout the liquid phase. Astarita and Savage (1982) showed that this assumption may be considered valid when

$$\left|[B_j]_i - [B_j]_o\right| << [B_j]_o \tag{66}$$

The diffusion of A through the film then becomes

$$D\,\frac{d^2[A]}{dx^2} = g\left([B_j]_o\right)\left[f\left([A]\right) - f\left([A']\right)\right] \tag{67}$$

where $g\left([B_j]_o\right) = g_o$ and $f\left([A']\right)$ are constants and uncoupled from the equations for $[B_j]$. Assuming the validity of Equation 66, then

$$[A'] = [A]_o \tag{68}$$

If the rate of the forward reaction is first order with respect to $[A]$, Equation 67 may be rewritten as

$$D\,\frac{d^2[A]}{dx^2} = g_o\left([A] - [A]_o\right) \tag{69}$$

where g_o now contains the reaction-rate constant. Introducing the dimensionless concentration

$$W = \frac{[A] - [A]_o}{[A]_i - [A]_o} \tag{70}$$

Equation 69 becomes

$$D\,\frac{d^2 W}{dx^2} = g_o\,W \tag{71}$$

with the boundary conditions

$$\begin{aligned} &at\ x = 0 \quad W = 1 \\ &at\ x = \delta \quad W = 0 \end{aligned}$$

The solution to Equation 71 is readily obtained, and combining it with Equation 56 results in the expression

$$I = \frac{I_F}{\tanh(I_F)} \tag{72}$$

where

$$I_F = \frac{(Dg_o)^{1/2}}{k_L}$$

Since I_F is the value of I when $I >> 1$, I_F is referred to as the fast reaction regime enhancement factor (Astarita and Savage, 1982).

The enhancement factor I_F can be determined readily for the absorption and stripping of CO_2 in hot carbonate solutions. Assuming that the controlling reaction is that of Equation 3, the reaction rate of CO_2 can be expressed as

$$r = k[OH^-][CO_2] \tag{73}$$

Then by comparison with Equation 69

$$g_o = k[OH^-] \tag{74}$$

From the equilibrium constant of the reaction of Equation 26

$$K_1 = \frac{[HCO_3^-][OH^-]}{[CO_3^=]} \tag{75}$$

or

$$g_o = kK_1 \frac{[CO_3^=]}{[HCO_3^-]} \tag{76}$$

Recalling Equations 20 and 21

$$g_o = kK_1 \frac{m(1-y)}{2ym} = kK_1 \frac{1-y}{2y} \tag{77}$$

Equation 72 then becomes

$$I_F = \frac{\left[\dfrac{DkK_1(1-y)}{2y}\right]^{1/2}}{k_L} \tag{78}$$

which is valid for absorption and stripping (Savage et al., 1980).

As the rate of reaction becomes larger, the concentrations of the B_j's near the interface become appreciably different from their bulk values and the assumption of Equation 66 is no longer valid. The solution in this region lies between that of the fast and instantaneous reaction asymptotes and is referred to as the **fast-instantaneous transition region.**

The first analysis of the fast-instantaneous transition region was presented by Van Krevelen and Hoftijzer (1948) who used the assumption that to calculate the concentration gradient at the gas-liquid interface

$$\text{gradient at interface} = \left.\frac{d[A]}{dx}\right|_i \tag{79}$$

the solution needs only to be accurate near the interface. This assumption was later employed by Astarita and Savage (1982) along with the approach used in the previous analysis to obtain a solution in the fast-instantaneous transition region. The derivation began by combining Equations 51 and 65

$$D\,\frac{d^2[A]}{dx^2} = g\Big([B_j]\Big)\,\Big[f\Big([A]\Big) - f\Big([A']\Big)\Big] \tag{80}$$

At the interface

$$g\Big([B_j]\Big) = g\Big([B_j]_i\Big) = g_i = \text{constant} \tag{81}$$

and

$$[A']_i = \frac{\prod [B_j]_i^{-\nu_j}}{K} \tag{82}$$

For a reaction that is first order with respect to A, Equation 80 becomes

$$D\,\frac{d^2[A]}{dx^2} = g_i\Big([A] - [A']_i\Big) \tag{83}$$

which is uncoupled from the equations for $[B_j]$. Combining the solution to Equation 83 with Equation 56

$$I = \frac{[A]_i/[A]_o - [A']_i/[A]_o}{[A]_i/[A]_o - 1} \frac{S}{\tanh(S)} - \frac{1 - [A']_i/[A]_o}{[A]_i/[A]_o - 1} \frac{S}{\sinh(S)} \tag{84}$$

where

$$S = \frac{(Dg_i)^{1/2}}{k_L} \tag{84a}$$

From Equation 82, the term $[A']_i/[A]_o$ in Equation 84 becomes

$$\frac{[A']_i}{[A]_o} = \prod_j \left[\frac{[B_j]_i}{[B_j]_o} \right]^{-\nu_j} \tag{85}$$

To use Equation 84, the values of $[B_j]_i$ must be known. The following procedure was developed by Astarita and Savage (1982) to calculate these values.

$$\frac{d^2[B_j]}{dx^2} = \nu_j \frac{d^2[A]}{dx^2} \tag{86}$$

for all B_j with non-zero ν_j. Integrating Equation 86

$$\frac{d[B_j]}{dx} = \nu_j \left[\frac{d[A]}{dx} - \left. \frac{d[A]}{dx} \right|_i \right] \tag{87}$$

Integrating Equation 87 from $x = 0$ *to* $x = \delta$

$$[B_j]_o - [B_j]_i = \nu_j \left[[A]_o - [A]_i - \delta \left. \frac{d[A]}{dx} \right|_i \right] \tag{88}$$

Recalling that

$$N_A = -D \left. \frac{d[A]}{dx} \right|_i$$

$$k_L = \frac{D}{\delta}$$

$$I = \frac{k_L^*}{k_L}$$

$$N_A = k_L^* \Big([A]_i - [A]_o \Big)$$

Equation 88 can be rearranged to

$$\frac{[B_j]_o - [B_j]_i}{[A]_i - [A]_o} = -\nu_j(I - 1) \tag{89}$$

Equation 89 can be used to calculate the value of $[B_j]$ for those components whose ν_j is not equal to zero.

Next consider the B_j whose value of ν_j is zero (those that do not appear in the overall reaction) but whose concentration appears as an argument of the function

$$g\Big([B_j]\Big) \qquad j = 1,2.....N$$

through some rate controlling step in the sequence of reactions. Assuming the function g has the form

$$g\Big([B_j] \Big) = k \prod_j \Big([B_j]^{q_j} \Big) \tag{90}$$

Substituting Equation 90 into Equation 84a, and from the definitions of I_F and g_o given below Equations 72 and 67, respectively, the following expression can be obtained:

$$S = \frac{\Big(Dg_o\Big)^{1/2}}{k_L} \prod_j \left[\frac{[B_j]_i^{q_j}}{[B_j]_o^{q_j}} \right]^{1/2} = I_F \left[\prod_j \left(\frac{[B_j]_i}{[B_j]_o} \right)^{q_j} \right]^{1/2} \tag{91}$$

Equation 89 may then be rearranged to

$$\frac{[B_j]_i}{[B_j]_o} = 1 - \left[\frac{[A]_i}{[A]_o} - 1\right] \frac{[A]_o}{[B_j]_o} \nu_j(I - 1) \tag{92}$$

In absorption

$$\frac{[A]_i}{[A]_o} > 1$$

while in stripping

$$\frac{[A]_i}{[A]_o} < 1$$

In the instantaneous reaction regime, Equation 92 becomes

$$\frac{[B_j]_i^*}{[B_j]_o} = 1 - \left[\frac{[A]_i}{[A]_o} - 1\right] \frac{[A]_o}{[B_j]_o} \nu_j(I_I - 1) \tag{93}$$

Equation 92 may then be rewritten as

$$\frac{[B_j]_i}{[B_j]_o} = 1 + \left[\frac{[B_j]_i^*}{[B_j]_o} - 1\right] \left(\frac{I - 1}{I_I - 1}\right) \tag{94}$$

Recalling that

$$K = \frac{\prod_j [B_j]^{*-\nu_j}}{[A]^*}$$

then

$$\frac{[A]_i}{[A]_o} = \prod_j \left(\frac{[B_j]_i^*}{[B_j]_o}\right)^{-\nu_j} \tag{95}$$

Knowing the interfacial partial pressure of A and the bulk liquid composition, Equation 95 may be solved for

$$\frac{[B_j]_i^*}{[B_j]_o} = F_j^* \tag{96}$$

Substituting Equation 96 into Equation 94

$$\frac{[B_j]_i}{[B_j]_o} = F_j = 1 + (F_j - 1)\left(\frac{I - 1}{I_I - 1}\right) \tag{97}$$

Substitution of Equations 85, 91, and 97 into Equation 84 yields the final result of Astarita and Savage (1982)

$$I = \frac{[A]_i/[A]_o - \prod\limits_j F_j^{-v_j}}{[A]_i/[A]_o - 1} \; \frac{I_F\left(\prod\limits_j F_j^{q_j}\right)^{1/2}}{\tanh\left[I_F\left(\prod\limits_j F_j^{q_j}\right)^{1/2}\right]}$$

$$- \frac{1 - \prod\limits_j F_j^{-v_j}}{[A]_i/[A]_o - 1} \; \frac{I_F\left(\prod\limits_j F_j^{q_j}\right)^{1/2}}{\sinh\left[I_F\left(\prod\limits_j F_j^{q_j}\right)^{1/2}\right]} \tag{98}$$

Equation 98 applies for both absorption and stripping, and it degenerates into the proper asymptotes of the fast and instantaneous reaction regimes (Astarita and Savage, 1982).

Savage et al. (1980) also extended this methodology to the absorption and stripping of CO_2 with hot carbonate solutions. Letting

$OH^- = B_1$

$CO_3^= = B_2$

$HCO_3^- = B_3$

then from Equation 73

$$\begin{aligned} q_1 &= 1 \\ q_2 &= 0 \\ q_3 &= 0 \end{aligned}$$

and from the reaction of Equation 1

$$\begin{aligned} \nu_1 &= 0 \\ \nu_2 &= 1 \\ \nu_3 &= -2 \end{aligned}$$

Equation 98 then becomes

$$I = \frac{[CO_2]_i/[CO_2]_o - F_3^2/F_2}{[CO_2]_i/[CO_2]_o - 1} \frac{I_F(F_1)^{1/2}}{\tanh\left(I_F(F_1)^{1/2}\right)}$$

$$- \frac{1 - F_3^2/F_2}{[CO_2]_i/[CO_2]_o - 1} \frac{I_F(F_1)^{1/2}}{\sinh\left(I_F(F_1)^{1/2}\right)} \qquad (99)$$

Recalling that

$$F_1 = \frac{F_2}{F_3}$$

Savage et al. (1980) showed that

$$I = \frac{[CO_2]_i/[CO_2]_o - F_3^2/F_2}{[CO_2]_i/[CO_2]_o - 1} \frac{I_F(F_2/F_3)^{1/2}}{\tanh\left(I_F(F_2/F_3)^{1/2}\right)}$$

$$- \frac{1 - F_3^2/F_2}{[CO_2]_i/[CO_2]_o - 1} \frac{I_F(F_2/F_3)^{1/2}}{\sinh\left(I_F(F_2/F_3)^{1/2}\right)} \qquad (100)$$

where

$$F_2 = 1 + (F_2^* - 1)\left(\frac{I - 1}{I_I - 1}\right)$$

$$F_2^* = \frac{1}{1 - y} - F_3^*\left(\frac{y}{1 - y}\right)$$

$$F_3 = 1 + (F_3^* - 1)\left(\frac{I - 1}{I_I - 1}\right)$$

$$F_3^* = \frac{\left([CO_2]_i/[CO_2]_o\right)y}{2(y - 1)}\left[\left(1 + \frac{4(1 - y)}{\left([CO_2]_i/[CO_2]_o\right)y^2}\right)^{1/2} - 1\right]$$

I_F is given by Equation 78 and I_I by Equation 58. Equation 100 is valid for absorption and stripping (Savage et al., 1980).

As noted by Joshi (1980), Equation 100 is implicit in I and requires a complex trial-and-error procedure to calculate the value of I. Hence, an approximate explicit expression for the enhancement factor may be desirable, even at the expense of accuracy. Using the method of DeCoursey (1974), I may be expressed as an explicit function of I_F and I_I.

$$I = -\frac{I_F^2}{2(I_I - 1)} + \left(\frac{I_F^4}{4(I_I - 1)2} + \frac{I_I I_F^2}{I_I - 1} + 1\right)^{1/2} \qquad (101)$$

To generalize this equation, an expression was developed by Joshi (1980) that approaches the proper asymptotes, and has an adjustable parameter, n. This expression is

$$I = \left[\left(1 + \frac{n^{\frac{n}{n-1}} X^{\frac{1}{n-1}} (X + 1)}{Q^{\frac{n}{2(n-1)}}} \right)^{1/n} + 1 \right] \left(\frac{Q^{\frac{n}{2(n-1)}}}{(nX)^{\frac{1}{n-1}}} \right) \qquad (102)$$

where $Q = 1 + I_F^2$ and $X = I_I - 1$. Comparing the closeness of fit between Equations 100 and 102, Joshi found a value of n equal to 3 gave a maximum error of 12%. Writing Equation 102 with $n = 3$

$$I = \left[1 + \left(\frac{5.2(X + 1)X^{0.5}}{Q^{0.75}} \right)^{0.5} - 1 \right] \left(\frac{Q^{1.5}}{3X} \right)^{0.5} \qquad (103)$$

The previous discussion has been limited to the absorption of a single gas. The simultaneous absorption of two gases with reaction has been examined numerically by Goettler and Pigford (1971) and Ramachandran and Sharma (1971). The case where one gas reacts instantaneously has been considered by Cornelisee et al. (1977), Hikita et al. (1979) and Barreto and Farina (1982). Barreto and Farina (1982) have developed a series of approximations for the enhancement factors for the absorption of two gases where one reacts instantaneously based on a numerical solution of the film theory equations.

There are, however, two problems associated with the use of these numerical solutions in a simulation program for a packed absorber or stripping column. The first is that the solutions contain a quantity that cannot be specified by theory alone. In the solution by Barreto and Farina (1982) for example the quantity is the film thickness. The second problem is that, based on published information, no algorithm for the design or simulation of a packed column with multicomponent mass transfer with chemical reaction has been developed.

PROMOTION OF MASS TRANSFER IN CARBONATE SOLUTIONS

The relatively slow rate of absorption of CO_2 in carbonate solutions has led to the development of additives referred to as rate promoters. All proprietary hot potassium carbonate processes employ a rate prompter (Say et al., 1985). A large number of substances have been shown to increase the rate of CO_2 absorption in potassium and sodium carbonate solutions. These include formaldehyde, methanol, phenol, ethanolamines (Killeffer, 1937), arsenious acid (Roughton and Booth, 1938), glycine (Jeffreys and Bull, 1964) and the enzyme carbonic anhydrase (Alper et al., 1980). The rate promoters used most often in industrial applications are arsenious acid and diethanolamine.

Astarita et al. (1981) have reviewed the rate promotion of CO_2 mass transfer in carbonate solutions and discussed the various mechanisms suggested to explain the effects of additives. These mechanisms may be divided into two categories: those dealing with surface phenomena and those concerning chemical effects.

Killeffer (1937) proposed that the addition of an amine reduces the surface tension of the solution and thus increases interfacial area. Jeffreys and Bull (1964) concluded that when glycine is used, glycinate ions accumulate at the surface of the liquid and catalyze the absorption by reacting with CO_2 at the interface. As noted by Astarita et al. (1981), the results of Jeffreys and Bull (1964) cannot be easily explained by a mechanism other than a surface phenomena. If the additive has one hydrophobic end and one hydrophylic end, it can locate at the gas-liquid interface; if the hydrophobic end is then the reactive site, this reaction may diminish the hydrophobic nature of the additive, and allow the additive-CO_2 intermediate to diffuse into the bulk of the liquid (Astarita et al., 1981).

Mechanisms involving the effects of chemical reaction on absorption were first proposed by Roughton and Booth (1938). In their work, the effect of arsenious acid on CO_2 mass transfer rates was interpreted as that of a homogeneous catalyst, that increased the rate of the primary reaction of CO_2:

$$CO_2 + OH^- \rightarrow HCO_3^- \tag{104}$$

The mechanism by which amines promote this step has been interpreted in terms of a complex mass-transfer-with-reaction mechanism (Shier and Danckwerts, 1969).

Astarita et al. (1981) have analyzed the promotion of CO_2 mass transfer using arsenious acid and amines, and developed a general mechanism for inorganic and organic promoters. From this theory, the mechanism may be written as

$$\begin{gathered} CO_2 + \text{PROMOTER} \rightarrow \text{INTERMEDIATE} \\ \text{INTERMEDIATE} + OH^- \rightarrow HCO_3^- + \text{PROMOTER} \end{gathered} \tag{105}$$

The difference between the homogeneous catalyst mechanism and the complex mass-transfer-with-reaction mechanism, referred to as the "shuttle" mechanism, is related to the relative rate of the second step in Equation 105.

In the case of arsenious acid, the reactions of Equations 105 become

$$CO_2 + H_2AsO_3^- \rightarrow \text{INTERMEDIATE} \tag{106}$$

$$\text{INTERMEDIATE} + OH^- \rightarrow HCO_3^- + H_2AsO_3^- \tag{107}$$

where Equation 107 actually represents a sequence of steps whose rate is much faster than that of Equation 106. Thus the reaction of Equation 107 may be considered as taking place immediately following the reaction of Equation 106 at the gas-liquid interface (Astarita et al., 1981).

With the amine rate promoter, the reactions of Equations 105 become

$$CO_2 + RR'NH \rightarrow RR'NCOOH \tag{108}$$

$$RR'NCOOH + OH^- \rightarrow HCO_3^- + RR'NH \tag{109}$$

While the reaction of Equation 108 is believed to take place at the gas-liquid interface, the reaction of Equation 109 is believed to take place significantly only in the bulk of the liquid. Diffusion of free amine back to the interface to again react with CO_2 must take place for the sequence to be completed (Astarita et al., 1981).

Since desorption is carried out at higher temperatures than absorption, and the rate of the reaction of Equation 109 increases with increasing temperature, an additive such as an amine that acts through a shuttle mechanism in absorption may act as a homogeneous catalyst in desorption. An additive that acts through the shuttle mechanism in desorption, however, would not result in significant promotion at the lower temperatures of absorption (Astarita et al., 1981).

A simulation program for an acid gas removal system using a hot potassium carbonate solution with a rate promoter must account for two effects of the rate promoter: the effect of the additive on the vapor-liquid equilibrium behavior of the system and its effect on the rates of absorption and desorption. The following discussion describes the two effects.

The thermodynamics of promoted carbonate solutions is considerably more complex than that of unpromoted solutions. In general, acid promoters tend to decrease the capacity of the solution for CO_2 slightly, while alkaline promoters such as amines tend to increase capacity slightly (Astarita et al., 1983). Amines that are used most commonly, such as diethanolamine, have no significant effect on the vapor-liquid equilibrium of CO_2 in K_2CO_3 solutions. This is thought to be due to the formation of stable carbamates with CO_2.

$$CO_2 + 2RR'NH \rightarrow RR'NCOO^- + RR'NH_2 \tag{110}$$

which tie up the amine in an essentially unreactive form (Say, 1984). However, amines act as a sink for CO_2 and slightly increase the capacity of the solution at high values of y, the degree of saturation of CO_2 (Astarita et al., 1983). The effect of an amine rate promoter on the equilibrium of H_2S has not been determined.

The effect of a rate promoter on the rate of absorption and desorption of CO_2 may be expressed by introducing a parameter referred to as the rate-promotion factor, E, into the mass transfer expression for the liquid phase. Expressing the flux of A in the liquid phase in an unpromoted solution as

$$N = Ik_L \left([A]_i - [A]_o \right) \tag{111}$$

the flux of A in a promoted solution becomes

$$N = EIk_L \left([A]_i - [A]_o \right) \tag{112}$$

where E is defined as

$$E = \frac{I\ (promoted)}{I\ (unpromoted)} \tag{113}$$

A theoretical expression for E corresponding to a given reaction kinetic regime, may be developed from the fluid dynamic models of the gas-liquid interface and the asymptotic solutions to the enhancement factor (Say et al., 1985).

In the case of an amine promoter, the maximum possible effect on mass transfer from the shuttle mechanism is obtained by considering the amine-CO_2 reaction to be instantaneous and irreversible at the interface. The resulting expression is given by Astarita et al. (1981) as

$$E = \left[1 + \frac{[Am]^2 k_L^2}{Dk[CO_2]_i^2} \right]^{0.5} \tag{114}$$

Rate promotion effects observed at high temperatures (>>100°C) are, however, larger than can be predicted by Equation 114 and thus larger than that possible via the shuttle mechanism (Astarita et al., 1983). It thus seems that at high temperatures, the rate of the reaction of Equation 109 becomes large enough so that it may take place near the interface. At such conditions, the amine may be a homogeneous catalyst whose effect is to speed up the rate of the reaction of CO_2 and $CO_3^=$ so that this reaction may be considered instantaneous (Astarita et al., 1983). If this is the case, the flux of CO_2 in the liquid phase may be expressed as

$$N = I_I k_L \left([CO_2]_i - [CO_2]_o \right) \tag{115}$$

with I_I given by Equation 58.

MODELING OF PACKED COLUMNS WITH CHEMICAL SOLVENTS

In absorption and stripping calculations, the degrees of freedom available are not sufficient to specify all variables in one of the exit streams, even after the feed streams are specified. Thus, the state of neither end of the column is known completely (von Stockar and Wilke, 1977). This often presents extremely difficult convergence problems, and sophisticated computational methods have been developed for the case of physical absorption (von Stockar and Wilke, 1977; Feintuch and Treybal, 1978; Srivastava and Joseph, 1984).

As noted previously, a procedure for the design or simulation of a packed column for multicomponent mass transfer with chemical reaction has not been published. In fact, expressions based on mass transfer rates for the design or simulation of packed towers for absorption and desorption of a single component with chemical solvents have been conspicuously absent from standard texts on mass transfer and separation operations such as those by Sherwood et al. (1975), King (1980), and Treybal (1980).

Pandya (1983) has suggested a method by which the complex procedure of Feintuch and Treybal (1978) may be applied to the absorption of a single component with chemical reaction. This method, however, becomes very complex in accounting for all heat effects; such complexity seems unwarrented for use with the hot potassium carbonate process since heat effects with this system are small. Alternatively, a complex simulation program for dynamic gas absorption and regeneration with chemical solvents has been developed by Systems Science and Software (Alexander, 1982). Due, however, to the proprietary nature of the licensing of this program, detailed information on this work is not available.

Danckwerts (1970) proposed a method where two coupled differential equations for the rate of absorption with reaction of a single component in a packed column could be developed and then integrated over the column. In the approach the rate of absorption was recognized to be equal to the difference between the liquid flows of A into and out of a packing section of height *dz* plus the rate of reaction of A with B in the packing section.

$$\text{Rate of Absorption} = \text{Change in Flow of Unreacted A in Liquid} + \text{Rate of Reaction of A with B}$$

or

$$N_A a dz = L dx_A + l r_A dz \tag{116}$$

As B is non-volatile,

$$\text{Rate of Reaction of B} = -\text{ Decrease in Flow Rate of Unreacted B}$$

or

$$z l r_B dz = -L dx_B \tag{117}$$

where l is the liquid hold-up per unit volume of packing, a is the interfacial area per unit volume of packing, and r_A and r_B are the rates of reaction of A and B in moles per unit volume of liquid. Except in special cases, the two differential equations can be solved only by double stepwise numerical integration (Danckwerts, 1970).

There is difficulty in using this method, however, if the gas-side resistance to mass transfer is significant. Since the rate of absorption of A is dependent on the interfacial mole fraction x_{Ai}

$$N_A a = Ik_L a(x_{Ai} - x_A) \tag{118}$$

the value of x_{Ai} must be known. Expressing the rate of absorption of A in terms of gas-phase mole fractions

$$N_A a = k_G a P(y_A - y_{Ai}) \tag{119}$$

$$Py_{Ai} = Hx_{Ai} \tag{120}$$

an expression for y_{Ai} may be obtained as

$$y_{Ai} = \frac{Py_A}{H} - \frac{N_A}{k_G aH} = \frac{Py_A}{H} - \frac{Ik_L a(x_{Ai} - x_A)}{k_G aH} \tag{121}$$

Equations 119 and 121 may then be used with Equations 116 and 117.

A single rate equation for the absorption and stripping of a single component with chemical reaction was introduced by Joshi (1980). This expression, which is similar to the HTU/NTU approach for physical absorption, has been shown to give good agreement when compared with published pilot plant data (Joshi et al., 1981). To derive the rate equation, first consider a differential element of packing of height dz over which the gas stream composition changes by an amount dy. From a steady-state material balance for the solute (component A)

$$\text{Rate of Change in Gas Flow of Solute} = \text{Rate of Solute Transfer} \tag{122}$$

$$-d(Gy_A) = N_A a dz$$

$$-Gdy_A - y_A dG = N_A a dz$$

If only one component (component A) is transferred, then

$$dG = -N_A a dz \tag{123}$$

and Equation 122 becomes

$$dz = \frac{-G dy_A}{(1 - y_A) N_A a} \tag{124}$$

Letting

$$G' = G(1 - y_A) \tag{125}$$

Equation 124 becomes

$$dz = \frac{-G' dy_A}{(1 - y_A)^2 N_A a} \tag{126}$$

Expressing the flux of A in terms of the overall gas-phase mass transfer coefficient

$$N_A = K_{oG}^{*} P(y_A - y_A^{*}) \tag{127}$$

where K_{oG}^{*} is the overall mass transfer coefficient based on the gas-side driving force, and including the effect of chemical reaction on the rate of absorption of A. y_A^{*} is the gas-phase mole fraction of the solute that would be in equilibrium with the bulk liquid mole fraction x_A. Defining R as

$$R = \frac{K_{oG}^{*}}{K_{oG}} \tag{128}$$

where K_{oG} is the overall mass transfer coefficient based on the gas-side driving force without reaction. The flux may be expressed as

$$N_A = R K_{oG} P(y_A - y_A^{*}) \tag{129}$$

Use of Equation 129 requires development of an expression for R.

For physical absorption, $K_{oG} a$ can be expressed as

$$K_{oG}a = \frac{1}{\dfrac{1}{k_G a} + \dfrac{H}{k_L a}} \tag{130}$$

A similar expression for K^*_{oG} may be developed.

$$K^*_{oG} = \frac{1}{\dfrac{1}{k_G} + \dfrac{H}{Ik_L}} \tag{131}$$

From Equations 128 and 130

$$R = \frac{1 + \dfrac{k_G H}{k_L}}{1 + \dfrac{k_G H}{Ik_L}} = \frac{1 + M}{1 + M/I} \tag{132}$$

where

$$M = \frac{k_G H}{k_L} \tag{132a}$$

Since K^*_{oG} can now be expressed in terms of R and K_{oG}, Equation 129 may be substituted into Equation 126 to yield

$$dz = \frac{-G'}{K_{oG}aP} \frac{dy_A}{(1 - y_A)^2(y_A - y^*_A)\dfrac{1 + M}{1 + M/I}} \tag{133}$$

Evaluating $K_{oG}a$ (Equation 130), M (Equation132a) and y^*_A from an equilibrium relationship, Equation 152 can be integrated numerically using an appropriate expression for I. Equation 133 may be used as a design equation for the height of packing to yield a specified separation or as a simulation equation to predict the separation from a specified packing height.

FACILITY DESCRIPTION

The pilot plant facility used in this study consisted of two major subsystems: a fluidized-bed gasifier with a raw gas cleaning system, and an acid gas removal system. In the raw gas cleaning system, gas from the gasifier passes through a hot cyclone separator where of most of the particulate matter is removed and a Venturi scrubber where the gas is quenched by direct contact with water for removal of remaining particulates, condensables and water-solubles. This system is referred to as the Gasifier-PCS system. In the acid gas removal system (AGRS), the gas is contacted with a solvent (a hot potassium carbonate solution in the study reported on here) that absorbs the carbon dioxide, hydrogen sulfide, and other soluble components. The solvent is then regenerated and returned to the absorber. Each system can be operated independently or the entire plant can be operated as an integrated unit.

A schematic diagram of the gasifier-PCS system is given in Figure 4, and the acid gas removal system in the configuration used for the potassium carbonate solvent is shown in Figure 5.

In the operation of the gasifier, crushed coal was fed to the gasifier from the feed hopper, while steam and oxygen were fed to the bottom of the reactor to form a fluidized bed. The gasifier was operated at about 790 kPa absolute (100 psig) and temperatures ranging from 870 to 1040°C. The gas from the gasifier was passed through the cyclone to remove most of the entrained particulate matter and was then quenched, cooled, and filtered before leaving the PCS system.

After leaving the PCS system, the gas was dried in a molecular sieve dehydrating tower, compressed to about 3550 kPa absolute (500 psig), cooled to approximately 15°C, and fed to the absorber.

Gas entering the AGRS from the Gasifier-PCS subsystem (or a synthetic gas mixture) was fed to the packed absorption column. Flowing counter-currently to this gas stream in the absorber was the K_2CO_3 solvent which absorbed the acid gases from the coal gas. The solvent and absorbed acid gases are fed to the regeneration units while a clean product gas leaves the absorber top. Absorber operating pressure in this study ranged from 1700 kPa to 3100 kPa. The absorber operating temperature varied depending on heat exchange equipment in the system and the stripper operating temperature.

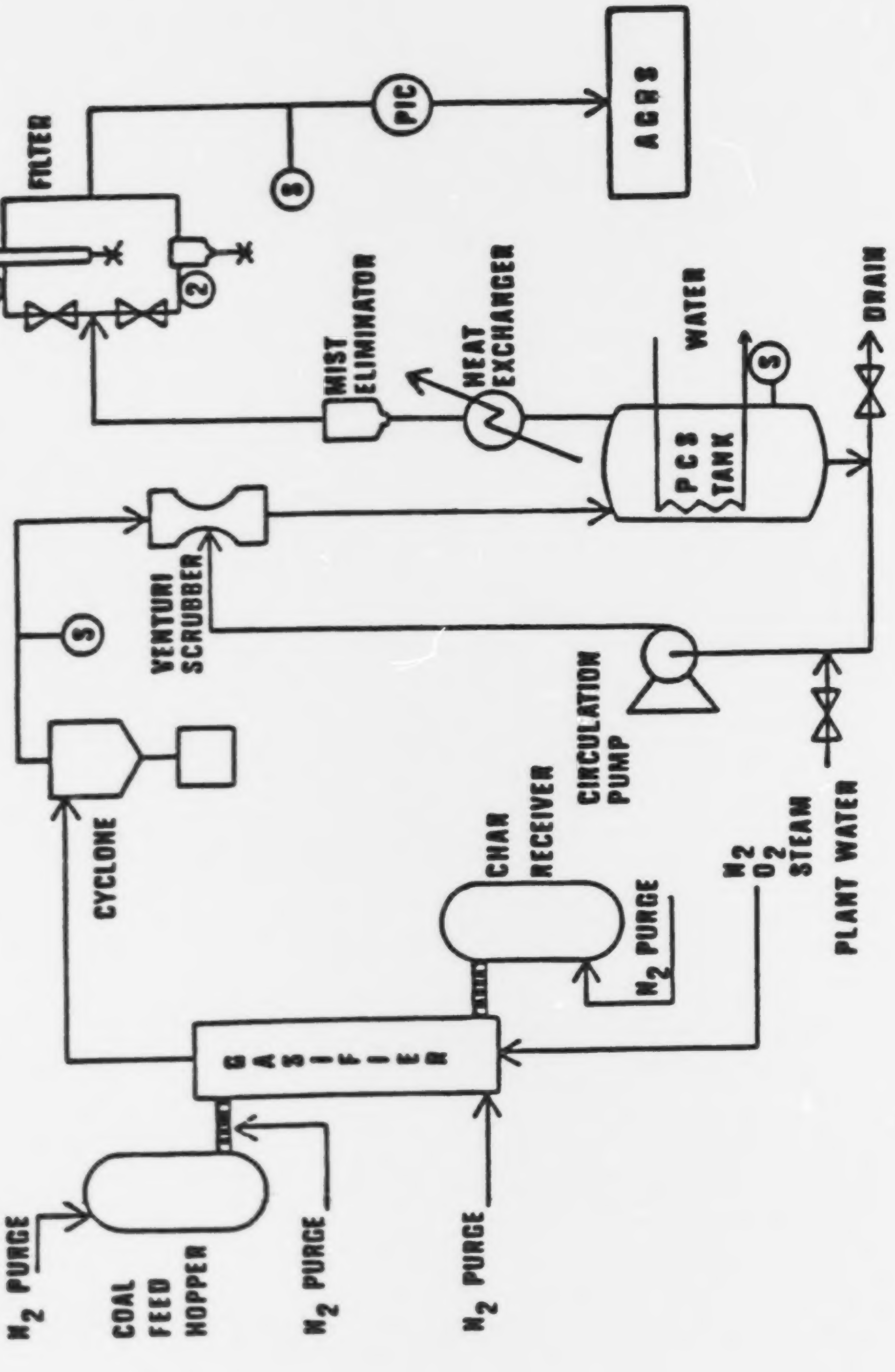
N_2 PURGE
COAL FEED HOPPER
N_2 PURGE
N_2 PURGE
GASIFIER
CHAR RECEIVER
N_2 PURGE
N_2
O_2
STEAM
PLANT WATER
CYCLONE
CIRCULATION PUMP
S
VENTURI SCRUBBER
PCS TANK
WATER
S
DRAIN
MIST ELIMINATOR
HEAT EXCHANGER
FILTER
1
2
S
PIC
AGRS

Figure 4 Gasifier/PCS System

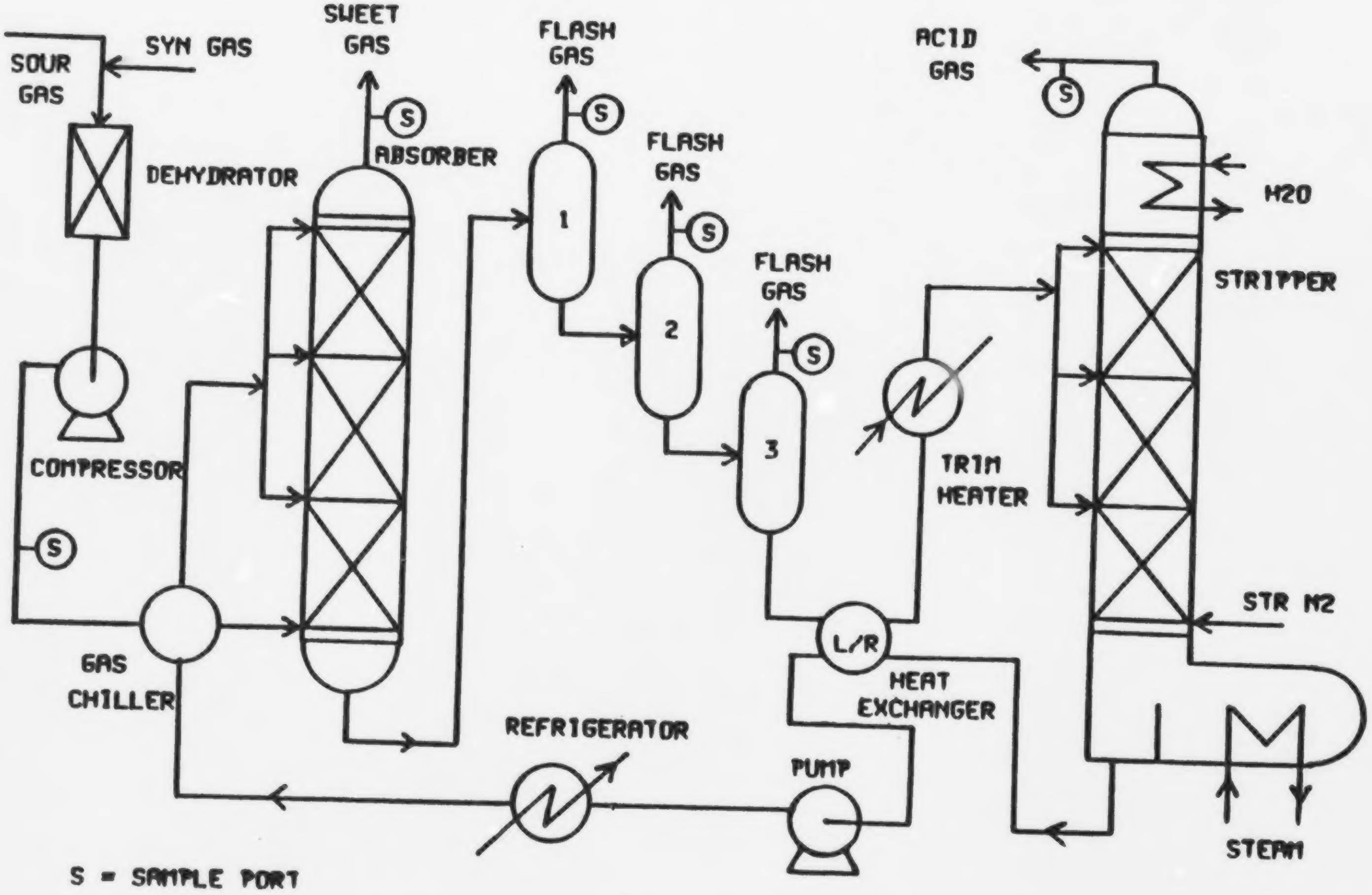
SOUR GAS
SYN GAS
DEHYDRATOR
COMPRESSOR
S
GAS CHILLER
SWEET GAS
S
ABSORBER
FLASH GAS
S
1
FLASH GAS
S
2
FLASH GAS
S
3
REFRIGERATOR
PUMP
L/R
HEAT EXCHANGER
TRIM HEATER
ACID GAS
S
H2O
STRIPPER
STR N2
STEAM
S = SAMPLE PORT

Figure 5 Acid Gas Removal System

During regeneration, the solvent and absorbed acid gases leaving the absorber are fed to a flash tank where the pressure is reduced to about 500 kPa. The resulting liquid stream is then fed to the packed stripping column, operated typically at 130 kPa. Flowing counter-currently to the solvent in the stripping column is steam produced by boiling the solvent in the reboiler. The acid gases are more soluble in the pure steam phase than in the solvent and are hence stripped from the solvent. The resulting clean K_2CO_3 solution is then returned to the absorber while the stripper exit gas and the gas from the absorber and the flash tank are sent to a flare.

The absorber and stripper columns consisted of three sections of packing, each of which contained 2.2 m of 0.0064-m (0.25-in) ceramic Intalox saddles. One, two or three sections of packing could be used in either the absorber or stripper. Each section of packing contained two redistributers of liquid flow to prevent channeling. The columns, flash tanks and all pipes were insulated so that heat absorbed from the surroundings was negligible.

Details of the instrumentation and process control of the facility are presented by Ferrell et al. (1980) and Willis (1981). The process is controlled with a Honeywell TDC 2000 process control computer that regulates 16 process control loops. Approximately 100 process sensors monitor temperatures, pressures, flow rates, and levels throughout the plant through a data acquisition system linked to a Digital PDP 11/23 computer.

EXPERIMENTAL RESULTS AND DISCUSSION

Procedures for start-up and operation of the pilot plant facility are given by Ferrell et al. (1980) and by Kelly (1981). Operation of the gasifier and the AGRS are started at the same time, and usually require approximately six hours for steady-state operation. For this study, steady state was defined as a period of operation during which measured process variables, such as flow rates, temperatures, pressures, and gas compositions, were constant. Once a steady-state condition had been reached, operation was continued for two to three hours while operating variables were recorded and samples of key streams were taken. During this steady-state period, measured values of all process variables were averaged over five minute intervals and stored by the data acquisition system.

Gas and liquid samples were taken periodically throughout a run from locations noted on Figures 4 and 5. Gas samples were taken in one-liter stainless steel or glass bombs; those used for analysis of trace components were taken in bombs internally coated with Teflon. A complete discussion of sampling and analysis is given in the quality assurance section of this report.

The closure of mass balances on the major components in the gas was used to evaluate the accuracy of measured flow rates and compositions for each run. Values used in testing closure were obtained by averaging the measured variables over a period of time (typically one hour) preceding the time at which steady-state samples were taken. If the overall mass balance closure was not within 5%, data associated with that sample period were not used in evaluating the operation. It should be noted that a few of the components included in sample analyses were present in such small amounts that slight errors could lead to mass balance closures that did not meet the criterion. In such cases, judgement was used to decide if the data on these components were to be used. Table 4 shows a typical data set of stream compositions and the calculated mass balance closure for one of the runs used in this study. Complete mass balance results and all gas analysis data for the runs of this study are given by Staton (1985).

TABLE 4
ANALYSES AND MASS BALANCES FOR TEST RUN ACIL-23

	Stream Composition (mol %)			
	Sour Gas	Sweet Gas	Flash Gas	Acid Gas
CO_2	27.490	24.340	80.720	90.000
H_2S	0.188	0.098	1.185	3.553
COS	0.003	0.003	0.007	0.005
H_2O	0.000	0.000	0.000	0.000
H_2	37.670	38.750	8.180	0.000
CO	11.130	11.580	2.410	0.000
N_2	19.650	20.030	7.580	5.990
CH_4	4.380	4.470	1.920	0.340
C_2H_4	0.218	0.221	0.236	0.044
C_2H_6	0.335	0.351	0.144	0.008

	Mass Balance (mol/h)						
	In	Out					
	Sour Gas	Sweet Gas	Flash Gas	Acid Gas	Total In	Total Out	Percent Recovery
CO_2	205.041	180.008	7.544	7.987	205.041	195.539	95.37
H_2S	1.405	0.722	0.111	0.315	1.405	1.148	81.69
COS	0.022	0.021	0.001	0.000	0.022	0.023	101.04
H_2O	0.000	0.000	0.000	0.000	0.000	0.000	0.00
H_2	280.972	286.578	0.764	0.000	280.972	287.343	102.27
CO	83.016	85.641	0.225	0.000	83.016	85.866	103.43
N_2	146.565	148.133	0.708	0.532	146.565	149.373	101.92
CH_4	32.669	33.058	0.179	0.030	32.669	33.268	101.83
C_2H_4	1.628	1.631	0.022	0.004	1.628	1.657	101.75
C_2H_6	2.498	2.598	0.013	0.001	2.498	2.612	104.57
TOTAL	745.88	739.56	9.35	8.87	753.82	756.83	100.4

Table 5 gives a listing of the AGRS operating conditions for the runs of this study, and Table 6 shows a summary of the CO_2, H_2S, and COS analyses in the sour gas (the AGRS feed gas) and sweet gas streams for each run. As can be seen, the composition of the sour gas varied significantly, making interpretation of results somewhat difficult. Table 7 shows the percentage removals of CO_2, H_2S, and COS for the runs with complete gas analyses.

The following sections present a brief description of the objectives and results for each run.

ACIL-23

The solvent used in this run was pure water. In this and several following runs, the liquid entering the absorber was cooled so that the absorber and flash tank operated at low temperatures (Table 5) to minimize the amount of water in gas samples taken from the absorber and flash tank exit streams. (Excess water in these samples would have interfered with the analyses.) At a later date, condensors were installed on these streams, and the heat exchanger between the reboiler and absorber was bypassed. Under the conditions of this run, the removal of the acid gas species was quite low.

ACIL-24

This was the first run using a 10% solution of potassium carbonate as the AGRS solvent. The absorber and flash tank were again operated at low temperatures. As can be seen in Table 6, no H_2S was detected in the sweet gas for this run, corresponding to 100% removal; however, only 56.7% of the CO_2 was absorbed. Thus, at low temperatures and at low concentrations of K_2CO_3, considerable selectivity can be obtained in the absorption of H_2S. Only 22.7% of the COS was removed, however.

ACIL-25

In this run, the conditions of Run ACIL-24 were repeated, except the absorber pressure was reduced from 3082 kPa to 1703 kPa (Table 5). As can be seen in Table 6, H_2S removal decreased only slightly to 97.9% while CO_2 removal decreased to 38.1%. Hence, an even greater selective absorption of H_2S was obtained at this absorber pressure. The removal of COS was changed only slightly by the reduction in absorber pressure.

TABLE 5
ACID GAS REMOVAL SYSTEM OPERATING CONDITIONS

Run Number Date	ACIL-23 7/14/83	ACIL-24 7/26/83	ACIL-25 8/11/83	ACIL-26 8/30/83	ACIL-27 9/13/83
Solvent Composition %					
Water	100	90	90	90	90
K_2CO_3	0	10	10	10	10
Diethanolamine	0	0	0	0	0
Solvent Circulation Rate (L/min)	3.3	3.3	3.3	3.3	3.3
Absorber					
Pressure (kPa)	3095	3082	1703	2400	1474
Packing Height (m)	4.33	4.33	4.33	4.33	2.16
Sour Gas Flow (mol/h)	746	762	830	800	666
Liquid Inlet Temp (C)	33	34	35	35	34
Gas Inlet Temp (C)	40	41	42	40	41
Flash Tank					
Pressure (kPa)	515	496	496	1000	613
Liquid Inlet Temp (C)	32	35	36	35	34
Stripper					
Pressure (kPa)	131	131	131	131	134
Packing Height (m)	4.33	4.33	4.33	4.33	4.33
Liquid Inlet Temp (C)	33	37	37	37	35
Steam Flow (kg/h)	13.6	13.1	12.5	13.0	14.5
Steam Temp (C)	174	173	174	174	175

TABLE 5 (CONTINUED)
ACID GAS REMOVAL SYSTEM OPERATING CONDITIONS

Run Number	ACIL-28	ACIL-29	ACIL-30	ACIL-31	ACIL-32
Date	10/13/83	11/15/83	12/1/84	1/10/84	2/8/84
Solvent Composition %					
Water	90	80	80	80	80
K_2CO_3	10	20	20	20	20
Diethanolamine	0	0	0	0	0
Solvent Circulation Rate (L/min)	3.3	3.3	3.3	3.3	3.3
Absorber					
Pressure (kPa)	3083	1790	1785	1782	3156
Packing Height (m)	4.33	2.16	4.33	2.16	2.16
Sour Gas Flow (mol/h)	767	798	780	748	799
Liquid Inlet Temp (C)	27	102	100	117	102
Gas Inlet Temp (C)	37	19	20	17	14
Flash Tank					
Pressure (kPa)	498	533	577	570	572
Liquid Inlet Temp (C)	30	94	91	103	94
Stripper					
Pressure (kPa)	131	134	134	238	134
Packing Height (m)	4.33	4.33	4.33	4.33	4.33
Liquid Inlet Temp (C)	31	96	93	105	96
Steam Flow (kg/h)	17.7	17.6	17.3	21.8	16.0
Steam Temp (C)	173	172	172	172	171

TABLE 5 (CONTINUED)
ACID GAS REMOVAL SYSTEM OPERATING CONDITIONS

Run Number Date	ACIL-33 2/22/84	ACIL-35 3/21/84	ACIL-36 4/4/84	ACIL-38 5/3/84	ACIN-1 5/16/84
Solvent Composition %					
Water	80	70	70	70	65
K_2CO_3	20	30	30	30	30
Diethanolamine	0	0	0	0	5
Solvent Circulation Rate (L/min)	3.3	3.3	2.91	2.91	3.3
Absorber					
Pressure (kPa)	1785	1780	3158	3152	1776
Packing Height (m)	2.16	2.16	2.16	2.16	2.16
Sour Gas Flow (mol/h)	760	743	659	686	759
Liquid Inlet Temp (C)	116	104	100	100	104
Gas Inlet Temp (C)	19	20	22	25	24
Flash Tank					
Pressure (kPa)	578	505	509	571	570
Liquid Inlet Temp (C)	106	97	94	92	97
Stripper					
Pressure (kPa)	134	134	135	134	135
Packing Height (m)	4.33	4.33	4.33	4.33	4.33
Liquid Inlet Temp (C)	102	94	89	88	93
Steam Flow (kg/h)	19.6	23.1	14.3	16.0	16.4
Steam Temp (C)	172	173	173	171	172

TABLE 5 (CONTINUED)
ACID GAS REMOVAL SYSTEM OPERATING CONDITIONS

Run Number Date	ACIN-2 5/30/84	ACIN-3 6/13/84	ACIN-5 6/27/84	ACIN-6 7/12/84	ACIN-7 7/24/84
Solvent Composition %					
Water	65	65	65	80	80
K_2CO_3	30	30	30	20	30
Diethanolamine	5	5	5	0	0
Solvent Circulation Rate (L/min)	3.3	5.5	3.3	3.3	3.3
Absorber					
Pressure (kPa)	1774	1773	1772	1763	1763
Packing Height (m)	2.16	2.16	2.16	2.16	2.16
Sour Gas Flow (mol/h)	725	699	739	730	736
Liquid Inlet Temp (C)	105	110	93	101	105
Gas Inlet Temp (C)	24	30	30	32	30
Flash Tank					
Pressure (kPa)	567	567	565	553	556
Liquid Inlet Temp (C)	96	102	88	94	97
Stripper					
Pressure (kPa)	148	154	134	134	134
Packing Height (m)	6.49	4.33	4.33	4.33	4.33
Liquid Inlet Temp (C)	92	101	86	89	93
Steam Flow (kg/h)	17.4	24.2	*	30.2	32.2
Steam Temp (C)	172	173		172	172

* Str N_2 flow = 270 mol/h
Str N_2 temperature = 26°C

TABLE 5 (CONTINUED)
ACID GAS REMOVAL SYSTEM OPERATING CONDITIONS

Run Number Date	ACIN-8 8/14/84	ACIN-9 8/29/84
Solvent Composition %		
Water	80	75
K_2CO_3	20	20
Diethanolamine	0	5
Solvent Circulation Rate (L/min)	2.91	2.91
Absorber		
Pressure (kPa)	1761	1754
Packing Height (m)	2.16	2.16
Sour Gas Flow (mol/h)	681	674
Liquid Inlet Temp (C)	103	101
Gas Inlet Temp (C)	30	29
Flash Tank		
Pressure (kPa)	555	549
Liquid Inlet Temp (C)	94	95
Stripper		
Pressure (kPa)	134	133
Packing Height (m)	4.33	4.33
Liquid Inlet Temp (C)	91	91
Steam Flow (kg/h)	28.9	15.9
Steam Temp (C)	172	173

TABLE 6
SUMMARY OF SOUR AND SWEET GAS COMPOSITIONS (MOLE %)

Run No	Sour Gas CO_2	Sour Gas H_2S	Sour Gas COS	Sweet Gas CO_2	Sweet Gas H_2S	Sweet Gas COS
ACIL-23	27.5	0.188	0.0030	24.3	0.098	0.0029
ACIL-24	28.4	0.196	0.0057	13.9	ND	0.0049
ACIL-25	29.5	0.242	0.0029	20.3	0.0056	0.0027
ACIL-26	28.5	-	-	17.0	-	-
ACIL-27	25.5	0.250	0.0056	18.2	0.0078	0.0050
ACIL-28	25.4	0.401	0.0064	10.3	ND	0.0047
ACIL-29	23.4	0.276	0.0099	2.49	0.0036	0.0021
ACIL-30	27.9	0.271	0.0053	9.36	0.0039	0.0013
ACIL-31	24.8	0.178	0.0086	0.76	0.0016	0.0010
ACIL-32	20.7	0.176	0.0116	0.40	ND	0.0014
ACIL-33	28.4	0.203	0.0034	2.57	0.0022	0.0011
ACIL-35	29.8	0.161	0.0029	2.12	0.0019	0.0011
ACIL-36	29.4	0.165	0.0132	1.39	0.0006	0.0034
ACIL-38	29.6	0.226	0.0051	0.73	0.0016	-
ACIN-1	24.3	0.280	0.0111	0.52	0.0018	0.0012
ACIN-2	24.6	0.312	0.0156	0.53	0.0007	0.0022
ACIN-3	23.0	0.223	0.0153	0.63	0.0014	0.0015
ACIN-5	24.3	0.264	0.0117	9.02	0.0070	0.0096
ACIN-6	23.8	0.199	0.0118	2.81	0.0008	0.0039
ACIN-7	23.6	0.191	0.0104	0.50	ND	0.0018
ACIN-8	25.1	0.263	0.0117	1.19	0.0007	0.0028
ACIN-9	23.6	0.279	0.0132	0.25	0.0010	0.0007

ND = none detected < 5 ppm for H_2S

TABLE 7
REMOVAL OF CO_2, H_2S AND COS

Run	CO_2	H_2S	COS
		% Removed	
ACIL-23	12.2	48.6	4.5
ACIL-24	56.7	100	22.7
ACIL-25	38.1	97.9	20.0
ACIL-27	40.0	97.3	24.3
ACIL-28	67.8	100	39.6
ACIL-29	91.4	98.7	81.5
ACIL-30	73.6	98.8	64.7
ACIL-31	97.8	99.0	92.2
ACIL-32	98.4	100	90.3
ACIL-33	93.3	99.1	76.9
ACIL-35	94.8	99.2	72.7
ACIL-36	96.5	99.7	80.5
ACIL-38	98.2	99.5	-
ACIN-1	98.4	99.5	91.7
ACIN-2	98.4	99.8	89.4
ACIN-3	97.8	99.5	92.5
ACIN-5	70.2	97.9	35.6
ACIN-6	90.8	99.7	74.4
ACIN-7	98.4	100	87.0
ACIN-8	96.4	99.8	81.3
ACIN-9	99.2	99.7	95.8

ACIL-26

This run was made to provide information on the operation of the stripping column for a parallel study. Although complete gas analyses were not performed for this run, periodic samples of the sweet gas were taken and partial analyses completed. The results are shown in Figure 6. The percentages of the major species in the sweet gas were approximately constant, including that of CO_2, even though the steam flow to the reboiler was varied significantly. At these conditions, the concentrations of these species in the sweet gas were insensitive to the range of regeneration conditions employed. Such behavior indicates that the absorption of the acid gases was controlled by equilibrium with the solvent at the bottom of the absorber.

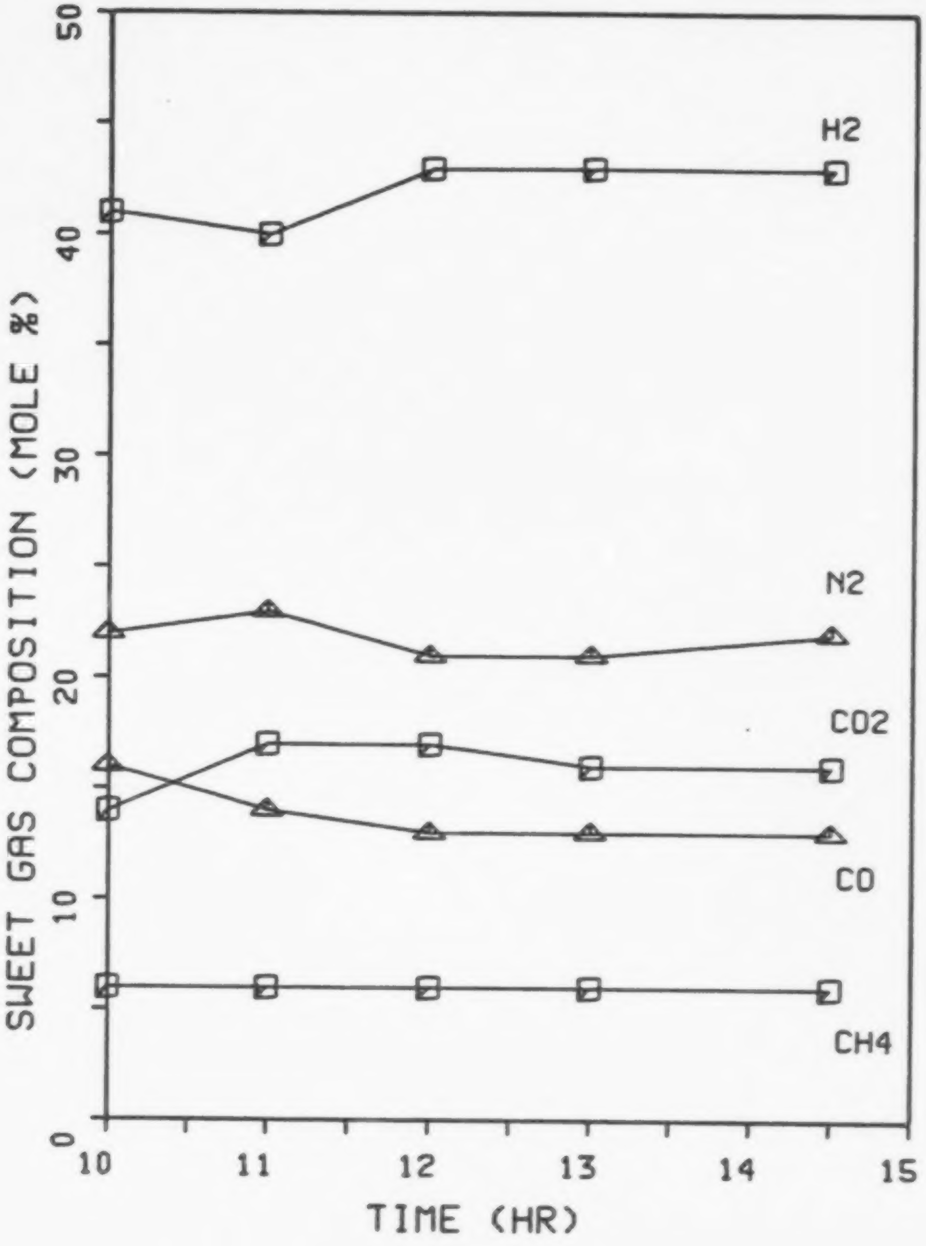

Figure 6 Sweet Gas Analyses for Run ACIL-26

ACIL-27

In this run, two system variables were examined. First, the reboiler was operated with a much lower steam flow rate than in previous runs (Table 5). The flow rate of the steam to the reboiler was sufficient to heat the solvent to its boiling point, but it was insufficient to boil up a detectable amount of water vapor into the stripper packing. Periodic sweet gas samples were taken, and analyzed for sulfur gases during this run. The results are given in Figure 7 which shows that the H_2S content of the sweet gas was increasing significantly during the entire run. It can be concluded that operating the reboiler in this manner does not adequately strip H_2S from the solvent. This is supported by the low H_2S recovery (approximately 32%) in the mass balance for this run.

The CO_2 content of the sweet gas for samples taken at times 13:00 and 14:00 were essentially the same. Also, CO_2 removal in this run was essentially the same as in Run ACIL-25 which was operated with normal reboiler boilup. Thus it seems operation of the reboiler without boilup did not significantly affect the removal of CO_2 using the AGRS conditions of this run and a 10% K_2CO_3 solution.

The second variable examined in this run was the packing height in the absorber. At time 13:00, the height of packing in the absorber was changed to 4.33 m (2 sections of packing) from 2.16 m (1 section). As can be seen in Figure 7, this had no noticable effect on the COS content of the sweet gas or on the rate of increase of H_2S in the sweet gas. As mentioned previously, CO_2 contents of the sweet gas taken during operation with one and two sections of packing in the absorber were essentially the same. It would then appear that with the 10% solution of K_2CO_3 as the AGRS solvent and one section of packing in the absorber, the absorber column was operating in a near equilibrium condition.

ACIL-28

Several variables were also examined in this run. First, this run repeated the conditions of Run ACIL-24 (the first run using 10% K_2CO_3) to determine if the solvent had experienced a loss of activity through irreversible interactions with the coal gas. As shown in Table 7, 100% of the H_2S was removed in this and Run ACIL-24. CO_2 and H_2S removals, however, increased slightly. It would thus seem that no loss of activity was experienced.

Also examined in this run was the effect of absorber temperature on sweet gas

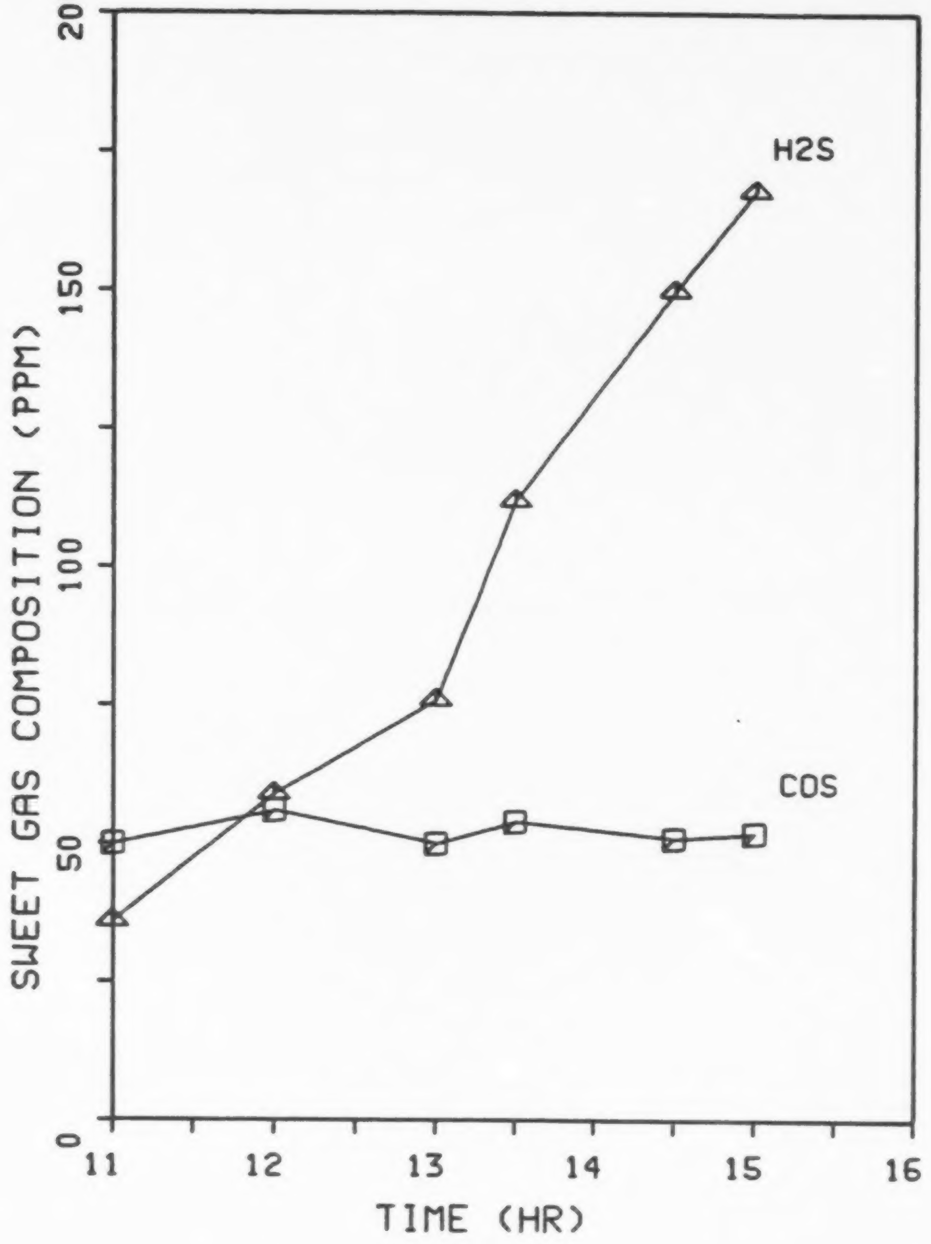

Figure 7 Sweet Gas Analyses for Run ACIL-27

composition. The temperature of the liquid stream entering the absorber was increased suddenly by by-passing the heat exchanger between the reboiler and absorber. The composition of the sweet gas was determined from periodic samples taken as this temperature changed. The increase in absorber temperature resulted in a slight increase in the CO_2 content of the sweet gas. This suggests that at these conditions, the absorption of CO_2 was controlled by equilibrium between the gas and liquid phases at some point in the column.

ACIL-29

This run was the first that used a 20% solution of K_2CO_3 as the AGRS solvent. The absorber was operated at the same pressure as in Run ACIL-25. The heat exchanger between the reboiler and absorber was not used in this and all following runs, so that the absorber operated at a higher temperature (approximately 100°C) than in previous runs (approximately 35°C). As shown in Table 7, CO_2 removal increased significantly from that of Run ACIL-25 to 91.4% while H_2S removal increased slightly to 98.7%. COS removal increased to 81.5%.

ACIL-30

In this run, the conditions of Run ACIL-29 were repeated, except that the height of packing in the absorber was 4.33 m instead of 2.16 m. As shown in Table 7, CO_2 removal dropped to 73.6% while H_2S removal was unchanged. Also, COS removal dropped to 64.7%. This decrease in the percentages of CO_2 and COS removed can be attributed to a large change in the CO_2 content of the sour gas stream. As can be seen in Table 6, sour gas in Run ACIL-29 contained 23.4% CO_2. while it was 27.9% in Run ACIL-30. Since additional packing in the absorber did not improve separation, it would appear that at these conditions the absorber column was operating in what is referred to as a pinched condition; that is, the solvent and gas are in equilibrium at some point in the column and additional packing has no effect on the CO_2 removal.

ACIL-31

In this run, the conditions of Run ACIL-29 were repeated except that the stripper was operated at a higher pressure (238 kPa) than in Run ACIL-29 (134 kPa). Although an increase in stripper pressure should decrease regeneration, it also causes an increase in the reboiler operating temperature (Table 5) by increasing the boiling point of the solvent. As shown in Table 7, CO_2 removal increased to 97.8% from 91.4% while that for H_2S remained at approximately 99%. COS removal increased to 92.2%. It is not clear, however, if this improved performance was primarily the result of an improvement in regeneration or absorption, since the temperature of the absorber for this run was also higher than that for Run ACIL-29 (Table 5).

ACIL-32

In this run, the AGRS was operated using a 20% solution of K_2CO_3 with the absorber operated at high pressure, as in Run ACIL-24. As shown in Table 7, CO_2 removal increased from that of Run ACIL-24 (56.7%) to 98.4%. As in Run ACIL-24, 100% of the H_2S was removed. COS removal in this run was 90.3%, consideribly higher than in Run ACIL-24 (22.7%).

ACIL-33

In this run, the absorber was operated at the same temperature as in Run ACIL-31; however, the stripper was operated at the reference pressure of 133 kPa to determine if the increased performance obtained in Run ACIL-31 was primarily a result of a change in regeneration or in absorption. As shown in Table 7, CO_2 removal was 93.3%, which is between that of Runs ACIL-29 (91.4%) and ACIL-31 (97.8%). H_2S removal was 99.1% and the percentage removal of COS was 76.9%, which is below that of Runs ACIL-29 (81.5%) and ACIL-31 (92.2%). As shown in Table 6, the composition of the sour gas in these three runs was significantly different and this may have affected the removals. The results for this run, however, correspond more closely to Run ACIL-29, suggesting the increased performance seen in Run ACIL-31 may be due primarily to an increase in the regeneration efficiency at the higher stripper operating temperature.

ACIL-35

This run was the first using a 30% solution of K_2CO_3 as the AGRS solvent. Although the conditions were the same as in run ACIL-29, the system operating temperature was slightly higher due to the higher boiling point of the 30% solution (Table 5). As shown in Table 7, CO_2 removal was 94.8%, higher than in Run ACIL-29 (91.4%). H_2S removal increased to 99.2% and the percentage removal of COS decreased slightly from that of Run ACIL-29 to 72.7%. It is possible that COS removal decreased because the physical solubility of COS in the solution was less at the higher K_2CO_3 concentration.

ACIL-36

In this run, a 30% solution of K_2CO_3 was used and the conditions were the same as in Run ACIL-35 except the absorber was operated at the higher pressure as in Run ACIL-32 (Table 5). As shown in Table 7, CO_2 removal was 97%, down slightly from that of run ACIL-32. The removal of H_2S was 99.7%. This was the first run at the higher absorber pressure where H_2S was detected in the sweet gas and hence the percentage removal was less than 100%. Since there was only 6 ppm H_2S in the sweet gas (Table 6), and the lower detection limit for H_2S is 5 ppm, the removal of H_2S is considered approximately the same as in the other runs at this high absorber pressure but with 10 and 20% K_2CO_3 solutions. As shown in Table 7, COS removal was 80.5 %.

ACIL-38

This run repeated the conditions of Run ACIL-36 to provide information on the reproducibility of the experimental data. As shown in Table 7, CO_2 recovery was 98.2%, compared to 96.5% in Run ACIL-36. H_2S recovery was 99.5%, compared to 99.7% in ACIL-36. No COS was detected in the sweet gas for this run. This result was, however, thought to be due to an error in sampling or analysis since COS was present in the sweet gas in all other runs of this study. The removals for CO_2 and H_2S agree well with those of Run ACIL-36 and indicate good reproducibility.

ACIN-1

The solvent used in this run was a solution of 30% K_2CO_3 and 5 weight percent diethanolamine (DEA). The conditions repeated those of Run ACIL-35 (Table 5) to provide information on the effect of an amine additive on AGRS performance when treating coal gas. Previous experimental results using one and two sections of packing in the absorber had indicated that the absorber was operating in what is referred to as a pinched condition. Consequently, any increase in the rate of absorption of CO_2 due to the amine would not be observed. As shown in Table 7, CO_2 removal was 98.4%, H_2S removal was 99.5% and COS removal was 91.7%. There appears to be a slight increase in the removals of CO_2 and COS over that in Run ACIL-35, suggesting that the amine has a small effect on the equilibrium of CO_2

ACIN-2

This run repeats the conditions of ACIL-29 except that 3 sections of packing were used in the stripping column rather than 2 sections (Table 5). As can be seen in Table 7, the removal of CO_2 increased to 98.4% from 91.4% in ACIL-29. H_2S removal was approxiately constant while COS removal increased from 81.5% to 89.4%. Since the composition of the sour gas in these two runs was approximately the same, these data suggest that providing the additional packing in the stripping column increased the removals of CO_2 and COS.

ACIN-3

In Run ACIN-3 the conditions of Run ACIL-29 were repeated except that a higher solvent circulation rate and a lower sour gas feed rate were used to provide a higher liquid-to-gas ratio in the absorber. The flow rate of steam to the reboiler was also increased over that of Run ACIL-29 (Table 5) in an attempt to keep regeneration conditions constant. As can be seen in Table 7, CO_2 removal was 97.8%, compared to 91.4% for ACIL-29. H_2S removal increased slightly from 98.7% to 99.5% and COS removal increased from 81.5% to 92.5%. These increases are, however, small compared to the increase in the absorber liquid-to-gas ratio (90 percent).

ACIN-5

In this run, stripping was accomplished with an inert gas stream (N_2) rather than with reboiled water vapor. The reboiler was operated with a small flow rate of steam to the heating coils to maintain the system at an elevated temperature, but at a steam flow rate smaller than that required to generate a detectable vapor stream in the packing. As can be seen in Table 7, CO_2 removal was 70.2%, H_2S removal was 97.9% and COS removal 35.5%. Although the removal of H_2S was much higher than that for CO_2 and COS, examination of the H_2S content of the sweet gas stream (Table 6) shows that H_2S removal was far from what is generally considered acceptable.

ACIN-6

In Run ACIN-6, the conditions of Run ACIL-29 were repeated, except that a higher reboiler steam flow rate was used (Table 5). As can be seen in Table 7, CO_2 removal was 90.8%, compared to 91.5% in Run ACIL-29. H_2S removal increased from 98.7% in ACIL-29 to 99.7% and COS removal decreased from 81.5% to 74.4%. As shown in Table 6, the concentrations of these species in the sour gas stream in these two runs were approximately constant. It is not clear why the removal of CO_2 and COS decreased from that in Run ACIL-29.

ACIN-7

In this run the conditions of Run ACIN-6 were repeated. As can be seen in Table 7, the removal of CO_2 was 98.4%, H_2S removal was 100% and COS removal was 87.0%. These values are significantly higher than for Run ACIL-29 and ACIN-6, suggesting that the higher reboiler steam flow rate did give improved regeneration. It is believed that the lower removals in Run ACIN-6 were a result of the poor regeneration obtained in the previous run (ACIN-5) when the stripping column was operated with an inert gas (i.e., the system had not reached steady-state with respect to regeneration of the solvent.)

ACIN-8

In Run ACIN-8, the conditions of Run ACIN-7 were repeated except that the total solvent inventory was boiled for approximately 3 hours in the reboiler before startup. This was done to provide information on whether the steady-state AGRS operation was independent of the regeneration history of the solvent at startup. As can be seen in Table 7, the removal of CO_2 was 96.4%, of H_2S 99.8% and of COS, 81.3%. These removals are slightly lower than those of Run ACIN-7. This is thought to be due to the higher concentrations of these species in the sour gas for this run. These, results suggest that the steady-state AGRS performance is not dependent on the solvent regeneration history at start-up.

ACIN-9

In Run ACIN-9 the conditions of Run ACIL-29 were repeated with a 20% K_2CO_3 and 5% DEA solution as the AGRS solvent. This was to provide additional information on the effect of the addition of an amine additive on system performance. As in the case with a 30% K_2CO_3 solution, percentage removals of CO_2 H_2S and COS increased slightly over that of Run ACIL-29 (Table 7).

Figure 8 shows the percentage of the inlet CO_2 that was removed as a function of K_2CO_3 concentration for runs at two absorber pressures. As shown, the absorber pressure appeared to have a large effect on CO_2 removal at low concentrations of K_2CO_3. At both pressures tested, CO_2 removal was not increased significantly as the K_2CO_3 concentration was increased from 20% to 30%. H_2S removal was independent of K_2CO_3 concentration at the high absorber pressure and increased only slightly with K_2CO_3 concentration at the lower absorber pressure (Figure 9). The percentage removal of COS, shown in Figure 10, increased with absorber pressure but decreased as the concentration of K_2CO_3 was increased from 20% to 30%, at both pressures tested.

Selectivity, which is defined as the moles of H_2S absorbed per mole of CO_2 absorbed, is shown in Figure 11 as a function of K_2CO_3 concentration at both absorber pressures tested. As shown, the selectivity decreased with increasing K_2CO_3 concentration and increasing pressure; however, there appeared to be no change with absorber pressure using the 30% solution of K_2CO_3.

The previous results illustrate the complex nature of absorption and regeneration with chemical solvents. For example, changing process variables may results in an increase in the rate and driving force of a chemical reaction while resulting in a

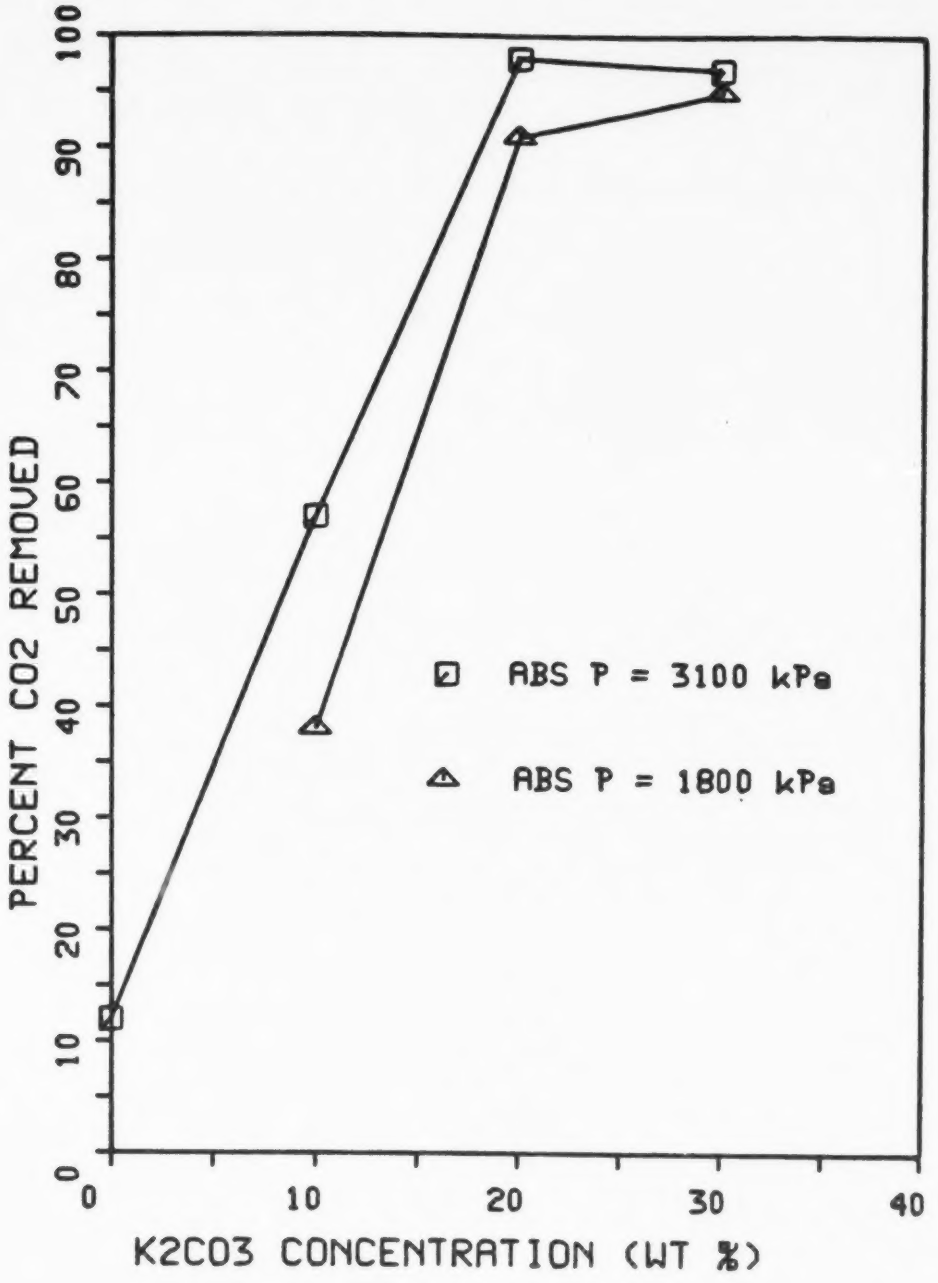

Figure 8 Experimental CO2 Removal

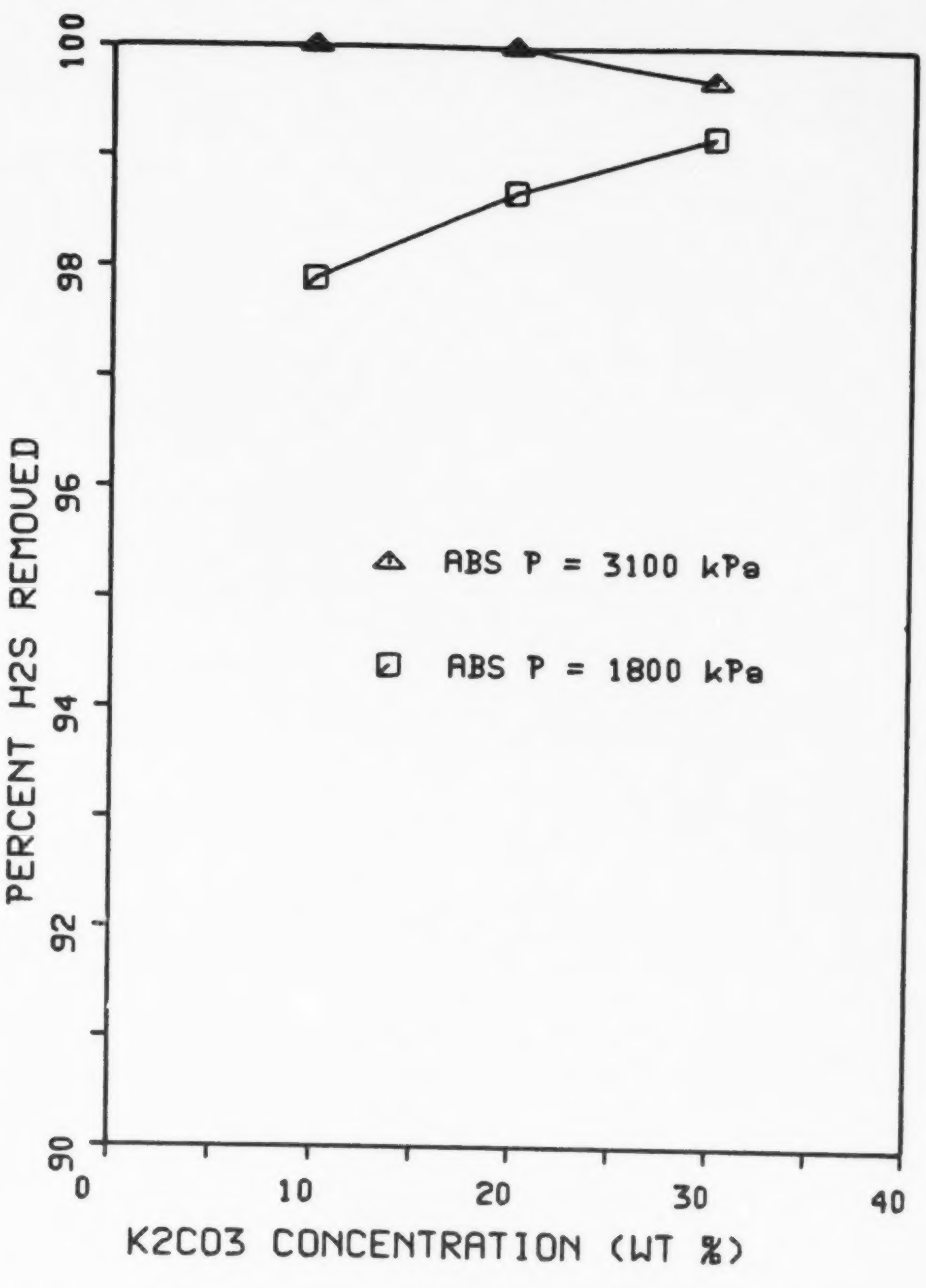

Figure 9 Experimental H2S Removal

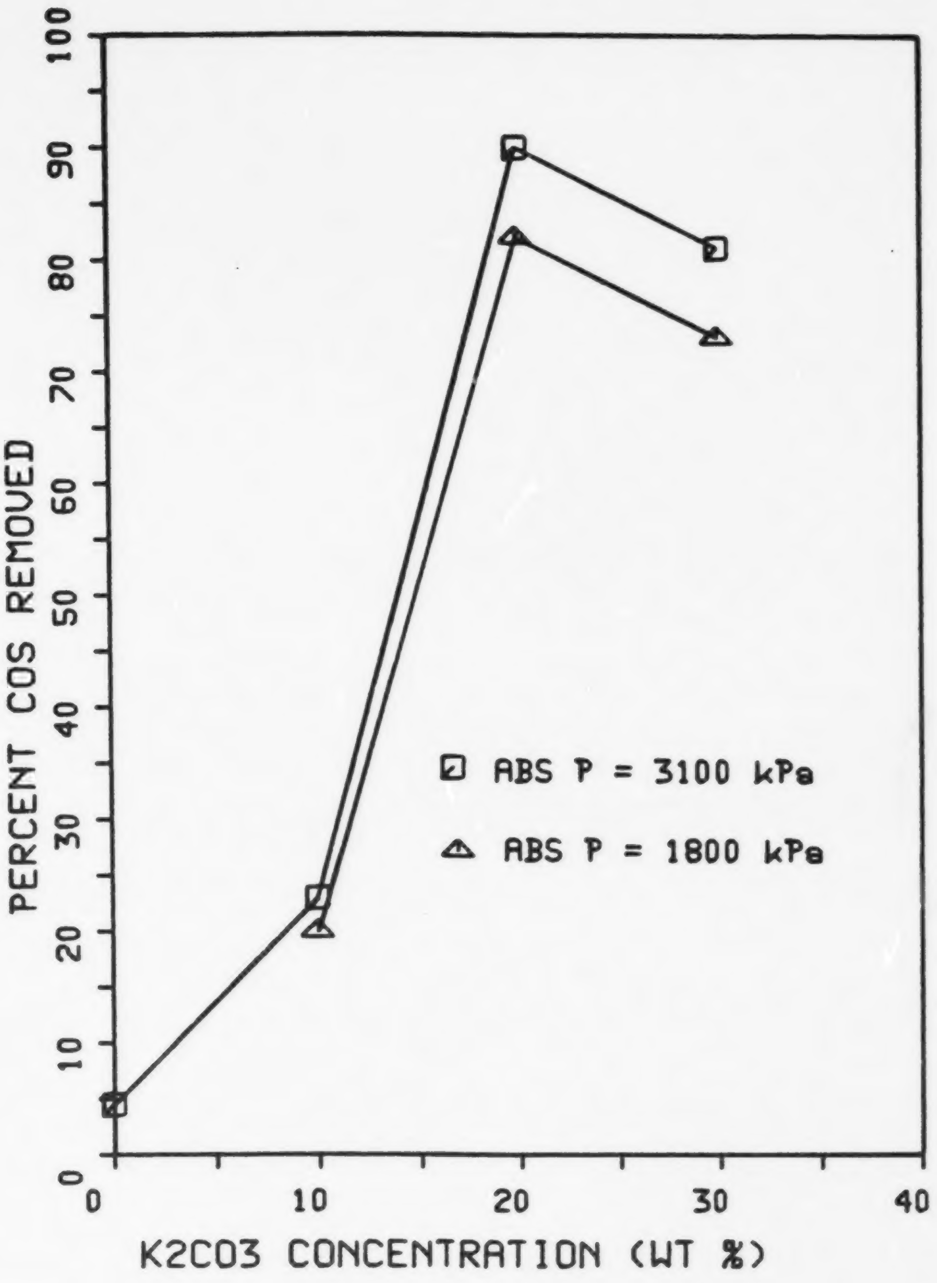

Figure 10 Experimental COS Removal

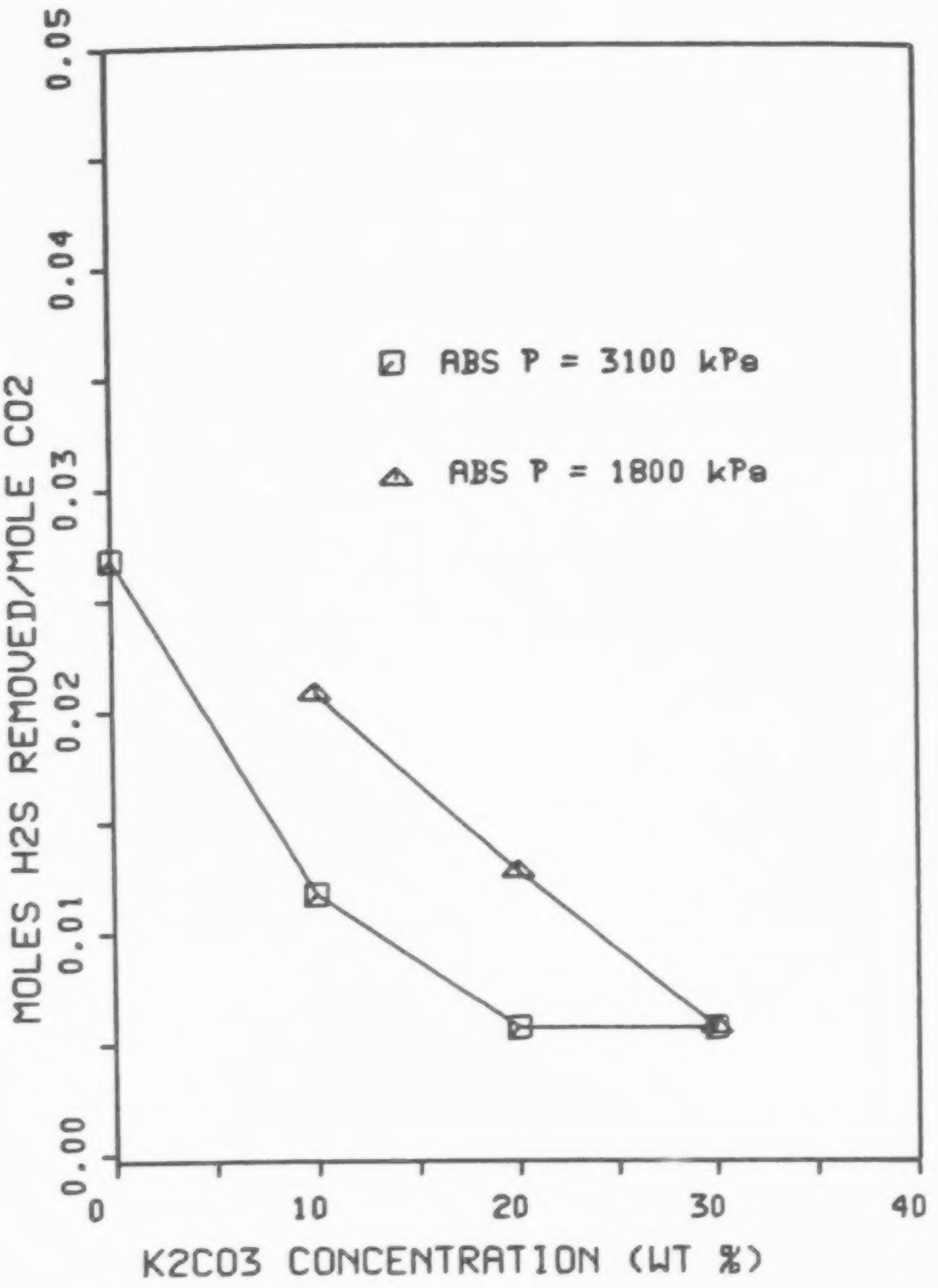

Figure 11 Experimental Selectivity

decrease in the physical solubility of gases in the solvent. These results support the need for an accurate process model to allow a better understanding of AGRS operation.

DEVELOPMENT OF SIMULATION MODEL

The model to be described here was developed to provide a better understanding of the hot potassium carbonate process, and to give a method for extension of pilot plant results to industrial situations. As noted previously, a rigorous procedure for the design or simulation of packed columns with multicomponent mass transfer accompanied by chemical reaction has not been published. Even in the case of absorption without reaction, extremely difficult convergence problems are often encountered since a complete description of neither the top nor the bottom of the column is usually known. In this section, the development of a simulation scheme for multicomponent absorption and stripping with chemical reaction will be presented. This simulation scheme avoids complex convergence problems through the formulation of a simplified model based on an examination of pilot plant experimental results, and information available in the literature.

Gas and liquid components are classified as follows:

1. The key reactive component is CO_2.
2. The non-key reactive components are H_2S and COS.
3. The inert gases are H_2, CO, N_2, CH_4, C_2H_4, and C_2H_6.
4. The volatile component of the solvent is H_2O.
5. The non-volatile solutes are $CO_3^{=}$ and HCO_3^{-}.

The model is based on the following simplifying assumptions:

1. Heat effects are negligible.
2. The absorption of inert components is controlled by equilibrium between the gas and liquid phases at the bottom of the absorber. All inerts are desorbed in stripping.
3. Non-key reactive components have no effect on the mass transfer rate of the key component.

4. Non-key reactive components whose reaction rates are greater than that of the key, for example H_2S, are assumed to be in equilibrium in the liquid phase. The absorption and stripping of these components are assumed controlled by equilibrium between the gas and liquid phases at the top of the absorber and stripper columns.
5. The absorption of COS, which reacts through hydrolysis only, is assumed to be a function of absorber temperature only. It is assumed that the reaction of COS is irreversible.
6. The volumetric flow rates of solvent through the absorber and stripper are constant.

The assumption of negligible heat effects may be considered valid since the heat of reaction of CO_2 in this solvent is relatively small (Bocard and Mayland, 1962), and the heat capacity of water is large. Pilot plant results in the present study and by others (Field et al., 1960) confirm that absorption, flashing, and stripping operations may be considered isothermal. For example, in Run ACIL-30 of this study, the solvent entered the absorber at 100°C and exited at 97°C. The temperature of the solvent entering the flash tank was 91°C and that of the liquid in the flash tank, 93°C (This apparent increase in temperature as a result of flashing may be attributed to conduction in the thermocouple that measured the temperature of the solvent prior to the flash tank liquid entrance.) The temperature throughout the stripping column corresponded to the solvent boiling point.

The second condition, which concerns the absorption of inert components, is based on the limited solubility of these components in K_2CO_3 solutions at the high absorber temperatures used in this process. Consider the plot of gas-phase mole fraction versus liquid-phase mole fraction in Figure 12. The slope of the equilibrium line is constant for slightly soluble gases and it is the ratio of the Henry's law constant to the pressure; the slope of the operating line for absorption is related to the ratio of liquid to gas flow rates. If the slope of the equilibrium line is greater than that of the operating line, then it is clear from Figure 12 that intersection of these two will occur at the top of the diagram, which corresponds to the bottom of the absorber. A large slope of the equilibrium line occurs when a component has a large Henry's law constant or a low solubility in the liquid.

The solubilities of the inert coal gas species (components that do not participate in a reaction with the solvent) are extremely small at the high absorber temperatures. Hence, on a diagram such as Figure 12, their equilibrium relationships approximate vertical lines. In this case, for any realistic liquid-to-gas ratio, an intersection between the equilibrium lines and operating lines will occur at the top of the diagram, representing an equilibrium or pinched condition at the bottom of the absorber.

If the composition of the liquid is expressed in terms of concentrations, and the

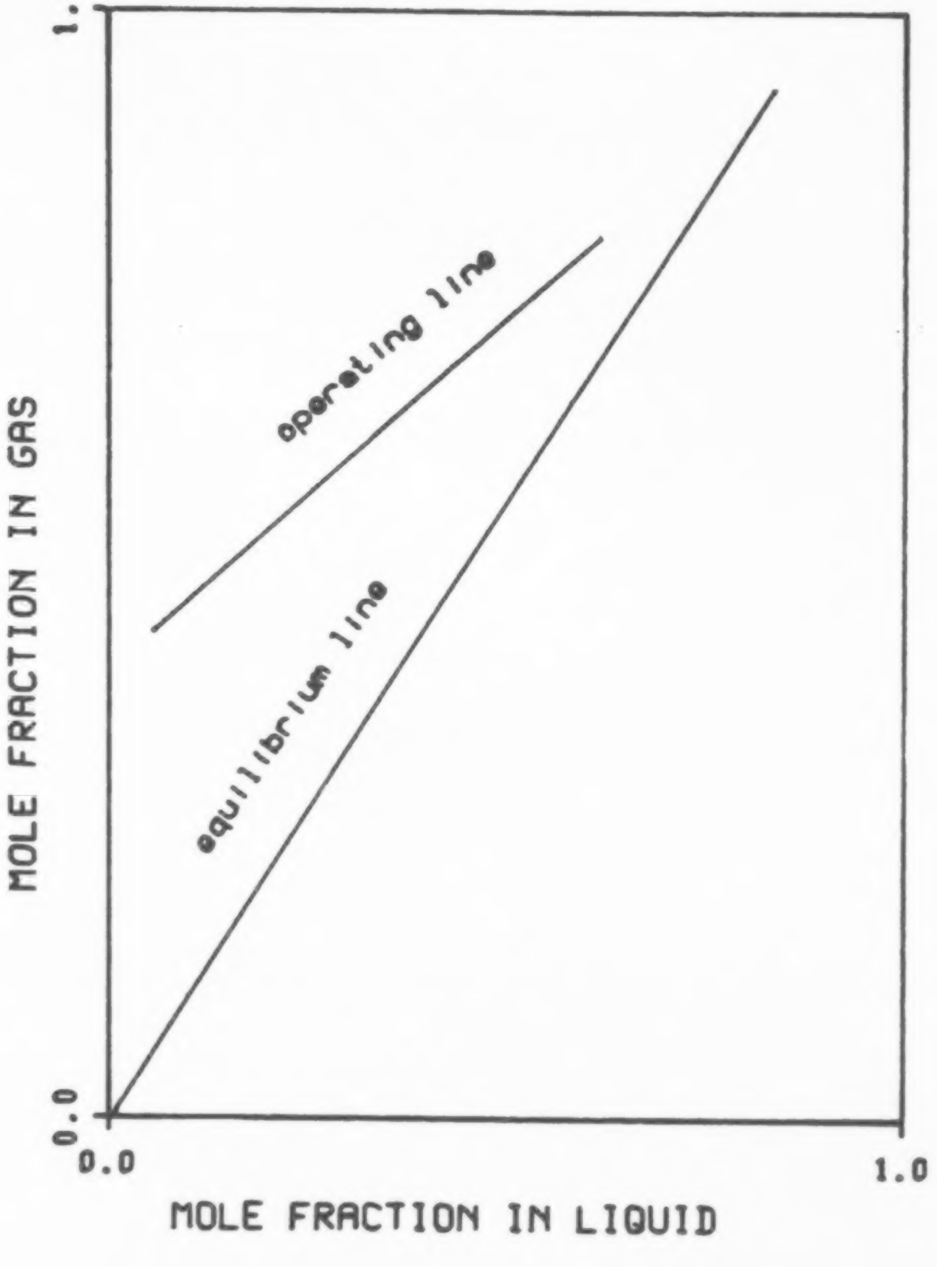

Figure 12 Absorption with Physical Solvents

volumetric flow rate of solvent is constant (Condition 6), then the flow rates of the inert components in the liquid stream leaving the absorber may be calculated from an equilibrium relationship and the composition of the gas entering the absorber. The flow rates of these components in the gas stream leaving the absorber may then be calculated by material balances. In stripping, since the solubilities of the inert species are very small, it may be assumed that for any realistic stripping operation, the concentrations in the reboiler exit liquid are zero.

Although the theory of mass transfer with chemical reaction of a single species is well developed, no rigorous expression is available to yield numerical values for the rates of absorption in the case of the simultaneous absorption with reaction of two gases. In the model developed here, the absorber and stripper algorithms are based on the rates of absorption and stripping of CO_2, referred to as the key component. It is assumed that H_2S has no effect on the mass transfer coefficient of CO_2 (condition 3 above) and that H_2S affects the absorption and stripping of CO_2 only by its effect on the equilibrium behavior of CO_2. This effect was expressed in Equations 40 through 53 for equilibrium compositions in the absorption and stripping algorithms. These equilibrium compositions were used to calculate initial estimates of the composition of the exiting gas stream in the absorption algorithm, the composition of the gas stream entering the packing from the reboiler in the stripping algorithm, and in equilibrium constraints to the absorption and stripping of CO_2.

Including the third condition that non-key reactive components have no effect on the mass transfer coefficient of the key component, allows use of the theory discussed in the development for the mass transfer enhancement factor of CO_2. First, there is an important physical aspect to consider: In a gas produced from coal, the amount of H_2S is always much smaller than the amount of CO_2. In this study, for example, a typical sour gas stream fed to the absorption column contained approximately 0.3 mole percent H_2S and approximately 25 mole percent CO_2. Thus, of the two gases that react with the reactive component of the solvent, the gas with the greater reaction rate is present in much smaller amounts. Second, there are two important points noted by Astarita et al. (1983) concerning simultaneous absorption and stripping of two gases where one reacts instantaneously, as is the case with H_2S. The mass transfer rate enhancement of the gas in the instantaneous regime is not affected by the presence of the other component, in other words CO_2 does not affect the absorption of H_2S. Further, if the component that reacts instantaneously has reached equilibrium in the liquid, then it does not affect the mass transfer rate enhancement of the other component. In other words, H_2S does not affect the enhancement of CO_2.

Condition 4 is that the H_2S is in equilibrium in the liquid phase, and that the absorption and stripping of H_2S is controlled by equilibrium between the gas and liquid phases at some point in the columns. Trial calculations and examination of pilot plant experimental results suggest that these equilibrium conditions between gas and liquid phases occur at the tops of the absorption and stripping columns.

The fifth condition involves COS. This species reacts through hydrolysis only, and does not compete with CO_2 and H_2S for the reactive component of the solvent. Examination of the pilot plant results show that in almost all cases, no COS was detected in the gas streams exiting the flash tank and stripping column. Based on this observation, all absorbed COS was assumed to be converted irreversibly to CO_2 and H_2S.

The rate of COS absorption in hot potassium carbonate solutions has been found to be much slower than that of CO_2 (Parrish and Neilson, 1974). It was noted that the hydrolysis of COS is only slightly dependent on solvent composition, but is highly dependent on temperature (Parrish and Neilson, 1974). Based on this information, the absorption of COS by a given solvent was assumed to be a function of absorber operating temperature only. The absorption of COS is discussed in detail later in this report.

DIFFERENTIAL ELEMENT

For both absorption and stripping, a differential element of packing of height dZ is shown in Figure 13. There are five unknowns associated with each differential element; $(Y_{key})_{n+1}$, y_{n+1}, $[key]_i$, the flux of the key component, and dZ. The following five differential equations may be solved for the five unknowns:

$$\frac{dY_{key}}{dZ} = \frac{-K_{oG}aP}{G'}(Y_{key} - Y^*_{key})(1 - Y_{key})^2 \frac{1 + M}{1 + M/I} \tag{134}$$

$$[key]_i = \frac{[key]_o + \dfrac{k_G P}{k_L I} Y_{key}}{1 + \dfrac{k_G H}{k_L I}} \tag{135}$$

$$dZ = \frac{dY_{key}}{dY_{key}/dZ} \qquad (dY_{key} \text{ is specified}) \tag{136}$$

$$(Y_{key})_{n+1} = (Y_{key})_n + dY_{key} \tag{137}$$

$$y_{n+1} = y_n + \left(\frac{G'}{Lm}\right)\left[\left(\frac{Y_{key}}{1 - Y_{key}}\right)_{n+1} - \left(\frac{Y_{key}}{1 - Y_{key}}\right)_n\right] \tag{138}$$

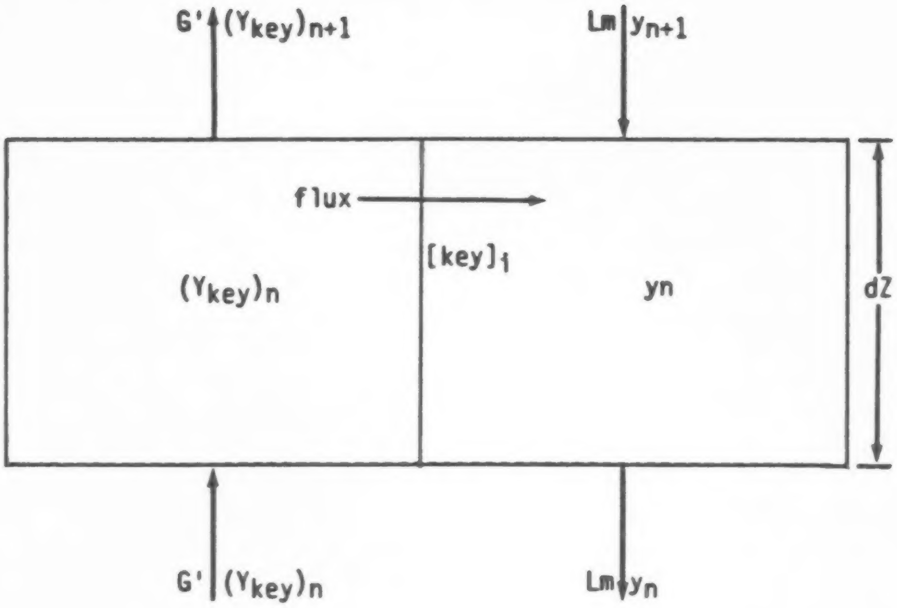
G' $(Y_{key})_{n+1}$
Lm y_{n+1}
flux
$[key]_i$
$(Y_{key})_n$
yn
dZ
G' $(Y_{key})_n$
Lm y_n

unknowns

$(Y_{key})_{n+1}$ y_{n+1} $[key]_i$ flux dZ

Figure 13 Differential Element of Packing

Equation 134 is the differential form of the design equation (Equation 133) introduced by Joshi (1980). Equation 135, which gives the interfacial concentration of the key component, may be derived by assuming that at steady state, the flux in the liquid and gas phases in a given differential element are equal. The change in the gas-phase mole fraction of the key component for each differential element is specified, and this allows the height of that differential element to be calculated from Equation 136. The mole fraction of the key component in the gas stream exiting a differential element may be calculated from Equation 137. Finally, the fractional saturation of the key component in the liquid entering a differential element is calculated by a material balance on the key component shown as Equation 138.

To use the above equations for absorption and stripping calculations, a finite element of height ΔZ is used and dY_{key}/dZ is replaced by $\Delta Y_{key}/\Delta Z$.

ABSORBER MODEL

Flow rates and compositions of the entering liquid and gas streams, and the packing height are specified in calculations to simulate an existing packed column. In design calculations, information on the removal of a certain component is given and packing height is calculated. The absorber calculations used in this model are in the simulation format.

Since the compositions and flow rates of the exiting liquid and gas streams are unknown, the calculations are initiated by estimating the mole fraction of the key component in the exiting gas stream. This estimate is obtained by assuming that the key component is in equilibrium (pinched) at the bottom of the column. The corresponding concentrations of the key component in the exit streams based on this assumption are shown in Figure 14.

To derive an equation for the linear operating line of Figure 14, consider a single plate or a section of packing in absorption or stripping. A material balance on reactive species A may be written as

$$G_{in} Y_{A,in} + L_{in}[A]_{t,in} = G_{out} Y_{A,out} + L_{out}[A]_{t,out} \tag{139}$$

In most chemical solvents, the physical solubilities of reactive solutes are much less than their chemical solubilities. Hence,

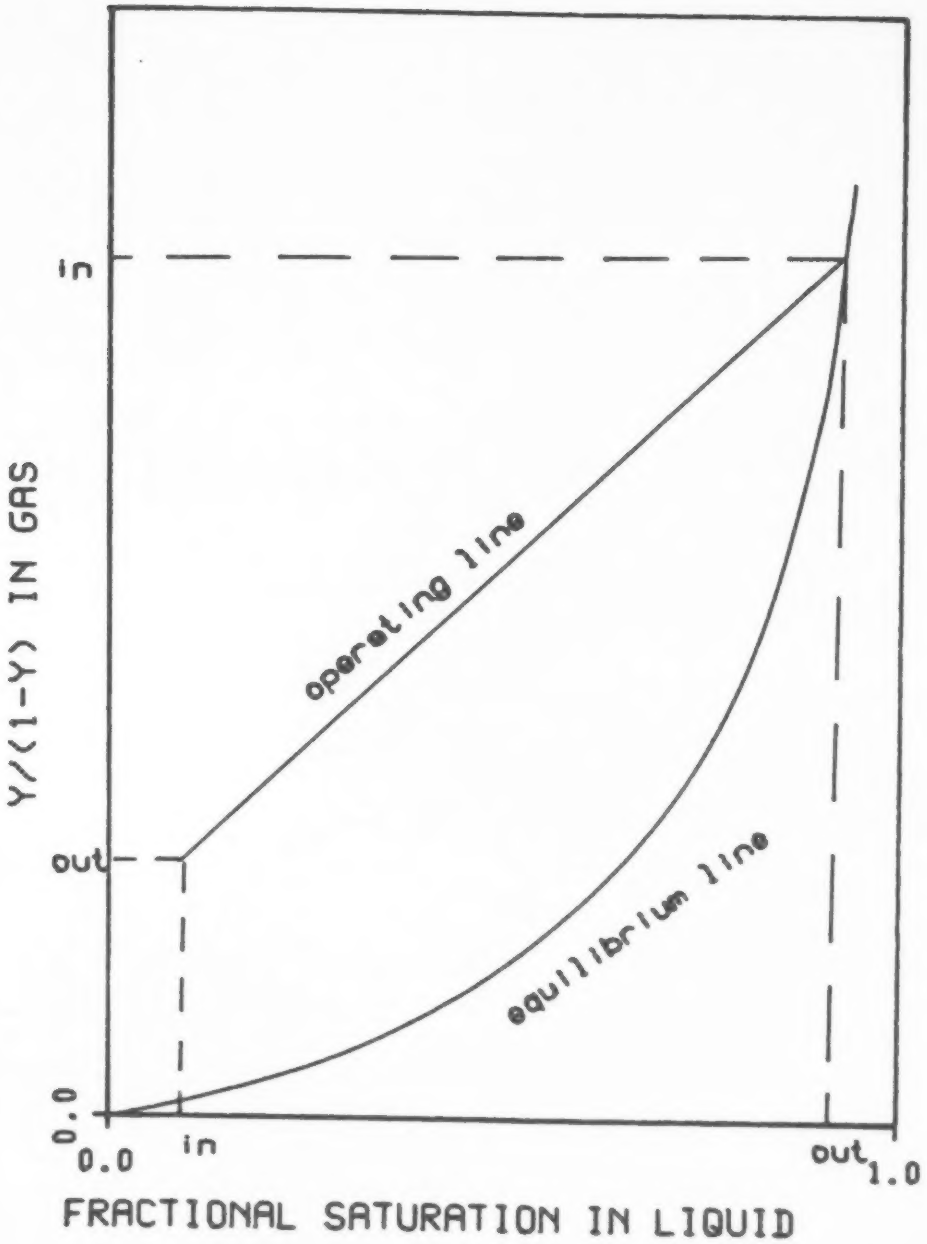

Figure 14 Bottom Pinch of Key Component

$$[A]_t \approx my_A \tag{140}$$

and Equation 139 may be rewritten as

$$G_{in} Y_{A,in} + Lmy_{A,in} = G_{out} Y_{A,out} + Lmy_{A,out} \tag{141}$$

Although L and m may change during absorption and desorption, the product, Lm, is constant.

If species A is the only component transfered between phases, a carrier gas flow rate may be defined as

$$G' = G(1 - Y_A) \tag{142}$$

and Equation 141 rewritten as

$$G'\left(\frac{Y_A}{1 - Y_A}\right)_{in} + Lmy_{A,in} = G'\left(\frac{Y_A}{1 - Y_A}\right)_{out} + Lmy_{A,out}$$

or

$$\left(\frac{Y_A}{1 - Y_A}\right)_2 = \left(\frac{Y_A}{1 - Y_A}\right)_1 + \frac{Lm}{G'}\,(y_{A,2} - y_{A,1}) \tag{143}$$

At a specified temperature and pressure, Equation 143 gives a linear operating line of slope Lm/G' for absorption and stripping with reaction.

If the ratio Lm/G' is larger than that which will allow a bottom pinch for the key component, a situation illustrated in Figure 15, then it is assumed in the initial calculations that the key component is pinched at the top of the column, as shown in Figure 16. Since the removal of H_2S ranged from 98% to 100% in the pilot plant operation, it was assumed at this point in the calculations that all entering non-key reactive components are absorbed to account for their effect on the equilibrium of the key component at the bottom of the absorber. The flow rate of inert gas, G', may be calculated with the assumptions of a bottom pinch for inert components and of a constant volumetric liquid flow rate through the packing, as discussed in the preceding section. The assumption that L is constant is not required to use Equation 143 since the product of L and m is constant.

Once initial estimates of the flow rates and compositions of the exiting streams are obtained, step-wise differential element calculations are initiated at the bottom of the

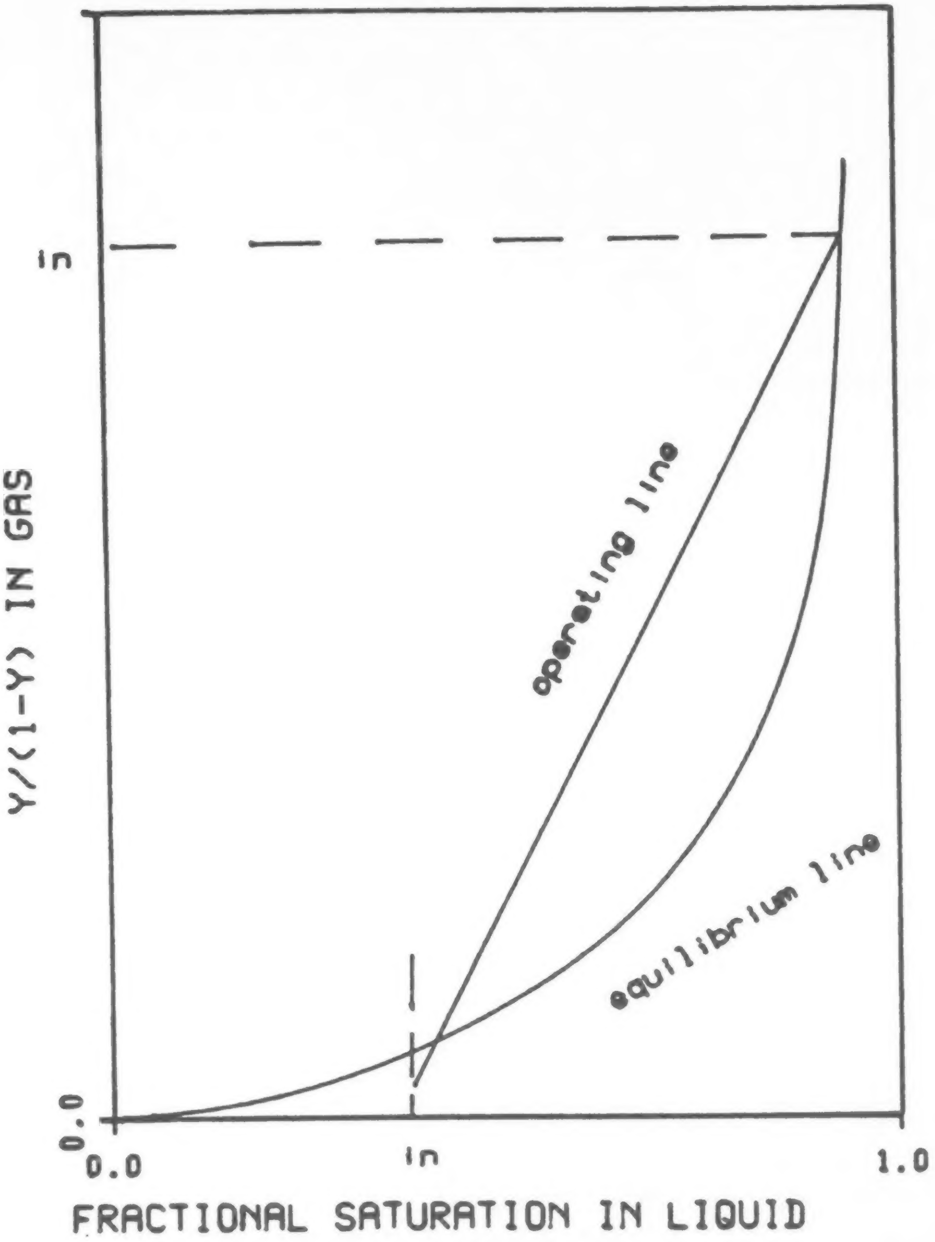

Figure 15 Absorption with High Liquid-to-Gas Ratio

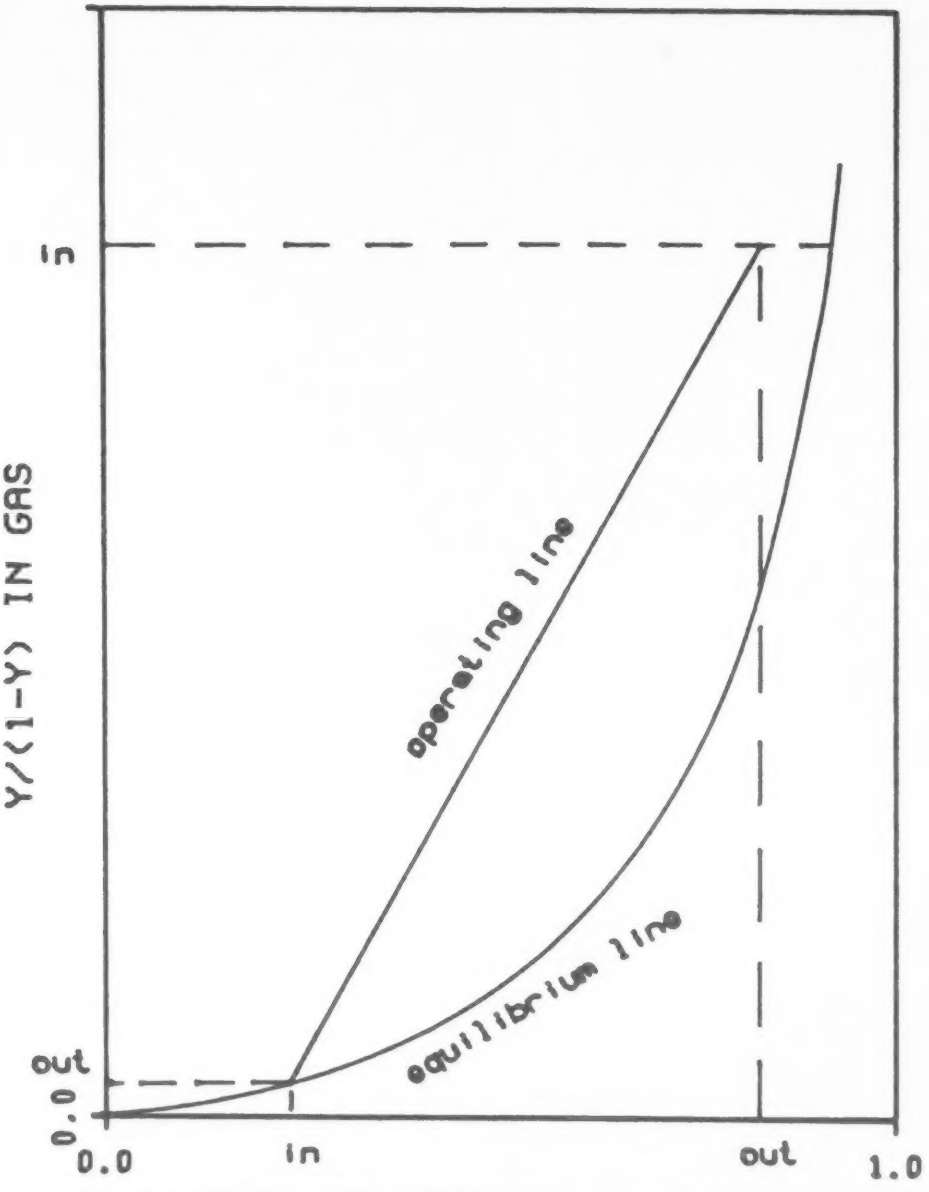

Figure 16 Top Pinch of Key Component

absorber column. Since calculations begin at the bottom of the column, $(Y_{key})_n$ and y_n are known and are assumed to be constant throughout the differential element n.

These step-wise calculations are continued until the sum of the heights of the differential elements reaches the specified packing height or until the driving force for transfer of the key component between the gas and liquid phases becomes zero (confirming the assumption of a top pinch). When this happens, the mole fraction of the key component in the gas stream leaving the final differential element is compared to the assumed value used to initiate the calculations. If a specified tolerance is not satisfied, a new guess of this mole fraction is made, and the corresponding exiting gas flow rate and composition, and exiting liquid composition are calculated from an overall balance on the key. The step-wise procedure is then reinitiated at the bottom of the column and is continued until convergence is achieved. This calculative technique is referred to as the shooting method.

After the absorber calculations on the key component are completed, the composition of the exit streams are corrected for the non-key components using the equilibrium and mass balance relationships discussed in the preceding section. The absorption of H_2S was assumed to be controlled by equilibrium between the gas and liquid streams at the top of the absorber. Pilot plant results that indicate the concentration of H_2S in the absorber exit gas is independent of the concentration of H_2S in the sour gas fed to the absorber support this assumption. Since the level of H_2S in the absorber exit gas stream was typically present in concentrations less than 10 ppm, the assumption of total H_2S absorption was valid to account for the effect of H_2S on the equilibrium of the key component at the bottom of the absorber. The absorption of COS was estimated by an emperical fit to information published by the Benfield Corporation (Parrish and Neilson, 1974) and is discussed later in this report.

FLASH TANK MODEL

The flash tank was assumed to have a holding time sufficient for chemical as well as physical equilibrium to occur. As stated previously, the flash tank was assumed to operate isothermally, so that the operating temperature and pressure were specified.

Calculative procedures for equilibrium stage operations with reaction have been developed, primarily for multicomponent distillation with reaction (Nelson, 1971). Since the packing algorithms expressed the composition of the liquid phase in terms of fractional saturation, a similar flash algorithm was needed. No such scheme was found in literature.

To derive the descriptive equations, consider a flash tank consisting of a single equilibrium stage at pressure P and temperature T. If f_i is the feed rate of component i, then

$$f_i = VY_i + L[i]_t \tag{144}$$

Expressing the total concentration of i in the exiting liquid stream as

$$[i]_t = C_i + y_i m$$

and specifying the exit gas and liquid streams to be in equilibrium

$$C_i = (P/H_i)Y_i$$

Equation 144 can be rewritten to give

$$f_i = VY_i + L\left[\left(\frac{P}{H_i}\right) Y_i + y_i m\right] \tag{145}$$

or

$$Y_i = \frac{f_i - Ly_i m}{V + L(P/H_i)}$$

Multiplying the numerator and denominator of Equation 163 by the molar density of the solvent, ρ_m (assumed to be constant)

$$Y_i = \frac{\rho_m f_i - \rho_m L y_i m}{\rho_m V + \rho_m L(P/H_i)} \tag{146}$$

At steady state, $\rho_m L = \rho_m F - V$, so that Equation 146 becomes

$$Y_i = \frac{\rho_m f_i - (\rho_m F + V) y_i m}{V\left[\rho_m - (P/H_i)\right] + \rho_m F(P/H_i)} \tag{147}$$

This is an explicit expression for the mole fraction of component i in the gas phase in terms of unknowns V and y_i.

Once a set of y_i has been assumed, Equation 147 may be used in the function

$$f(V) = \sum_i Y_i + Y_{solvent} - 1.0 = 0$$

where the mole fraction of the solvent in the gas can be approximated by

$$Y_{solvent} = \frac{P^*}{P}$$

to calculate V corresponding to the assumed set of y_i. Once V has been calculated, L may be obtained from

$$\rho_m L = \rho_m F - V$$

and the resulting set of y_i values calculated by

$$y_i = \frac{f_i - Y_i \left[V + L(P/H_i) \right]}{Lm} \tag{148}$$

The calculated set of y_i values may then be compared with the assumed set; if a specified tolerance is not satisfied, a new set is assumed, and the calculations repeated. Of course, the y_i values for the components that do not react with the reactive component of the solvent will be zero.

STRIPPER MODEL

The stripper column, which is operated with a reboiler and condenser, is represented by the model schematic shown in Figure 17. In stripper calculations, the packing is divided into a large number of elements and calculations in each element are essentially identical to those used in the absorber model. The primary difference between stripper and absorber calculations is that in the stripper calculations, the composition of the gas entering the column is not specified. This composition may, however, be determined by assuming the gas is in equilibrium with the reboiler exit liquid and estimating the liquid composition. The stripper calculations are thus initiated by assuming the composition of the reboiler exit liquid. This involves guessing only the

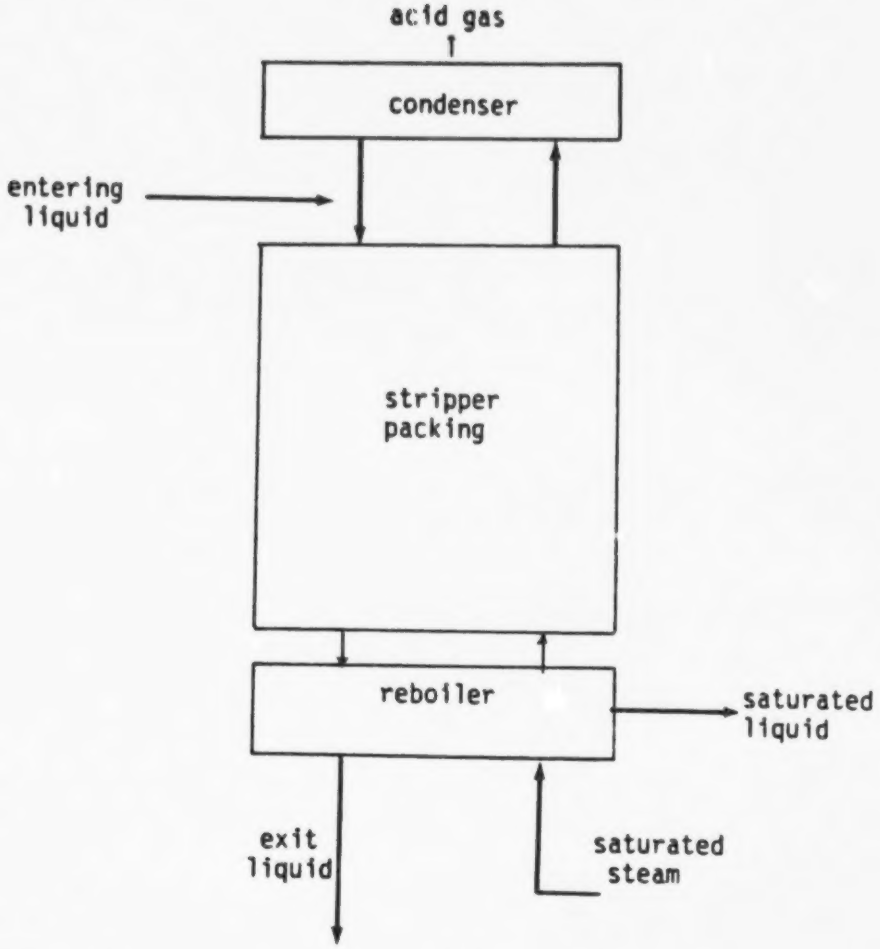
acid gas
condenser
entering liquid
stripper packing
reboiler
saturated liquid
exit liquid
saturated steam

Figure 17 Stripper Column Schematic

concentrations of the reactive components, since it is assumed that all inert components are desorbed in the stripper.

The flow rate of vapor entering the bottom of the stripper packing from the reboiler is calculated from the flow rate of steam to the reboiler, the latent heat of this steam and the latent heat of the solvent at the conditions of the stripper. The steam fed to the reboiler was assumed to be saturated vapor at the specified temperature, and the latent heat of the solvent was assumed to be that of water at the corresponding temperature. As it was assumed that no steam condenses in the stripper packing, the calculated vapor was the carrier gas flow G' in Equation 143.

The gas stream leaving the stripper is assumed to be at the condenser temperature, which is specified. It is assumed also that the gas stream leaving the condenser is saturated with solvent at the stripper pressure and condenser temperature. The amount of liquid returning to the packing from the condenser may then be calculated. Since the solubilities in pure water of all components present are extremely small, and the reactive component of the solvent is nonvolatile, the liquid returning to the packing from the condensor was assumed to be pure water.

As stated previously, since H_2S is present in small amounts, and its reaction with the solvent is considered instantaneous, the desorption of H_2S was assumed to be controlled by equilibrium between the gas and liquid phases somewhere in the stripping column. Trial equilibrium and mass balance calculations, and examination of pilot plant results suggest that this equilibrium is at the top of the stripper packing. Thus, the concentration of H_2S in the gas stream leaving the stripper packing was assumed to be that in equilibrium with the entering liquid. The concentration of H_2S in the reboiler exit liquid may then be calculated from a balance on H_2S across the stripper packing and the reboiler, and compared with the assumed value. This concentration must satisfy a specified convergence tolerence, as does the corresponding concentration of the key component.

As mentioned previously, all COS absorbed was assumed to be converted to CO_2 and H_2S. Thus, the concentration of COS is zero throughout the stripper column.

THERMODYNAMIC AND TRANSPORT PROPERTIES

The availability of accurate physical, thermodynamic, and transport property data or correlations is essential to the simulation of any chemical process. The following is a summary of the methods used to estimate these properties in the simulation of the hot potassium carbonate-coal gas operation.

DENSITY

Gas densities were calculated assuming ideal gas behavior. Liquid densities were correlated by an empirical fit to data presented in the Chemical Engineer's Handbook (Perry and Chilton, 1973) for the densities of potassium carbonate solutions:

$$\rho(\mathrm{g/ml}) = 1.1464 - 0.0006\mathrm{T(K)} + 0.0111(\mathrm{wt\%K_2CO_3}) \tag{149}$$

VISCOSITY

Individual gas viscosities were calculated by the Chapman-Enskog equation (Reid et al., 1977). Viscosities of gas mixtures were estimated with the Chapman-Enskog equation and the Wilke approximation (Reid et al., 1977).

Solvent viscosities were correlated by an empirical fit to data given by Kohl and Riesenfeld (1979) for the viscosities of potassium carbonate solutions:

$$\ln \mu\ (\mathrm{cP}) = 2.515 + 0.03077(\mathrm{wt\%K_2CO_3}) - 9.953\times 10^{-3}\ \mathrm{T(} \tag{150}$$

The viscosity of water was also used in a correlation for the diffusivity of CO_2 in potassium carbonate solutions. Viscosities of water were calculated by the method of Ertl and Dellien (Reid et al., 1977).

VAPOR PRESSURE OF SOLVENT

At various points in the algorithms, the gas stream was assumed to be saturated with water. The equilibrium partial pressure of water was calculated with the vapor pressure of water over K_2CO_3 solutions at the corresponding conditions. This vapor pressure was correlated by an emperical fit to data presented by Tosh et al. (1959):

$$\log P^*(\text{psia}) = 6.665 - \frac{2100}{T(K)} \tag{151}$$

LATENT HEAT OF VAPORIZATION

To estimate the amount of vapor generated in the reboiler, values for the latent heat of water were required. The latent heat of saturated steam was assumed to be a function only of temperature and was correlated by an empirical fit to data given by Felder and Rousseau (1986):

$$\lambda_v(\text{kJ/kg}) = 2581.42 - 3.1428T(^\circ\text{C}) \tag{152}$$

The latent heat of vaporization of the solvent was assumed to be that of water at the reboiler temperature. This approximation is recommended by Bocard and Mayland (1962), since heat effects with this solvent are small.

SURFACE TENSION

The surface tension of K_2CO_3 solutions was assumed to be equal to that of water at corresponding conditions. The surface tension of water was assumed to be a function only of temperature, as recommended by Perry and Chilton (1973), and using a reference value of 72.8 dynes/cm at 293 K (Reid et al., 1977). The critical surface tension for the packing used in the experimental work was 61 dynes/cm, as recommended by Perry and Chilton (1973).

DIFFUSIVITY

Binary gas diffusivities of CO_2 in the major coal gas components were calculated by the method of Fuller, Schettler and Giddings (Reid et al., 1977). Diffusivities of CO_2 in gas mixtures were calculated with the Stephan-Maxwell equation (Reid et al., 1977).

Diffusivities of CO_2 in K_2CO_3 solutions were calculated by the method of Ratcliff and Holdcroft (1963). This correlation employs values of the viscosity of K_2CO_3 solutions, the diffusivity of CO_2 in water, and the viscosity of water. Values for the diffusivity of CO_2 in water were estimated by the Wilke-Chang equation (Reid et al., 1977).

EQUILIBRIUM RELATIONSHIPS

Equilibrium relationships were used to calculate equilibrium compositions of gas and liquid phases and appear in key mass transfer rate expressions and expressions for the concentrations of reactive components in the liquid phase. The following is a summary of the methods used to calculate values for these relationships.

Henry's Law Constants

The solubilities of gases in aqueous K_2CO_3 solutions were expressed in terms of Henry's law constants. This was done using the method of Joshi (1980), who recommended using the corresponding Henry's law constant for the gas in water and the molarity of the solution:

$$\log\left(\frac{H}{H^o}\right) = 0.125\ m \tag{153}$$

Values for the Henry's law constant in water were estimated by the method of Wilhelm et al. (1977).

Reaction Equilibrium Constants

Equilibrium constants used in the algorithm are given below. Ideal solution behavior was assumed so that each equilibrium constant was expressed as a function of temperature only.

$$CO_2 + CO_3^{=} + H_2O \longleftrightarrow 2HCO_3^-$$

$$K_1 = \frac{[HCO_3^-]^2}{[CO_2][CO_3^{=}]} = 165 \exp\left(\frac{1312}{T(\mathrm{K})}\right) \tag{154}$$

Equation 154 was obtained by correlating data presented by Savage, et al. (1980).

$$H_2S + CO_3^{=} \longleftrightarrow HS^- + HCO_3^-$$

$$K_2 = \frac{[HS^-][HCO_3^-]}{[H_2O][CO_3^{=}]} = 911 \exp\left(\frac{600}{T(\mathrm{K})}\right) \tag{155}$$

Equation 155 was obtained by correlating data presented by Astarita et al. (1983).

$$COS + H_2O \longleftrightarrow CO_2 + H_2S$$

$$K_3 = \frac{[CO_2][H_2S]}{[COS]} = 22.1 \exp\left(\frac{4210}{T(\mathrm{K})}\right) \tag{156}$$

Equation 156 was obtained by correlating data presented by Ferm (1957).

$$CO_3^{=} + H_2O \longleftrightarrow HCO_3^- + OH^-$$

$$K_4 = \frac{[HCO_3^-][H_2S]}{[CO_3^{=}]} = 2487 \exp\left(\frac{-4797}{T(\mathrm{K})}\right) \tag{157}$$

K_4 was used in the solution of the mass transfer rate enhancement factor, and Equation 157 was obtained by correlating data presented by Savage, et al. (1980).

MASS TRANSFER COEFFICIENTS

Mass transfer rates of the key component in the absorber and stripper algorithms were expressed in terms of mass transfer coefficients and interfacial areas for mass transfer. The correlations that were used to estimate these quantities are given below and the nomenclature and units are as follows: a_t and a_w are the total and wetted surface areas of the packing in m^2/m^3, D is diffusivity in m^2/h, G is superficial mass velocity of the gas in kg/m^2·h, g is gravitational acceleration in m/h^2, k_G is the gas-phase mass transfer coefficient in kmol/m^2·h·atm, k_L is the liquid-phase mass transfer coefficient in m/h, L is the superficial mass velocity of the liquid in kg/m^2·h, R is the gas constant in m^3·atm/kmol·K, T is absolute temperature in Kelvin, μ is viscosity in kg/m·h, ρ is density in kg/m^3, σ is surface tension in dynes/cm, σ_c is the critical surface tension of the packing material in dynes/cm, and the subscipts G and L refer to gas and liquid, respectively.

Gas Phase Mass Transfer Coefficients

Values of gas-phase mass transfer coefficients were calculated using the correlation of Onda et al. (1968a). This correlation is an empirical fit to a large number of data sets and is recommended for mass transfer in packed columns (Astarita et al., 1983). The mass transfer driving force is expressed in terms of partial pressures, resulting in a gas phase mass transfer coefficient of units kmol/m^2-h-atm with this correlation.

$$k_g = 5.23 \left[\frac{G}{a_t \mu_G} \right]^{0.7} \left[\frac{\mu_G}{\rho_G D_G} \right]^{1/3} \left[a_t D^p \right]^{-2.0} \left[\frac{a_t D_G}{RT} \right] \qquad (158)$$

Liquid Phase Mass Transfer Coefficients

Values for liquid-phase mass transfer coefficients were also calculated using the correlation of Onda et al. (1968a). This correlation has been shown to give results that correspond more closely with measured data than do those using other correlations (Kelly, 1981). The mass transfer driving force is expressed in terms of concentrations, resulting in a liquid phase mass transfer coefficient of units m/h with this correlation.

$$k_L = 0.0051 \left[\frac{L}{a_w \mu_L} \right]^{2/3} \left[\frac{\mu_L}{\rho_L D_L} \right]^{-1/2} \left[a_t D^P \right]^{0.4} \left[\frac{\rho_L}{\mu_L g} \right]^{-1/3} \qquad (159)$$

Interfacial Area for Mass Transfer

The interfacial area for mass transfer between the gas and liquid phases was calculated with the correlation of Onda et al. (1968b). This correlation gives the ratio of the wetted surface area of packing to the total surface area of packing and assumes that the interfacial area for mass transfer is equal to the wetted surface area. The total surface area of packing was obtained from data given in Chemical Engineer's Handbook (Perry and Chilton, 1973).

$$\frac{a_w}{a_t} = 1 - \exp\left[\left(\frac{\sigma_c}{\sigma}\right)^{0.75}\left(\frac{L}{a_t\mu_L}\right)^{0.1}\left(\frac{L^2 a_t}{\rho_L^2 g}\right)^{-0.05}\left(\frac{L^2}{\rho_L \sigma a_t}\right)^{0.2}\right] \tag{160}$$

DESCRIPTION OF COMPUTER PROGRAMS

The computer programs developed in this study perform the calculations corresponding to the model discussed above. These programs are specific to the hot potassium carbonate process, with CO_2 designated as the key component. The main program (CARB) and all subroutines were written in FORTRAN-77 on the DEC VAX/VMS 11/750 computer in the Chemical Engineering Department at North Carolina State University. Codes for the main program and all subroutines are given by Staton (1985). The following is a brief description of these programs.

MAIN PROGRAM AND SUBROUTINES

CARB can simulate a packed absorption column, a flash tank, a packed stripping column, or a complete acid gas removal system consisting of these three units. The type of simulation is selected by specifying a value for MODE in the input data. Table 8 presents a description of the calculations corresponding to values of this flag.

Also included in CARB are three levels of program output, corresponding to brief, detailed and complete echoes of program calculations. The type of output is selected by specifying a value for FLAG1 in the input data. A description of these outputs and the corresponding values of FLAG1 are given in Table 9. Staton (1985) gives examples of the various program outputs.

TABLE 8
PROGRAM FORMATS

Specified Value of Flag MODE	Type of Simulation
1	Isothermal Packed Absorption Column
2	Isothermal Equilibrium Flash Tank
3	Isothermal Packed Stripping Column Operating with Condensor and Steam Heated Reboiler
4	Acid Gas Removal System Consisting of the Above Units

TABLE 9
LEVELS OF PROGRAM OUTPUT

Specified Value of Flag FLAG1	Description of Program Output
1	Normal output, echoes assumptions and results for each overall iteration in absorber, flash tank and stripping calculations, and for each AGRS iteration.
2	Detailed output, above echo plus information on each differential element in absorber and stripper calculations and for each iteration in flash tank calculations.
3	Complete output, gives detailed information on calculations in all subroutines, to be used with calculations for one differential element of packing in absorber or stripper simulations.

The major components in the coal gas streams fed to the AGRS in the pilot plant operation were included in the program. These components were assigned numbers following the sequence shown in Table 10. Values of stream flow rates, individual component molar flow rates, gas stream mole fractions and liquid stream concentrations are stored in a series of arrays following the numbering sequence shown in Figure 18. For example, FLOW(6) is the molar flow rate of the absorber exit gas stream, X(5,3) is the mole fraction of COS in the gas stream entering the absorber, and C(3,1) is the concentration of CO_2 in the liquid stream exiting the flash tank.

TABLE 10
COAL GAS SPECIES INCLUDED IN CARB

Assigned Number	Component
1 (key)	Carbon dioxide
2	Hydrogen sulfide
3	Carbonyl sulfide
4	Water
5	Hydrogen
6	Carbon monoxide
7	Nitrogen
8	Methane
9	Ethylene
10	Ethane

Values of thermodynamic variables are also stored in an array using the sequence 1 for absorber, 2 for flash tank and 3 for stripper. For example, H(2,5) represents the Henry's law constant for hydrogen at the conditions of the flash tank. K(1,2) represents the value of the reaction equilibrium constant for the reaction of equation 155 at the conditions of the absorber.

Names and descriptions of the main program and all subroutines are given in Table 11. Schematics of the calculative schemes corresponding to the four values of MODE are given in Figures 19 through 22. These schematics include the required data input for each type of simulation, as well as primary convergence tolerences. The calculative scheme used in the calculations at each differential element of packing in the absorber and stripper algorithms (subroutine DSEC) is given in Figure 23. More detailed information on program calculations is given in comment statements of the computer code.

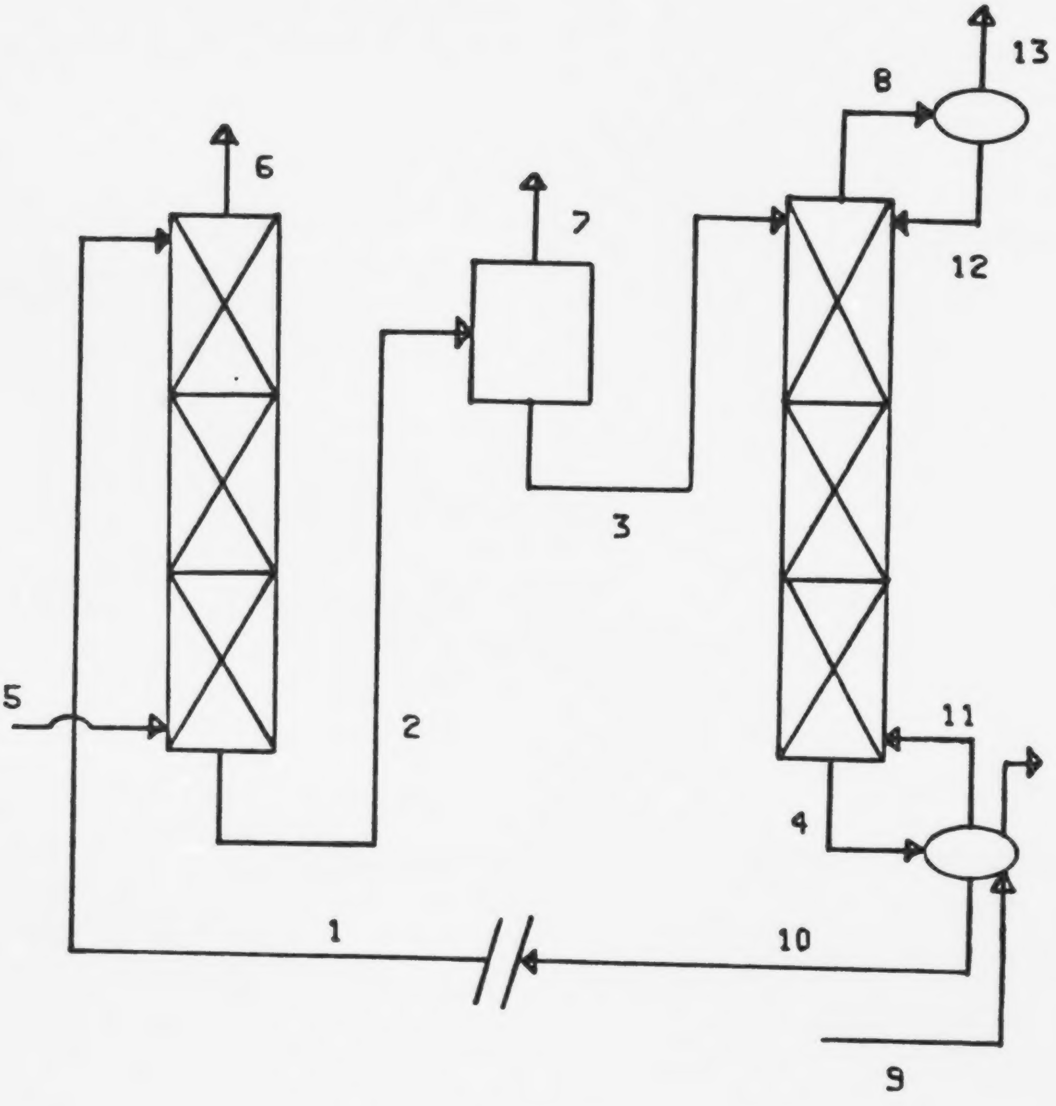
6
7
13
8
12
3
5
2
11
4
1
10
9

Figure 18 Stream Array Sequence

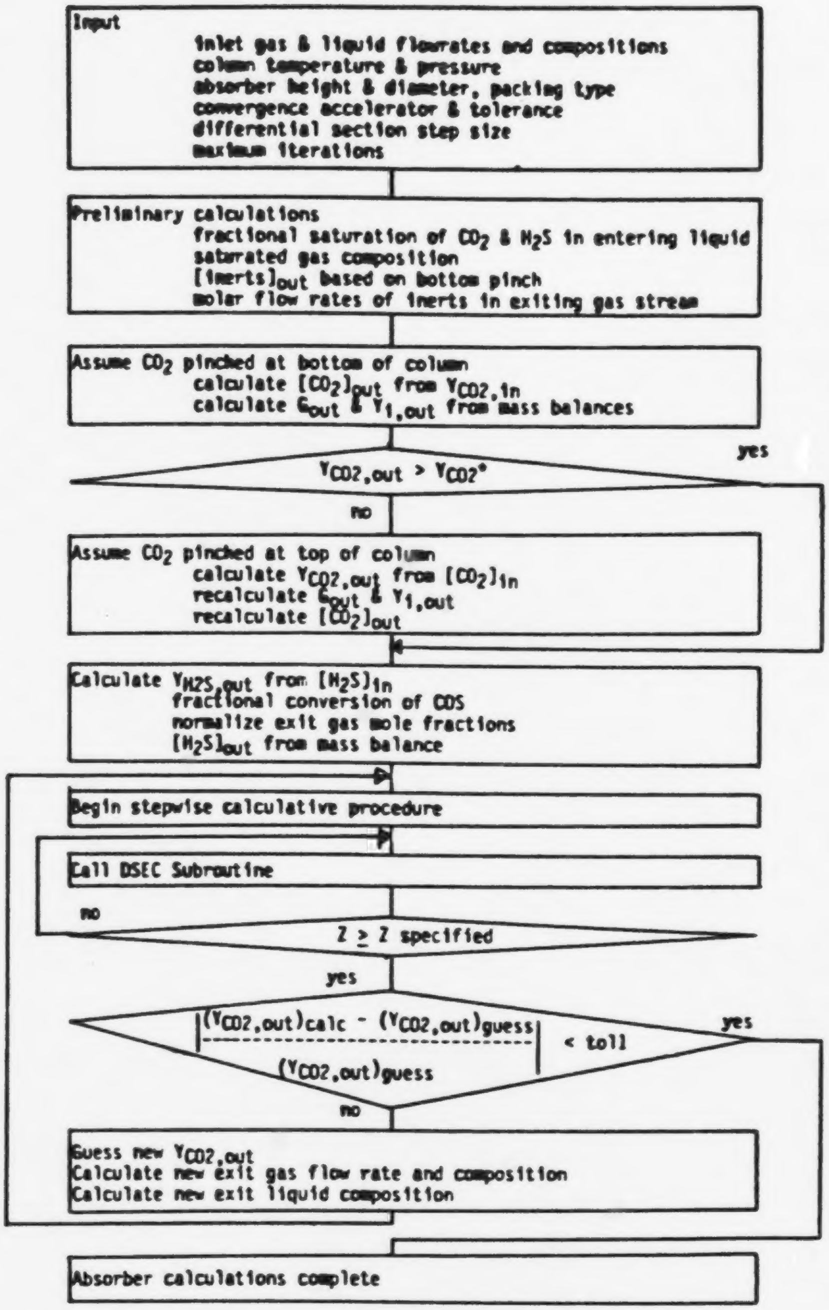
Input
inlet gas & liquid flowrates and compositions
column temperature & pressure
absorber height & diameter, packing type
convergence accelerator & tolerance
differential section step size
maximum iterations
Preliminary calculations
fractional saturation of CO_2 & H_2S in entering liquid
saturated gas composition
$[\text{inerts}]_{out}$ based on bottom pinch
molar flow rates of inerts in exiting gas stream
Assume CO_2 pinched at bottom of column
calculate $[CO_2]_{out}$ from $Y_{CO2,in}$
calculate G_{out} & $Y_{i,out}$ from mass balances
$Y_{CO2,out} > Y_{CO2}^*$
yes
no
Assume CO_2 pinched at top of column
calculate $Y_{CO2,out}$ from $[CO_2]_{in}$
recalculate G_{out} & $Y_{i,out}$
recalculate $[CO_2]_{out}$
Calculate $Y_{H2S,out}$ from $[H_2S]_{in}$
fractional conversion of COS
normalize exit gas mole fractions
$[H_2S]_{out}$ from mass balance
Begin stepwise calculative procedure
Call DSEC Subroutine
no
$Z \geq Z$ specified
yes
$\left| \frac{(Y_{CO2,out})_{calc} - (Y_{CO2,out})_{guess}}{(Y_{CO2,out})_{guess}} \right| < toll$
yes
no
Guess new $Y_{CO2,out}$
Calculate new exit gas flow rate and composition
Calculate new exit liquid composition
Absorber calculations complete

Figure 19 Absorber Calculative Scheme

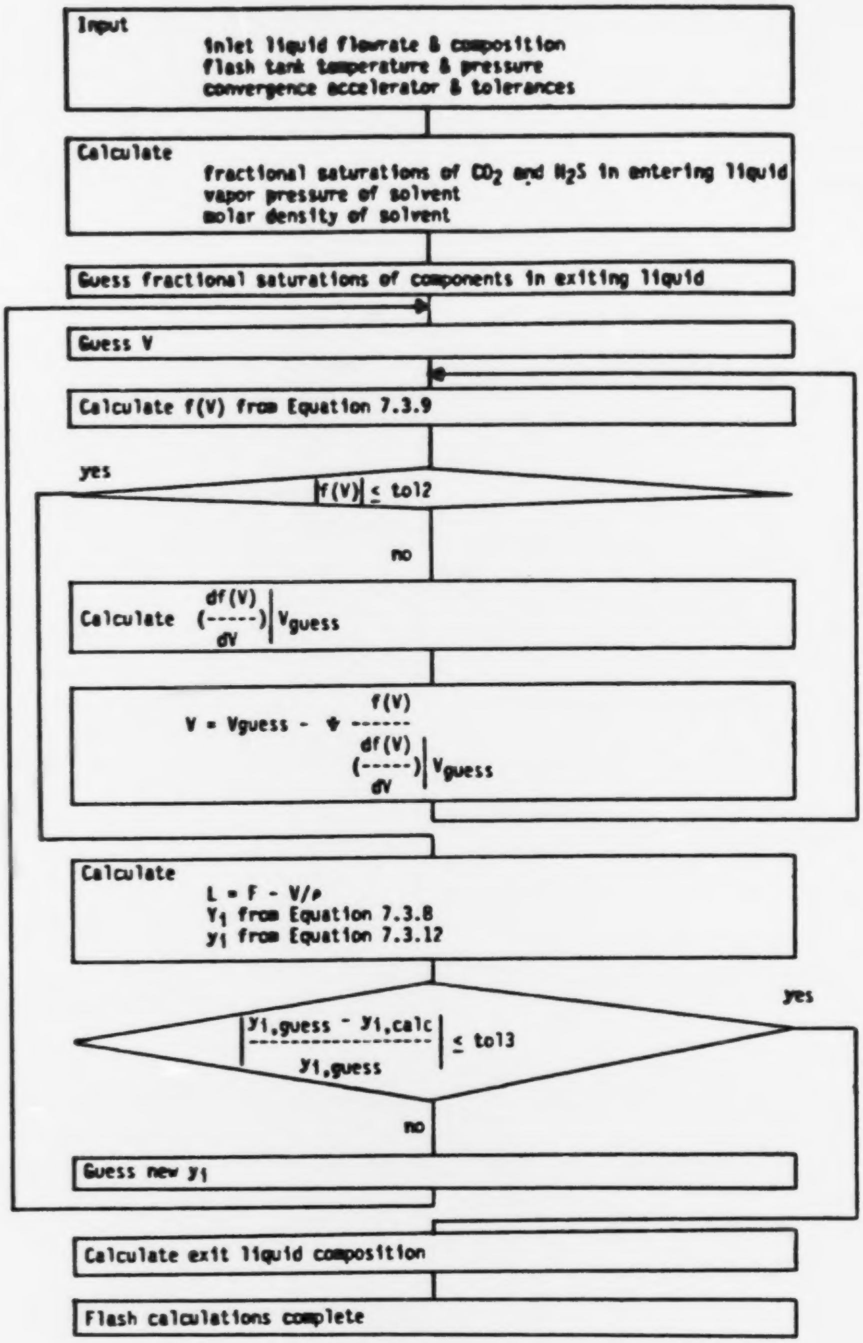
Input
inlet liquid flowrate & composition
flash tank temperature & pressure
convergence accelerator & tolerances
Calculate
fractional saturations of CO_2 and H_2S in entering liquid
vapor pressure of solvent
molar density of solvent
Guess fractional saturations of components in exiting liquid
Guess V
Calculate f(V) from Equation 7.3.9
yes
$|f(V)| \leq tol2$
no
Calculate $\left(\frac{df(V)}{dV}\right)\Big|_{V_{guess}}$
$V = V_{guess} - \psi \frac{f(V)}{\left(\frac{df(V)}{dV}\right)\Big|_{V_{guess}}}$
Calculate
$L = F - V/\rho$
Y_i from Equation 7.3.8
y_i from Equation 7.3.12
yes
$\left|\frac{y_{i,guess} - y_{i,calc}}{y_{i,guess}}\right| \leq tol3$
no
Guess new y_i
Calculate exit liquid composition
Flash calculations complete

Figure 20 Flash Calculative Scheme

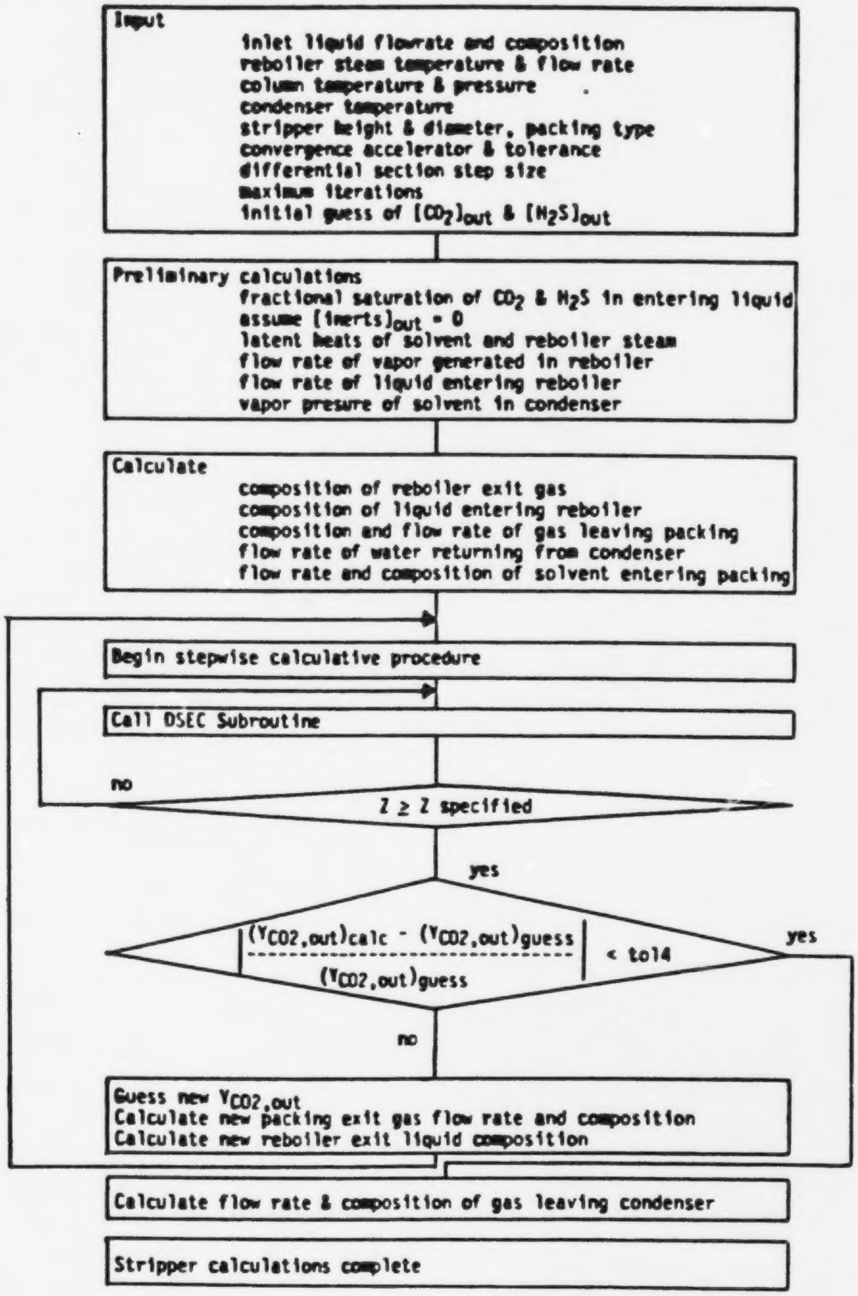
Input
inlet liquid flowrate and composition
reboiler steam temperature & flow rate
column temperature & pressure
condenser temperature
stripper height & diameter, packing type
convergence accelerator & tolerance
differential section step size
maximum iterations
initial guess of $[CO_2]_{out}$ & $[H_2S]_{out}$
Preliminary calculations
fractional saturation of CO_2 & H_2S in entering liquid
assume $[\text{inerts}]_{out} = 0$
latent heats of solvent and reboiler steam
flow rate of vapor generated in reboiler
flow rate of liquid entering reboiler
vapor presure of solvent in condenser
Calculate
composition of reboiler exit gas
composition of liquid entering reboiler
composition and flow rate of gas leaving packing
flow rate of water returning from condenser
flow rate and composition of solvent entering packing
Begin stepwise calculative procedure
Call DSEC Subroutine
no
$Z \geq Z$ specified
yes
$\left| \frac{(Y_{CO2,out})_{calc} - (Y_{CO2,out})_{guess}}{(Y_{CO2,out})_{guess}} \right| < tol4$
yes
no
Guess new $Y_{CO2,out}$
Calculate new packing exit gas flow rate and composition
Calculate new reboiler exit liquid composition
Calculate flow rate & composition of gas leaving condenser
Stripper calculations complete

Figure 21 Stripper Calculative Scheme

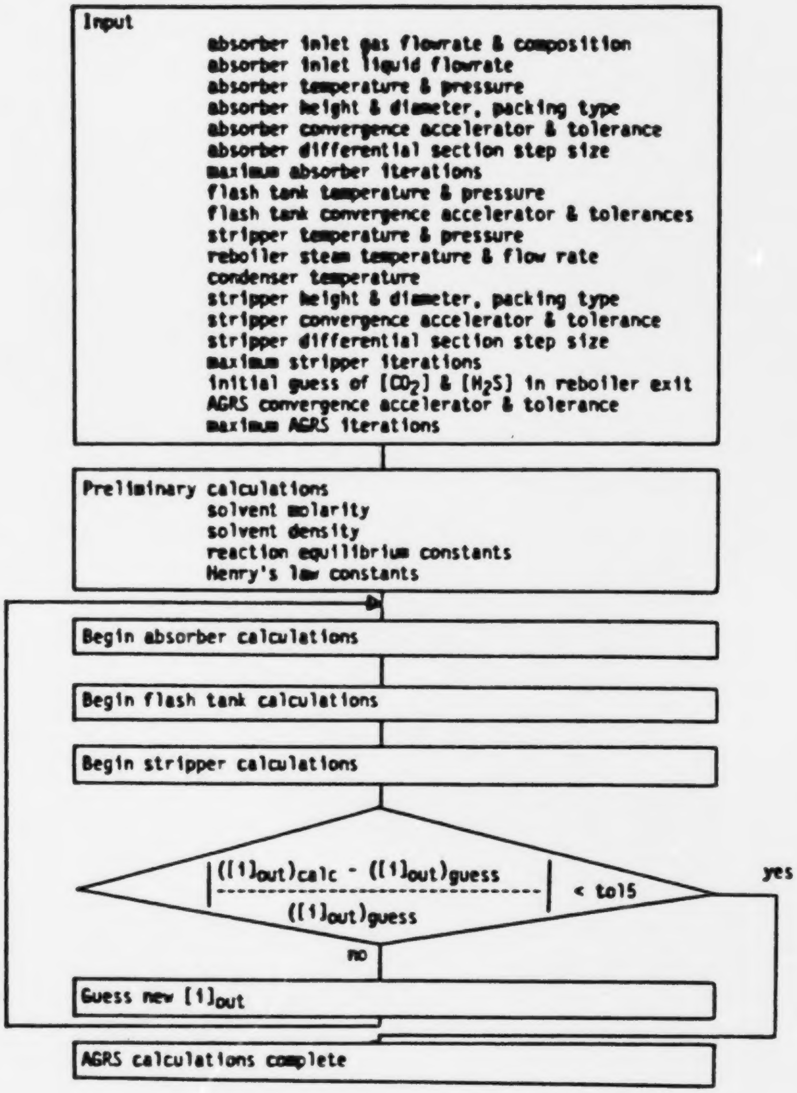
Input
absorber inlet gas flowrate & composition
absorber inlet liquid flowrate
absorber temperature & pressure
absorber height & diameter, packing type
absorber convergence accelerator & tolerance
absorber differential section step size
maximum absorber iterations
flash tank temperature & pressure
flash tank convergence accelerator & tolerances
stripper temperature & pressure
reboiler steam temperature & flow rate
condenser temperature
stripper height & diameter, packing type
stripper convergence accelerator & tolerance
stripper differential section step size
maximum stripper iterations
initial guess of $[CO_2]$ & $[H_2S]$ in reboiler exit
AGRS convergence accelerator & tolerance
maximum AGRS iterations
Preliminary calculations
solvent molarity
solvent density
reaction equilibrium constants
Henry's law constants
Begin absorber calculations
Begin flash tank calculations
Begin stripper calculations
$\left| \frac{([i]_{out})_{calc} - ([i]_{out})_{guess}}{([i]_{out})_{guess}} \right| < tol5$
yes
no
Guess new $[i]_{out}$
AGRS calculations complete

Figure 22 AGRS Calculative Scheme

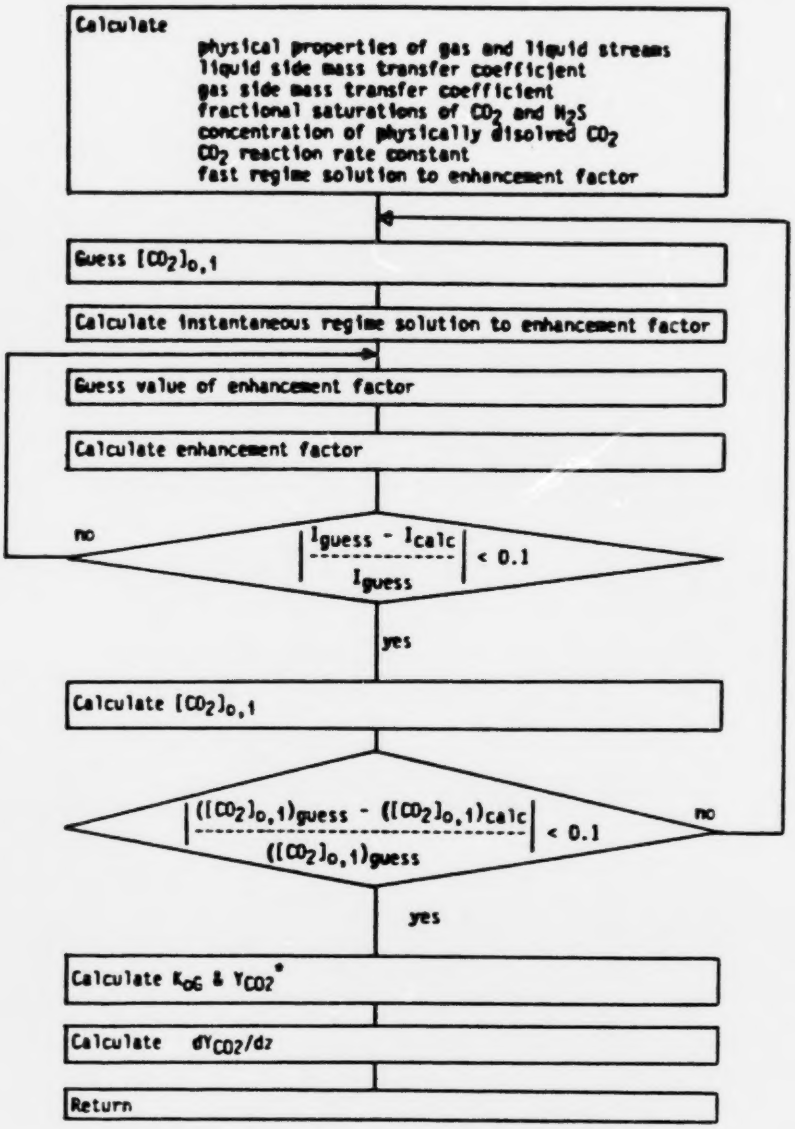
Calculate
physical properties of gas and liquid streams
liquid side mass transfer coefficient
gas side mass transfer coefficient
fractional saturations of CO_2 and H_2S
concentration of physically disolved CO_2
CO_2 reaction rate constant
fast regime solution to enhancement factor
Guess $[CO_2]_{o,i}$
Calculate instantaneous regime solution to enhancement factor
Guess value of enhancement factor
Calculate enhancement factor
no
$\left| \frac{I_{guess} - I_{calc}}{I_{guess}} \right| < 0.1$
yes
Calculate $[CO_2]_{o,i}$
$\left| \frac{([CO_2]_{o,i})guess - ([CO_2]_{o,i})calc}{([CO_2]_{o,i})guess} \right| < 0.1$
no
yes
Calculate K_{OG} & Y_{CO2}^*
Calculate dY_{CO2}/dz
Return

Figure 23 DSEC Calculative Scheme

TABLE 11
MAIN PROGRAM AND SUBROUTINES

Name	Description
CARB	Main program, coordinates all subroutines and reads in all input data
DSEC	Performs calculations at each differential element of packing in absorber and stripper algorithms
FLASH	Performs flash tank calculations
GMTC	Calculates values for physical and transport properties of gas phase and mass transfer coefficient of gas phase
LMTC	Calculates values for physical and transport properties of liquid phase and mass transfer coefficient of liquid phase
HENRY	Calculates values for Henry's law constants
RXN	Calculates values for reaction equilibrium constants
SOLV1	Solves for values of the equilibrium fractional saturations of CO_2 and H_2S, given the partial pressure of CO_2 and the total concentration of H_2S in the liquid
SOLV2	Solves for values of the equilibrium fractional saturations of CO_2 and H_2S, given the total concentrations of each in the liquid
PINCH	Finds the tangent intersection between operating line and equilibrium relationship in stripper calculations to give exit compositions and flowrates. Stripper calculations are completed with this subroutine if convergence cannot be obtained in iterative calculations due to an intersection between stripper operating and equilibrium lines

CONVERGENCE

The simplifying assumptions of the absorber and stripper models were used to avoid complex convergence problems. As a result, convergence was not a major problem in simulations of the pilot plant runs.

In flash tank calculations, values of the vapor flow rate, corresponding to an assumed set of fractional saturations in the flash tank exit liquid, were calculated using a Damped Newton's Method (Reklaitis et al. 1983). Convergence in all other calculations was accomplished by Modified Successive Substitution (Reklaitis et al. 1983).

Convergence tolerances in the DSEC subroutine for the enhancement factor and interfacial concentration of the key component were 10%. Convergence tolerances in other calculations were specified in the input data set. Table 12 gives the adjustable convergence parameters included in the programs, a description of their use and typical values used in the pilot plant simulations. These values were chosen after trial-and-error simulations indicated they allowed rapid convergence and reasonable accuracy.

COMPUTATIONAL REQUIREMENTS

Computational requirements varied depending on the type of simulation, the level of output and the number of iterations required for convergence. For the simulation of an acid gas removal system, with output corresponding to a FLAG1 value of one, a typical CPU time requirement for the DEC VAX/VMS 11/750 computer was five minutes.

TABLE 12
PROGRAM CONVERGENCE PARAMETERS

Name	Description	Typical Value
TOL1	Absorber Convergence Tolerance	0.05
TOL2	Flash Tank V Convergence Tolerance	0.05
TOL3	Flash Tank y Convergence Tolerance	0.05
TOL4	Stripper Convergence Tolerance	0.05
TOL5	AGRS Convergence Tolerance	0.05
ACC1	Absorber Convergence Accelerator	0.35
ACC2	Flash Tank Convergence accelerator	0.50
ACC3	Stripper Convergence Accelerator	0.15
ACC4	AGRS Convergence Accelerator	0.80
MAX1	Maximum Absorber Iterations	10
MAX2	Maximum Flash Tank Iterations	10
MAX3	Maximum Stripper Iterations	10
MAX4	Maximum AGRS Iterations	10
STEP1	Absorber Differential Element Size	0.001
STEP2	Stripper Differential Element size	0.001
FLAG3	If = 1: stop after 1 differential element in absorber calculations	0
FLAG5	If = 1: stop after 1 differential element in stripping calculations	0
CGES1	Initial guess of total concentration of CO_2 in reboiler exit liquid	0.3 - 0.9
CGES2	Initial guess of total concentration of H_2S in reboiler exit liquid	0 - 0.01

COMPARISON OF MODEL PREDICTIONS AND EXPERIMENTAL DATA

Model predictions and experimental data were compared using predicted and measured flow rates and compositions of gas streams exiting the process. Although quantitative analyses of the solvent streams were not done, estimates of the fractional conversion of carbonate to bicarbonate were obtained with pH measurements. These measurements were done for most runs and agreed with model predictions. For example, with a 20% K_2CO_3 solution, the fractional conversion of carbonate to bicarbonate was approximately 0.9 at the absorber exit, did not change significantly as a result of flashing, and was typically 0.4 at the reboiler exit. The relationship between pH and fractional conversion of carbonate to bicarbonate is given by Staton (1985).

Table 13 is an example of a detailed comparison between experimental data and model prediction for Run ACIL-24 of this study. Comparison tables such as Table 13 for all runs analyzed are given by Staton (1985). Excluded are those runs in which steady-state was not obtained (Runs ACIL-26 and ACIL-27), or stripping was accomplished with an inert gas (ACIN-5), or an amine rate promoter was used (Runs ACIN-1 and ACIN-9). Since the absorber and stripper packing heights in the pilot plant were sufficient to allow CO_2 to be at or near a pinched condition, addition of the amine rate promoter did not significantly affect experimental results. Since calculations to predict the rate promotion of CO_2 by such an additive could not be tested with pilot plant results, they were not included in the simulation program.

Measured and predicted flow rates of inert species in the sweet gas are in close agreement. This supports the assumption that the absorption of these components is controlled by equilibrium between the gas and liquid phases at the bottom of the absorber column. In regeneration, these species appear primarily in the flash tank exit gas, and their concentrations in the acid gas stream were typically lower than could be detected. Nitrogen, however, was detected in the acid gas stream for most runs. Since this component was used as a purge gas in the pilot plant, it was thought that excess N_2 entered the system through leaking purge valves: The mass balance recoveries for N_2 are higher than for other species in most runs.

TABLE 13
MODEL PREDICTIONS AND EXPERIMENTAL DATA FOR ACIL-24

Dry Total Flow Rates (mol/h)

Stream	Measured	Predicted
Sour gas	761.5	-
Sweet gas	672.4	664.6
Flash gas	12.6	4.3
Acid gas	126.7	130.3

Individual Component Flow Rates (mol/h)

	Sour gas	Sweet gas		Flash gas		Acid gas	
	Measured	Measured	Predicted	Measured	Predicted	Measured	Predicted
CO_2	216.49	93.73	103.55	9.37	1.80	121.28	126.18
H_2S	1.49	ND	0.0007	0.15	0.011	0.62	3.86
COS	0.044	0.034	0.039	0.001	0.0	ND	0.0
H_2O	-	-	1.10	-	0.47	-	3.26
H_2	275.44	276.81	274.13	1.57	1.21	ND	0.10
CO	112.55	116.92	111.96	0.60	0.54	ND	0.05
N_2	135.40	141.93	134.91	0.57	0.47	4.61	0.02
CH_4	36.70	38.12	36.43	0.28	0.23	ND	0.04
C_2H_4	1.34	1.36	1.31	0.02	0.02	0.008	0.01
C_2H_6	2.32	2.33	2.30	0.01	0.02	ND	0.004

As stated previously, the model assumes that all absorbed COS is converted irreversibly to CO_2 and H_2S. With few exceptions, no COS was detected in the exit streams from the flash tank and stripper. These results support the assumption regarding irreversibly of COS hydrolysis.

Measured and predicted gas stream flow rates are compared on a dry basis since the gas analysis methods used in this study could not measure the concentration of water vapor in the gas samples. Measured flow rates were assumed dry since condensors were installed in the gas lines ahead of the location of flow measurement and sampling.

Figures 24 through 26 show measured and predicted flow rates of the sweet, flash, and acid gas streams. Dashed lines on these figures represent 95% confidence intervals for the measured values, based on an analysis of the corresponding flow transmitter calibration curve.

As can be seen in Figure 24, measured and predicted sweet gas flow rates are in close agreement. Most predicted values fall within the 95% confidence interval for the measured value. Flow rates of this stream varied significantly as a result of large changes in the amount of CO_2 absorbed

Relative deviations between measured and predicted flash gas flow rates are quite large for some runs (Figure 25). Reducing convergence tolerances in flash calculations did not significantly change predicted values. These deviations are believed to be a result of errors in the measurement of this flow rate. These measured values were obtained by measuring the pressure drop across a laminar flow element, which is proportional to the flow rate. Water condensing in this element increases the pressure drop and gives a measured flow rate that is higher than the actual flow. The three runs using a 10% solution of K_2CO_3 were made before condensors were installed ahead of flow rate measurement and sampling locations. The three data points on Figure 25 representing the largest deviation between measured and predicted values, correspond to these three runs. It should also be noted that 200 mol/h of gas was typically absorbed in the absorber column and desorbed in regeneration. Relative to these flows, the deviations between measured and predicted flash gas flow rates are small.

Measured and predicted acid gas flow rates are shown in Figure 26. Flow rates of this stream also varied considerably as solvent composition and AGRS conditions were changed. Predicted values fall within the 95% confidence interval for the measured value indicating good agreement between pilot plant operation and model predictions. Removals of CO_2, H_2S, and COS are presented as percentages of the rates at which the compounds were fed to the absorber. This approach was taken because the concentrations of CO_2, H_2S, and COS in the sour gas fed to the AGRS varied significantly.

Measured and predicted percentage removals of CO_2 (the key component) are given in Figure 27. The upper region of Figure 27 is shown in greater detail in Figure 28. As shown in Figure 27, the removal of CO_2 varied greatly as the solvent composition and AGRS operating conditions were varied. Data points in Figures 27 and 28 fall randomly about the diagonal, demonstrating no bias in either the experimental measurements or

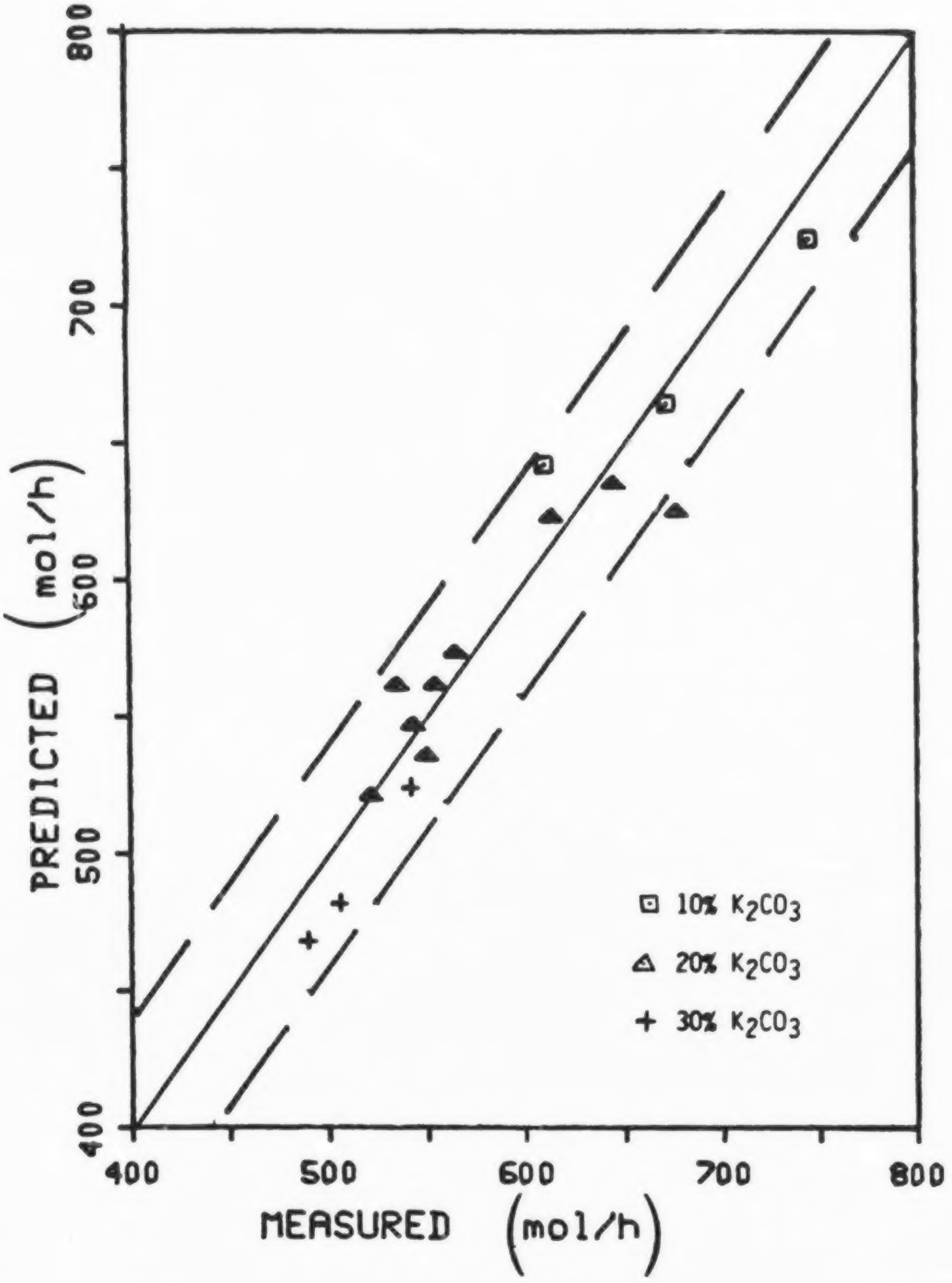

Figure 24 Measured and Predicted Sweet Gas Flow Rates

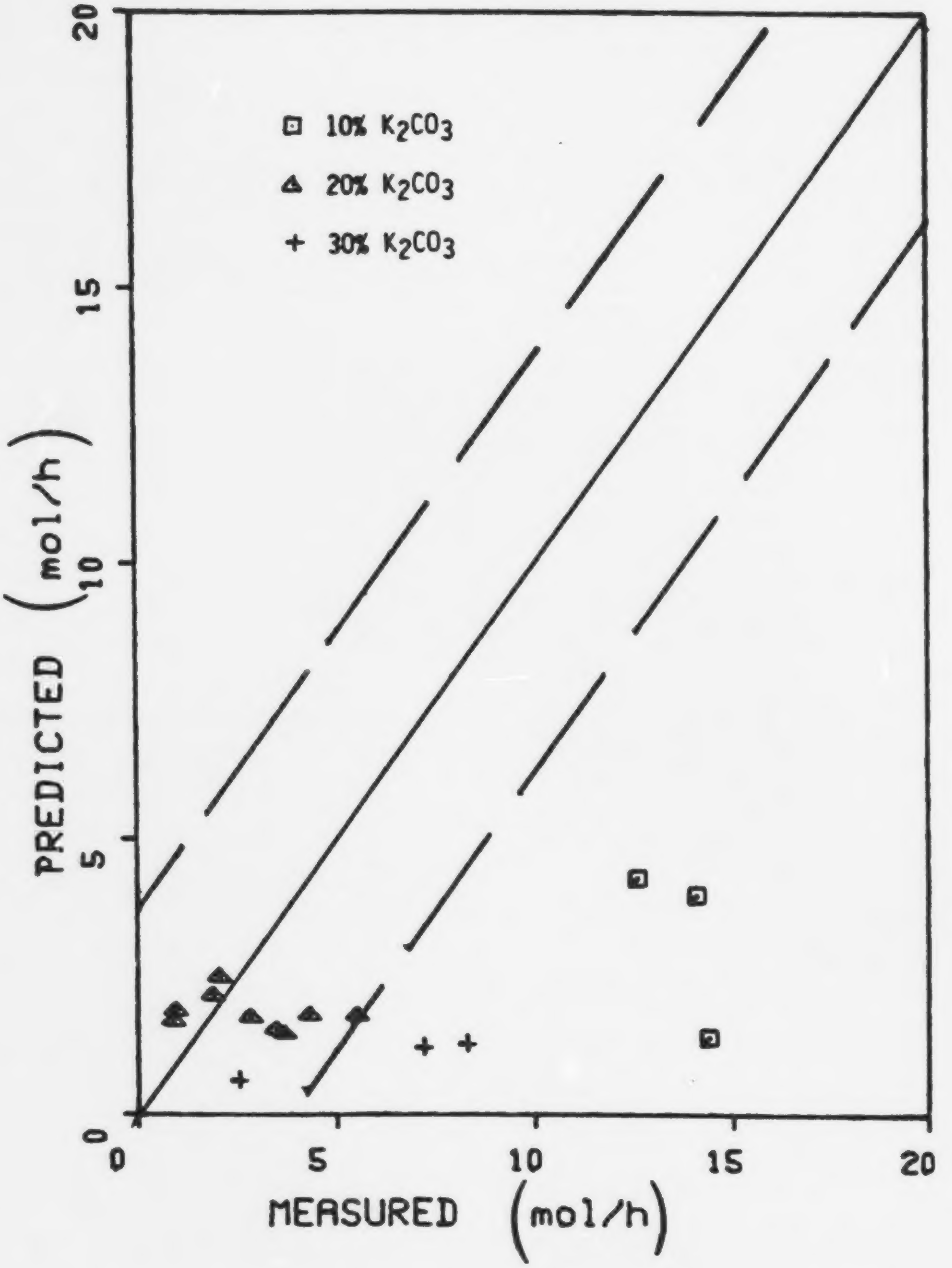

Figure 25 Measured and Predicted Flash Gas Flow Rates

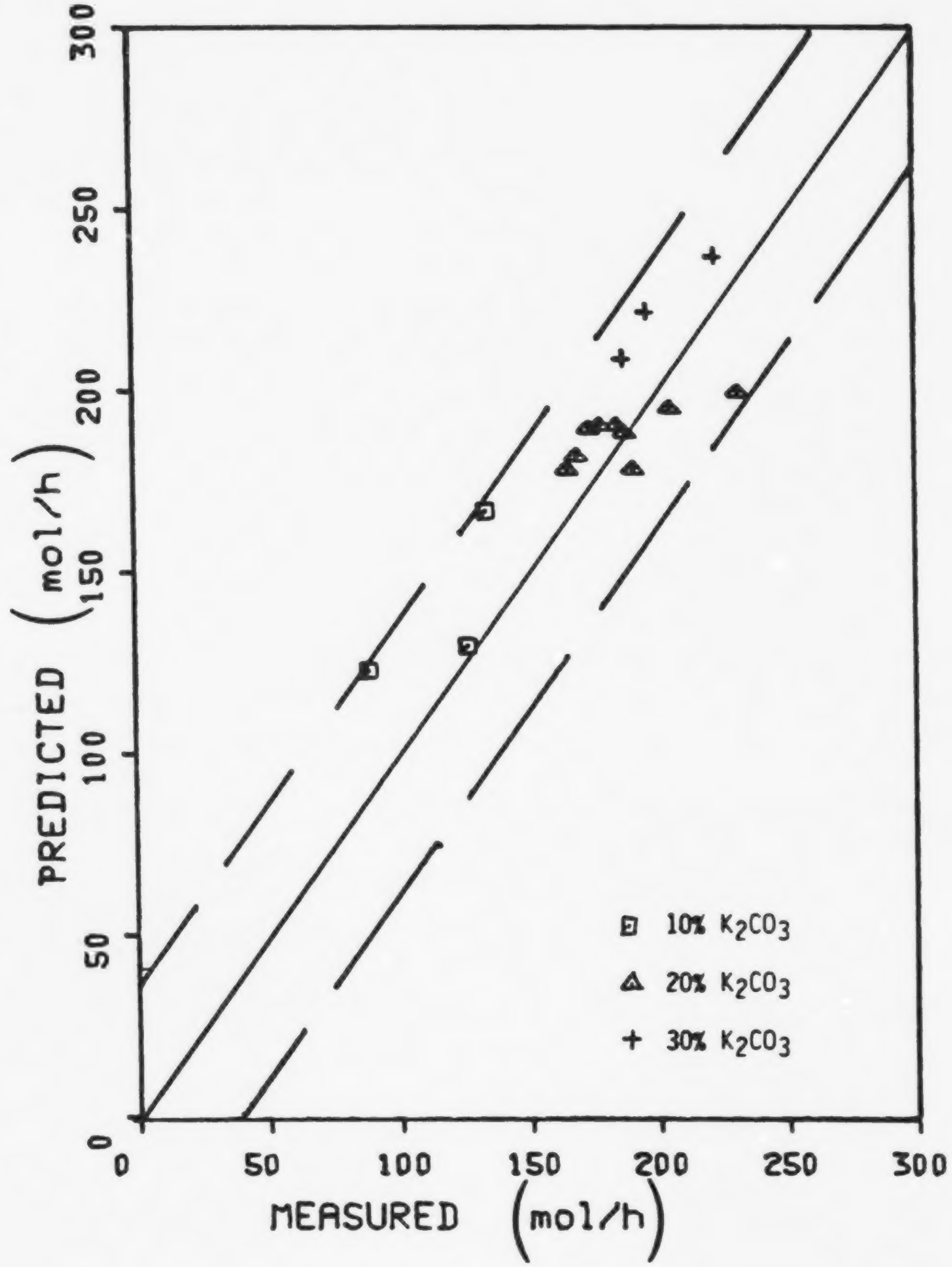

Figure 26 Measured and Predicted Acid Gas Flow Rates

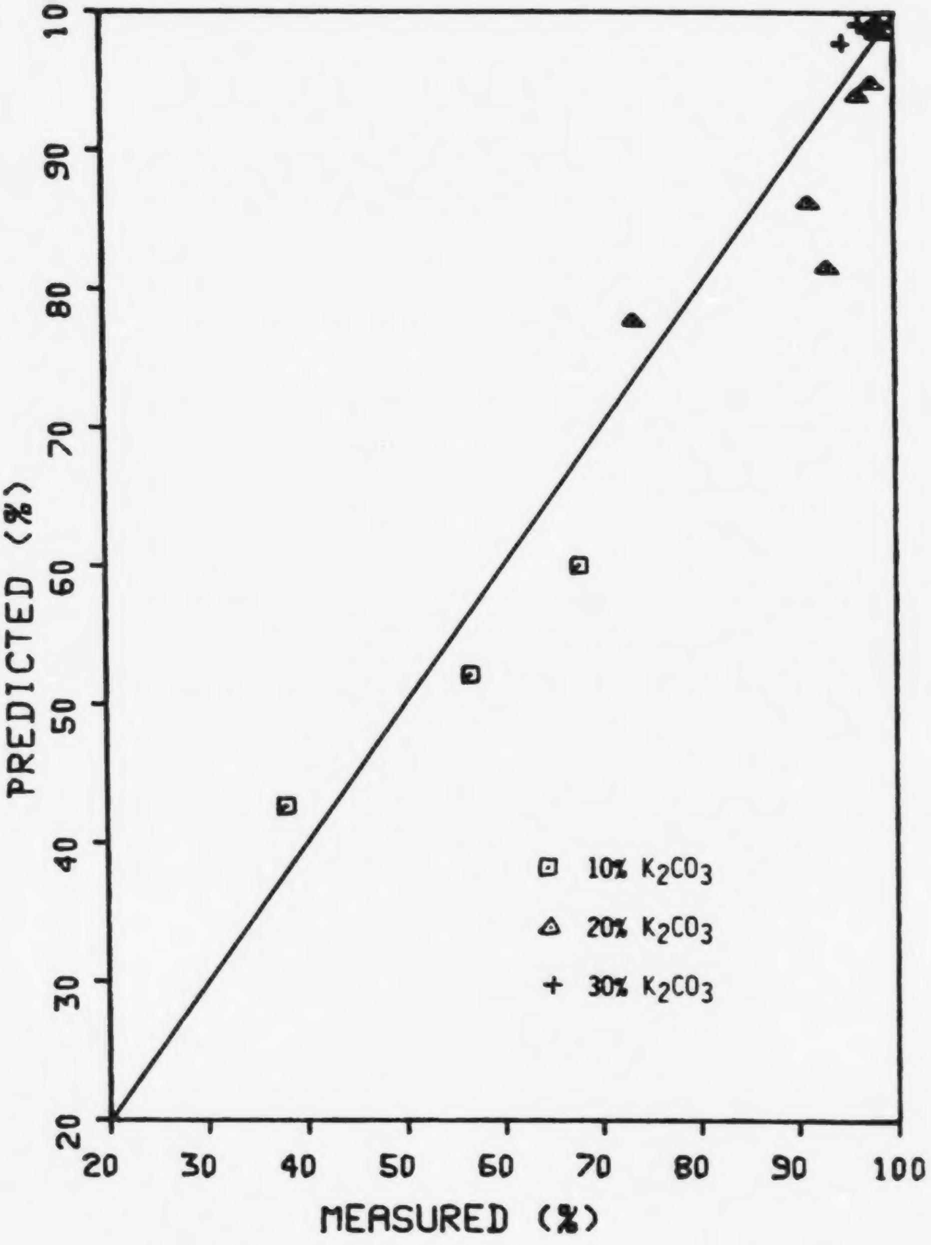

Figure 27 Measured and Predicted Removals of CO2

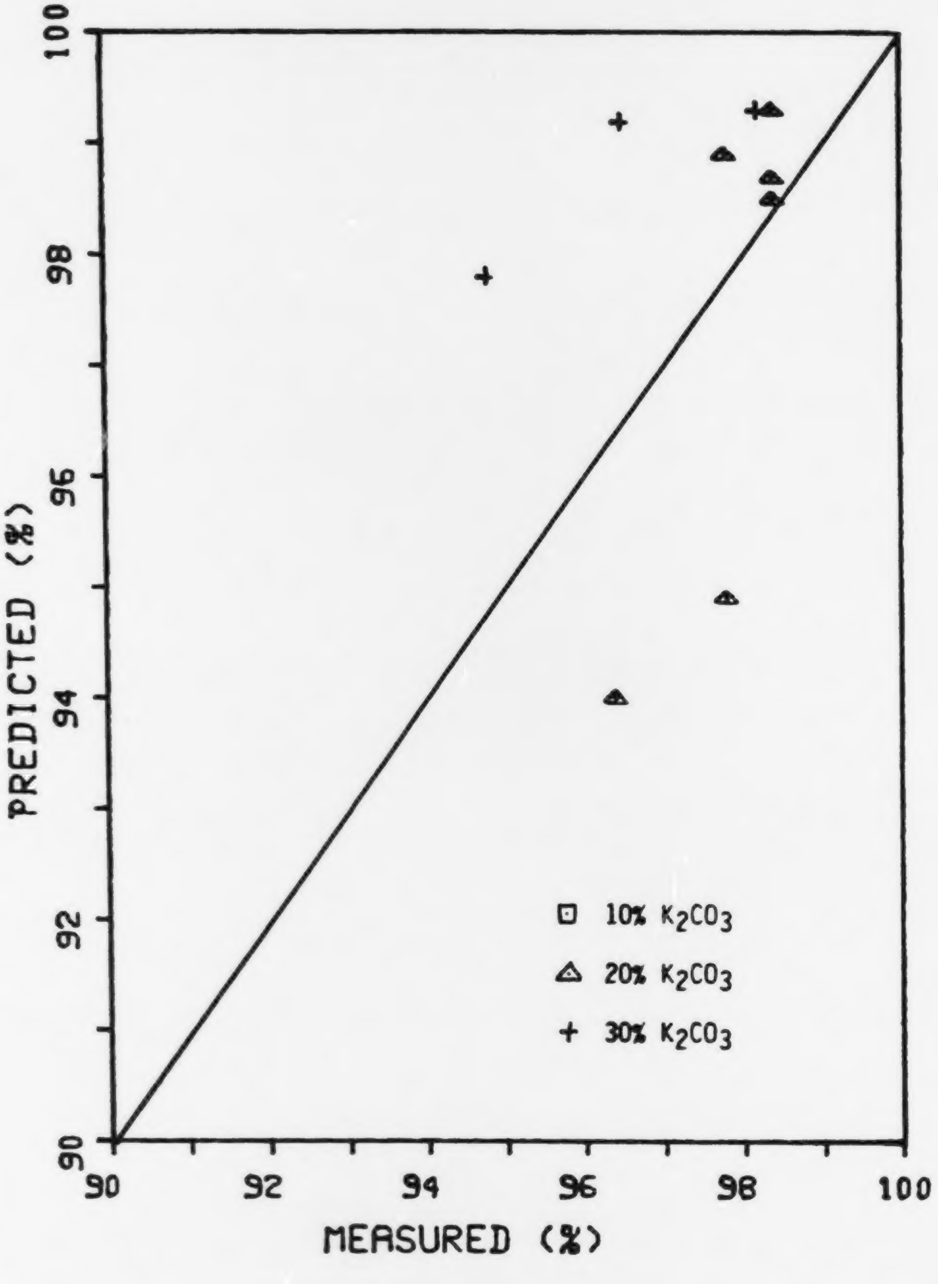

Figure 28 Measured and Predicted Removals of CO2 Greater Than 90%

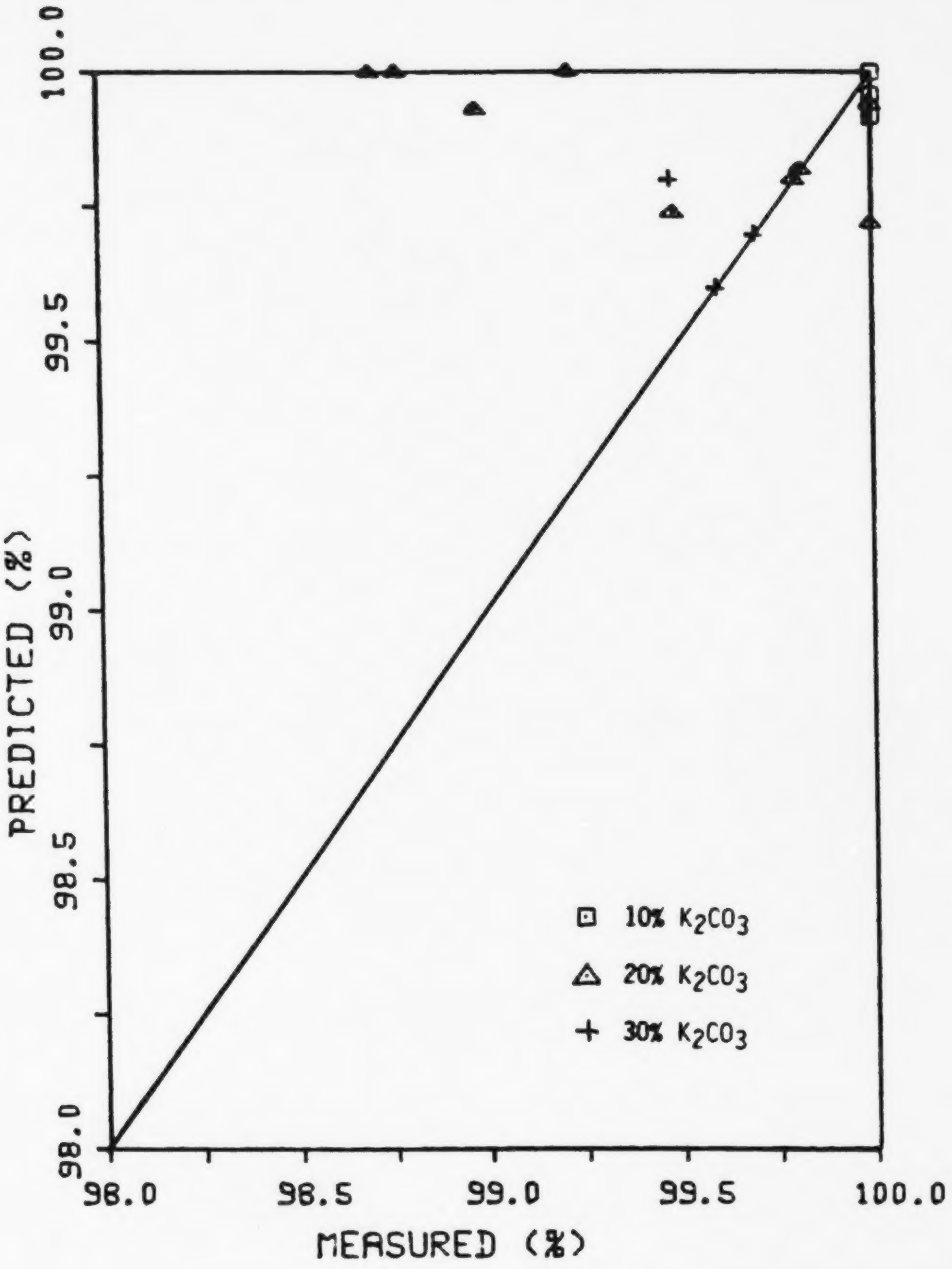

Figure 29 Measured and Predicted Removals of H2S

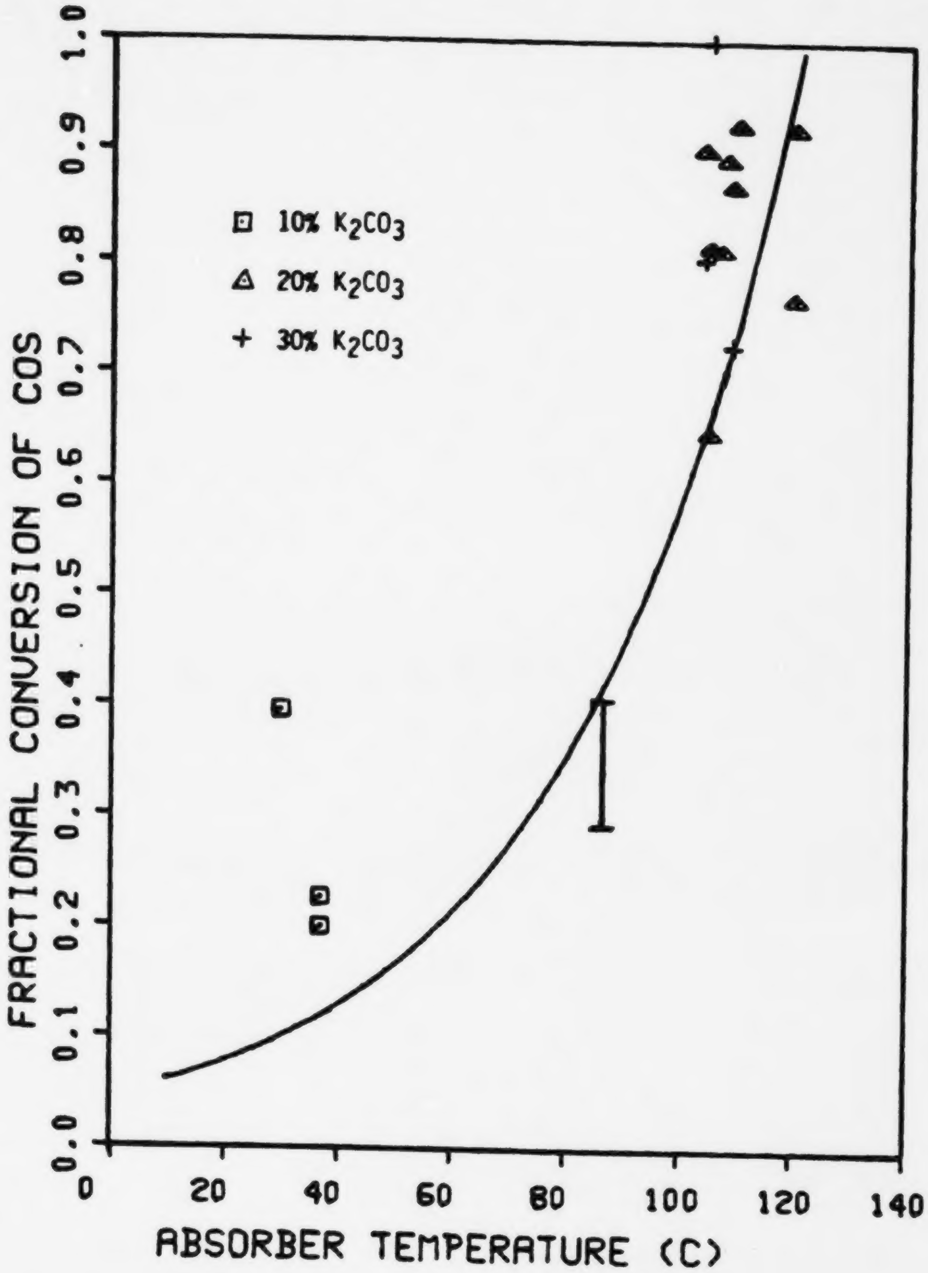

Figure 30 Fractional Conversion of COS

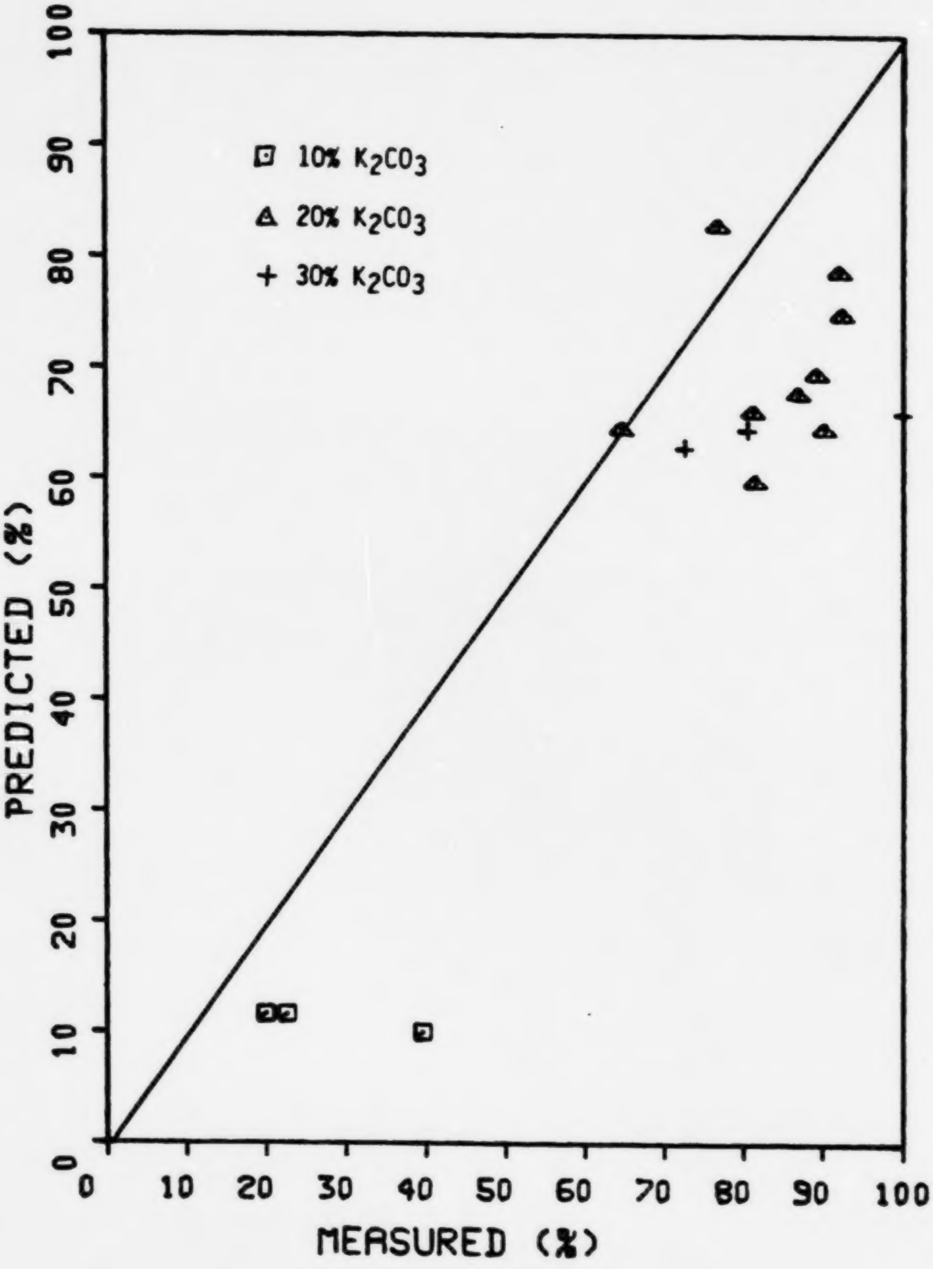

Figure 31 Predicted Removals of COS with Equation 12.1

the model predictions. The agreement between measured and predicted values is considered good.

Measured and predicted removals of H_2S are shown in Figure 29. It should be noted that the total scale on Figure 29 is 98% to 100%, and that points far from the diagonal represent a small deviation between measured and predicted values. Agreement between measured and predicted removals of H_2S is considered very good, supporting the assumption that the absorption and regeneration of H_2S are controlled by equilibria at the tops of absorber and stripping columns. This agreement also indicates that the equilibrium equations used in the model for the relationship between the equilibriums of reactive components in the liquid give good results.

As mentioned previously, COS removal was assumed to be a function only of absorber temperature, based on information given by the Benfield Corporation (Parrish and Neilson, 1974) and General Electric Corporation (Rib et al., 1983). Parrish and Neilson (1974) reported that the rate of hydrolysis of COS was a strong function of temperature (doubling with a 50°F increase) but it was insensitive to solvent composition. Parrish and Neilson (1974) reported that in pilot plant operation at a temperature of 250°F, 99.4% of the COS was removed. An Arrhenius relationship for the removal of COS as a function of absorber temperature was fitted to this information:

$$\xi = 0.0474 \exp \left(0.0251\ T(^{\circ}C)\right) \tag{161}$$

where ξ is the fractional conversion of COS. Rib et al. (1983) reported that 30% to 40% of COS was removed in a pilot plant at 85°C. Shown in Figure 30 are a curve representing Equation 161, a vertical line representing the information of Rib et al. (1983), and the measured pilot plant removals of COS in the experimental work of this study. As shown in Figure 30, agreement between these three independent sets of data is good; however in most cases, removals of COS measured in the present study are higher than were observed in the other studies. This is thought to be a result of the relatively large absorber packing height used in the present study. The data points representing the experimental removals of COS with the largest deviations from Equation 161 are from runs where two sections of packing were used in the absorber. Other runs of this study employed one section of absorber packing.

Model predictions of the absorption of COS were made with Equation 161 and are shown in Figure 31. As can be seen, measured values are typically greater than the corresponding predicted value. Since the parameters in Equation 161 are dependent on the characteristics of an absorption column, a similar expression was fitted to the pilot plant data obtained in this study:

$$\xi = 0.1614 \exp \left(0.01502\ T(^{\circ}C)\right) \tag{162}$$

Figure 32 shows a comparison of measured and predicted removals of COS using Equation 162. Clearly, the agreement is better than that obtained using Equation 161, and supports the assumption that COS removal is a function only of absorber temperature.

Model simulations aid with the explanation of observations from the experimental study. For example, in Run ACIL-25, reducing the absorber pressure resulted in more selective removal of H_2S. This agrees with model predictions that were discussed earlier. In Run ACIL-26, changes in the reboiler steam flow rate did not appear to affect the sweet gas CO_2 concentration. Model simulation indicated that at these conditions, the absorption of CO_2 was controlled by a pinched condition at the bottom of the absorber. In this case, the concentration of CO_2 would be expected to be insensitive to regeneration.

In Run ACIL-27, the flow rate of steam to the reboiler was sufficient to heat the solvent to its boiling point, but was insufficient to boil a detectable amount of water vapor into the stripper packing. This resulted in a large increase in the sweet gas H_2S concentration, but had no significant effect on the corresponding concentration of CO_2. Model simulation indicated that at these conditions the absorption of CO_2 was again controlled by a pinch at the bottom of the absorber, while the absorption of H_2S was controlled by a pinched condition at the top of the absorber and consequently was highly sensitive to regeneration.

In Runs ACIL-27 and ACIL-30, using 2 sections of packing in the absorber did not give greater removal of CO_2 than was obtained with 1 section. Model simulation confirmed that at the conditions of these runs, 1 section of packing was sufficient for the absorption of CO_2 to be controlled by equilibrium or a pinched condition. In Run ACIL-28, an increase in absorber temperature resulted in a decrease in CO_2 absorption. Model simulation also confirmed that at these conditions the absorption of CO_2 was controlled by a pinched condition. In this case, an increase in the absorber temperature would result in a decrease in absorption due to a decrease in the solubility of CO_2 in the solvent.

In Run ACIN-2, increasing the stripper packing from 2 to 3 sections resulted in an increase in CO_2 absorption. Model simulation confirmed that at these conditions, the desorption of CO_2 was not controlled by equilibrium or, in other words, the stripper column was not pinched with respect to CO_2.

Finally in Runs ACIN-1 and ACIN-9, the addition of an amine additive for promotion of the mass transfer rate of CO_2 did not result in a large change in the concentration of CO_2 in the sweet gas. Since the amine does not cause a large change to the equilibrium behavior of CO_2 in K_2CO_3 solutions, it was concluded that the absorption

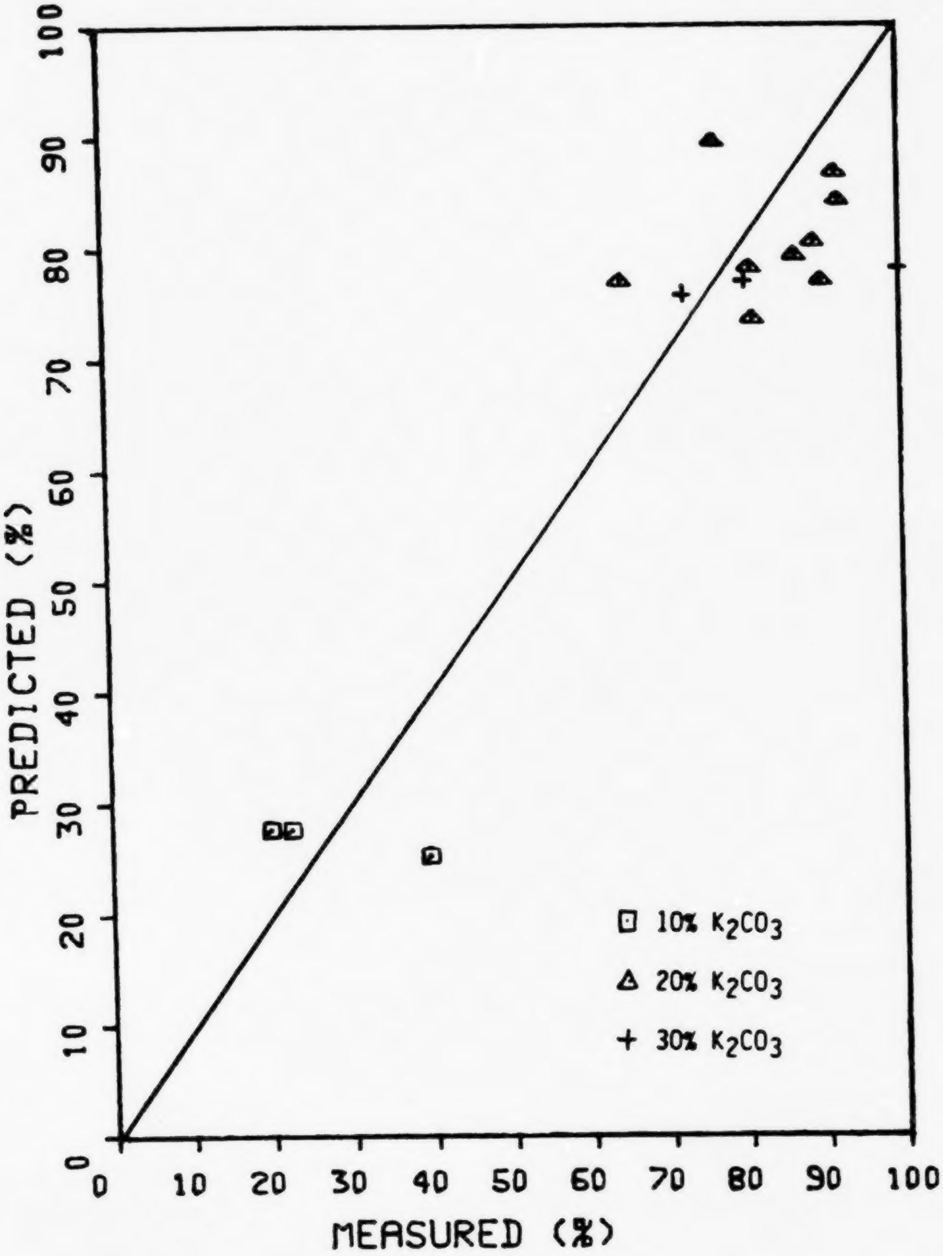

Figure 32 Predicted Removals of COS with Equation 12.2

of CO_2 was controlled by a pinched condition in these runs. This was confirmed by model simulation.

The model developed in this study for an acid gas removal system employing a chemical solvent is based on the mass transfer rate of a key component. The absorption and stripping of other components is characterized using equilibrium and mass balance relationships. An isothermal equilibrium flash algorithm was developed using the thermodynamic approach of Astarita et al. (1983).

The agreement between model predictions and pilot plant experimental data is considered quite good, supporting the assumptions used in the model. Although the computer programs developed in this study are specific to the hot potassium carbonate process, it is thought that a similar approach may be used with other chemical solvents to develop simulation programs to predict acid gas removal system operation.

APPLICATIONS

In the previous section, the model developed in this work was compared to experimental data obtained in a pilot plant facility. In addition to assisting with interpretation of pilot plant results, the model may be used to extend these results to situations not attainable in pilot plant operation. In this section, examples of how the model may be used are presented.

PARAMETRIC STUDIES

An important application of a system model is the examination of the effects of changes in process variables on system operation. This may be accomplished as part of a complex optimization procedure or as a simple one-variable sensitivity analysis.

To illustrate the use of the model in parametric studies, the mole fraction of CO_2 in the absorber exit gas was examined as AGRS operating variables were varied. Run ACIL-29 was chosen as the base set of conditions because AGRS operating conditions used in this run were typical of those used in the experimental work of this study, and because model simulations of this run indicated that the absorption of CO_2 in this run was not controlled by pinched conditions in the absorption or stripping columns.

Absorber pressure was examined first. Figure 33 shows predicted mole fractions of CO_2 in the absorber exit gas stream as a function of absorber pressure. Other AGRS operating variables in these simulations were identical to those of Run ACIL-29. As shown in Figure 33, changing the absorber pressure gave significant changes in the removal of CO_2 from the crude coal gas; the mole fraction of CO_2 in the absorber exit gas decreased from approximately 7% to 0.25% as the absorber pressure was increased from 1000 kPa to 5000 kPa.

Figure 34 shows predicted mole fractions of CO_2 in the absorber exit gas as a function of absorber temperature. As shown, the sweet gas mole fraction of CO_2 decreased as the absorber temperature was increased from 50°C to 100°C, but increased as the absorber temperature was increased above 100°C. This is a result of the effects of

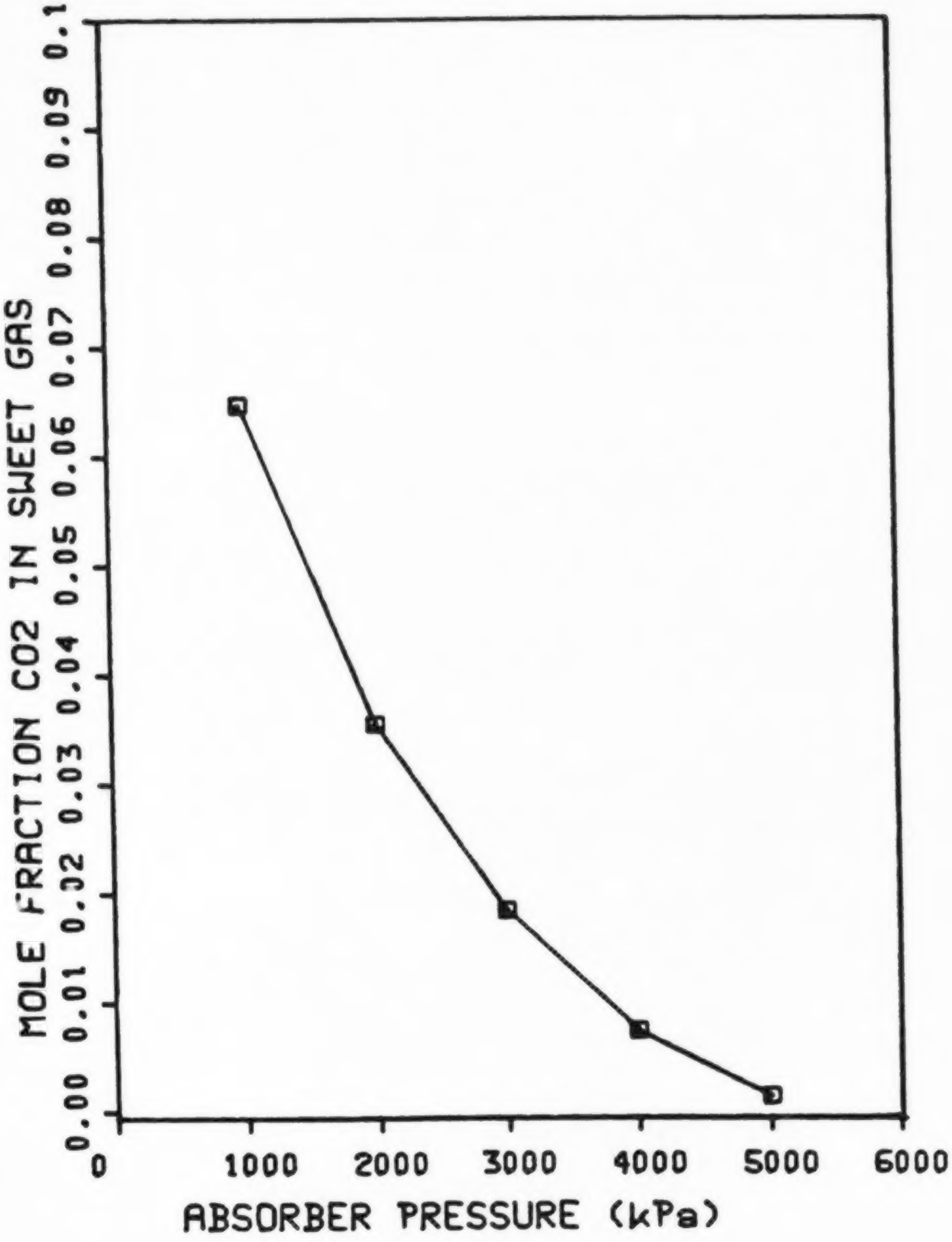

Figure 33 Effect of Absorber Pressure on Absorption of CO2

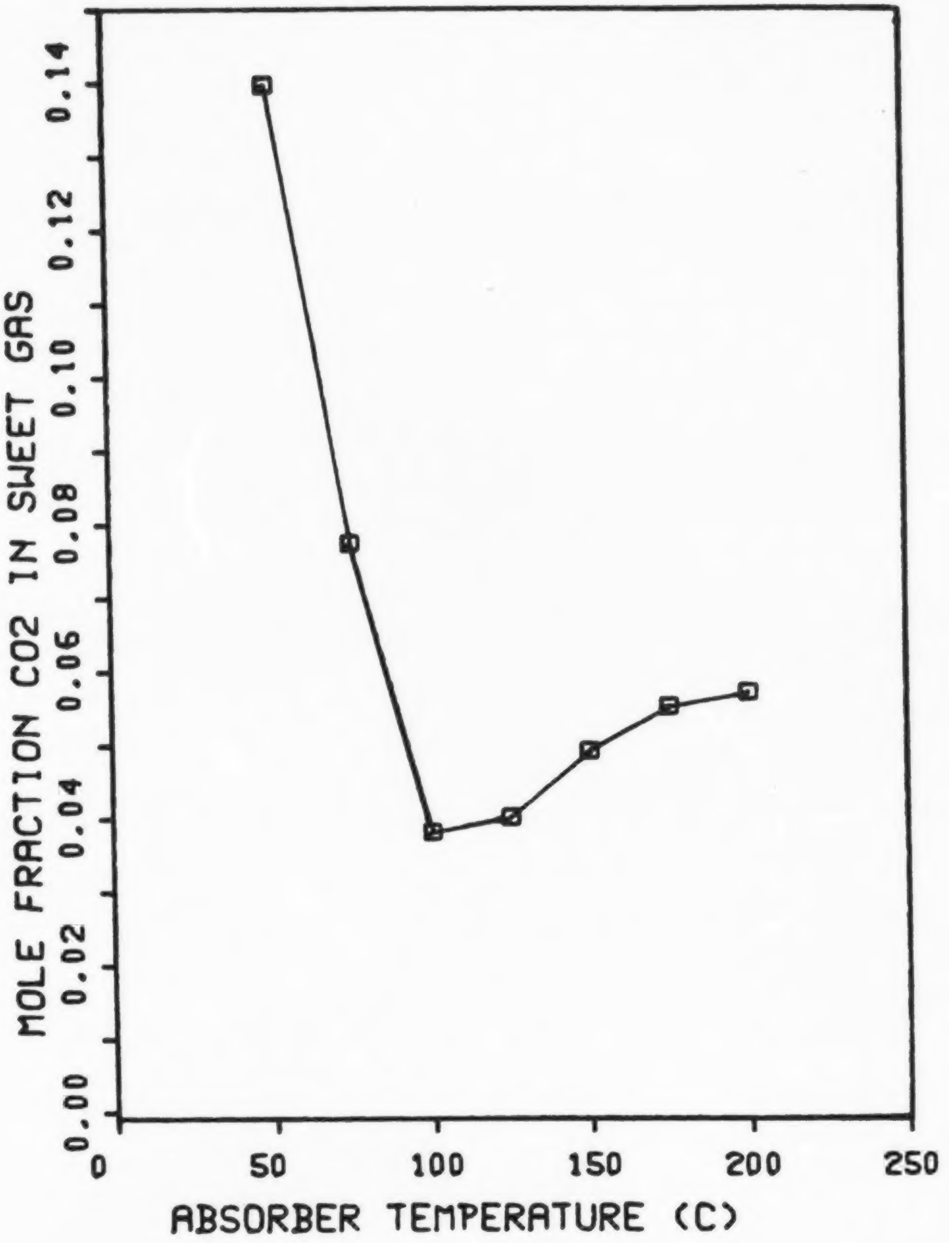

Figure 34 Effect of Absorber Temperature on Absorption of CO2

temperature on the mass transfer rate and equilibrium of CO_2. At low temperatures, the rate of absorption of CO_2 is mass-transfer limited, and increases with temperature. At a temperature of 100°C, the rate of mass transfer of CO_2 was sufficient to cause the occurance of a pinched condition, and the absorption of CO_2 became controlled by equilibrium between the gas and liquid phases at some point in the column. As the temperature was increased further, the absorption of CO_2 decreased as a result of the decreasing solubility of CO_2 in the solvent.

These effects may be seen in detail by examining the effects of temperature, with other independent variables held constant, on the mass transfer rate and equilibrium of CO_2 in a single differential element in the absorber. Figure 35 gives calculated values of the enhancement factor as a function of absorber temperature. At 50°C there is little mass transfer rate enhancement and the calculated value of the enhancement factor was approximately 1. The enhancement factor, however, increased with temperature, and was approximately 9 at 200°C. The discontinuity in Figure 35 represents a transition from the general solution for the enhancement factor to that given by the instantaneous reaction regime asymptotic solution. Also increasing with temperature were the physical mass transfer coefficients for the gas and liquid phases. In Figure 36, this is represented by an increase in the overall mass transfer coefficient, K_{oG}.

Shown in Figure 37 as a function of absorber temperature is the equilibrium mole fraction of CO_2, $Y^*_{CO_2}$ in Equation 133. Since the mass transfer rate of CO_2 is expressed with an overall mass transfer coefficient, changes in $Y^*_{CO_2}$ represent a corresponding change in the driving force for mass transfer of CO_2 between the gas and liquid phases. As seen, $Y^*_{CO_2}$ increased as the temperature increased from 50°C to 100°C, but decreased with further increases in temperature. This may be explained by recalling that the equilibrium partial pressure of CO_2 is proportional to the ratio of the Henry's law constant to the reaction equilibrium constant (Equation 42). At low temperatures, the reaction equilibrium constant decreases rapidly as the temperature is increased, and the ratio increases. At higher temperatures, the reaction equilibrium constant decreases more slowly as the temperature is increased, and a decrease in the Henry's law constant causes the ratio to also decrease.

Figure 38 shows predicted mole fractions of CO_2 in the absorber exit gas as a function of absorber inlet gas flow rate. Since other variables in these simulations were maintained at that of Run ACIL-29, increasing the absorber inlet gas flow rate corresponded to decreasing the liquid-to-gas ratio in the absorber. As shown in Figure 38, this had a significant effect on the mole fraction of CO_2 in the absorber exit gas.

Also examined was absorber packing height. Shown in Figure 39 are predicted mole fractions of CO_2 in the absorber exit gas as a function of absorber packing height. Increasing the height resulted in a decrease in the mole fraction of CO_2 in the absorber exit gas, until the packing reached a height that was sufficient to cause a pinched

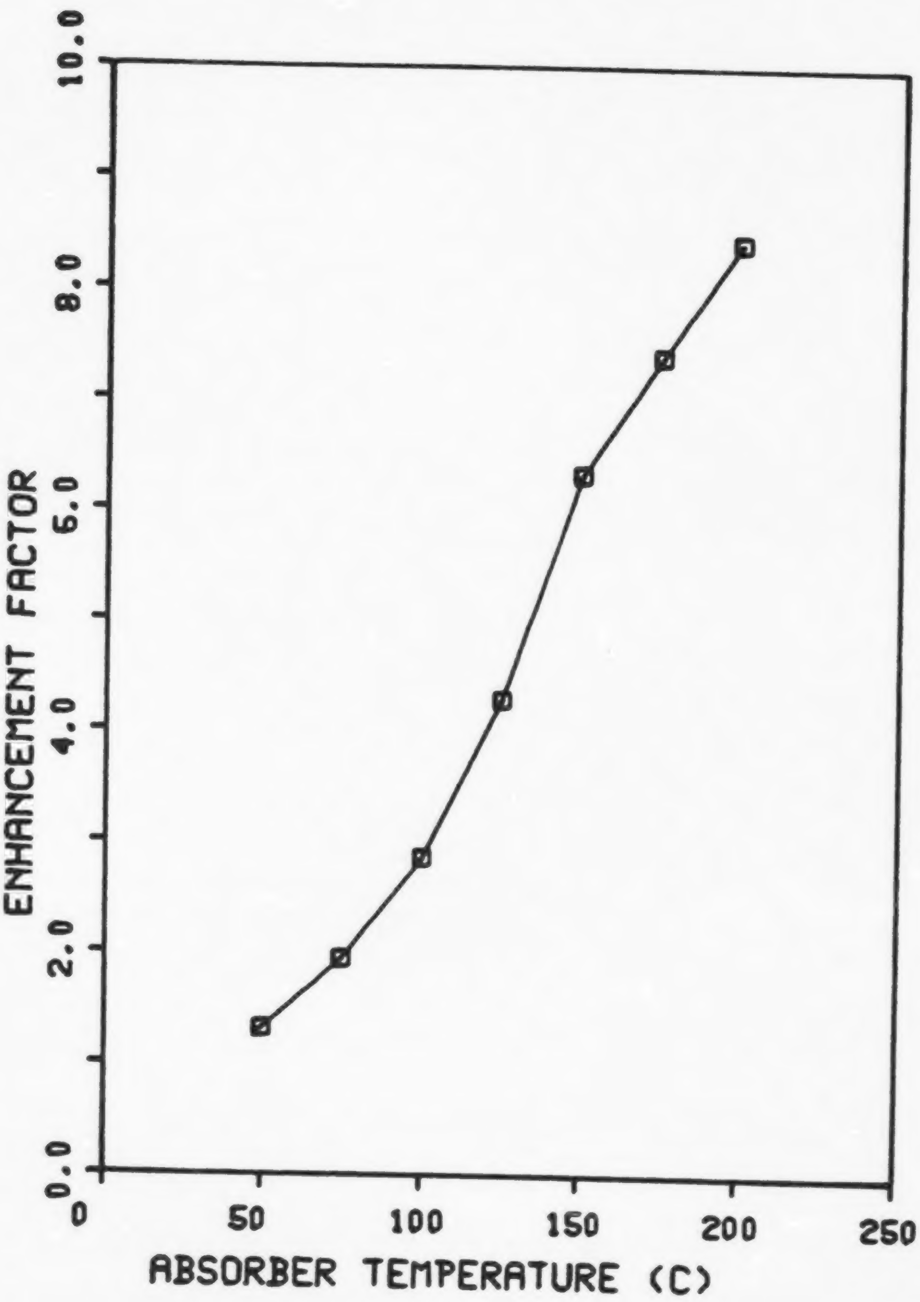

Figure 35 Effect of Absorber Temperature on Enhancement Factor

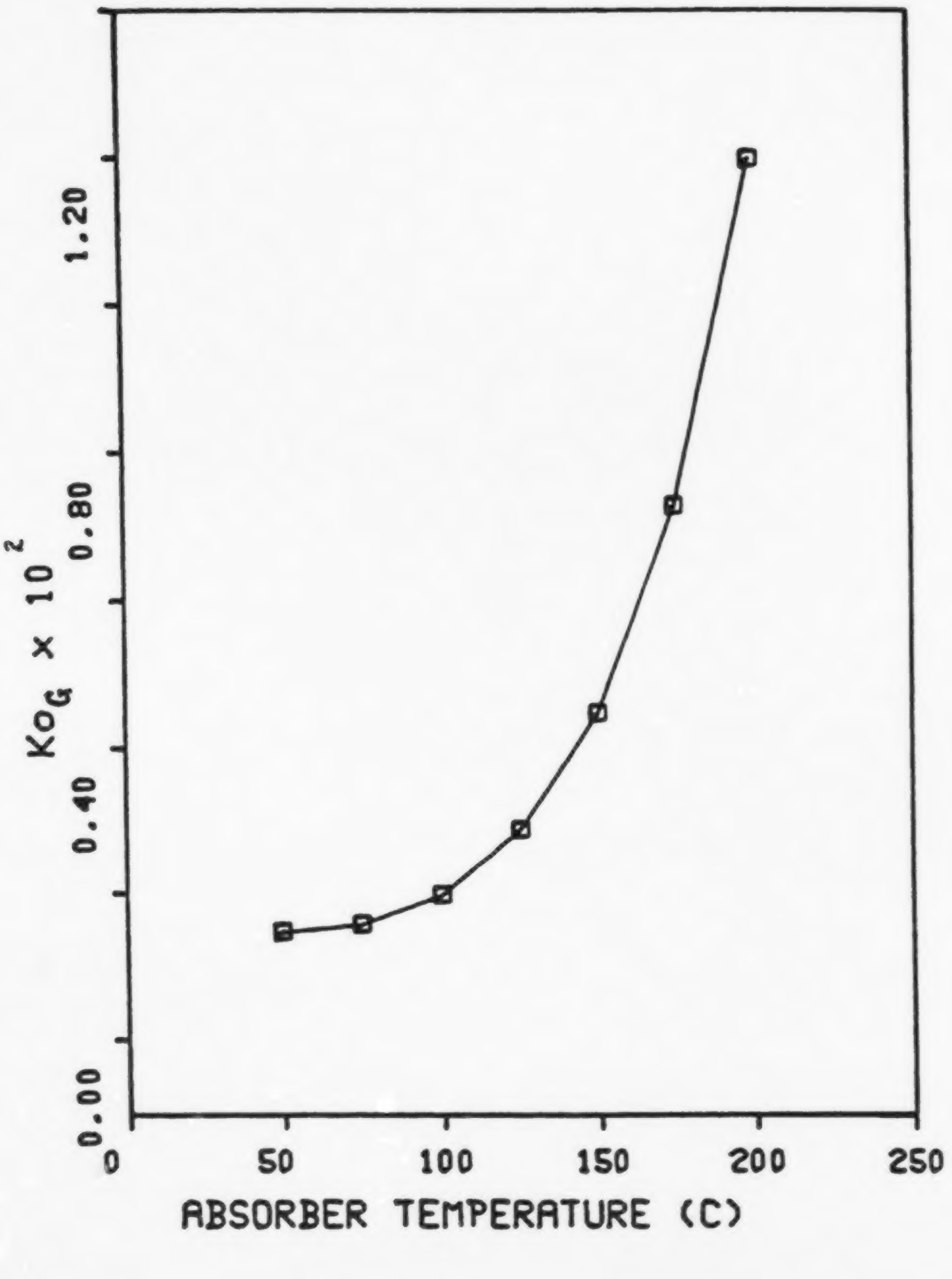

Figure 36 Effect of Absorber Temperature on Overall Mass Transfer Coefficient of CO2

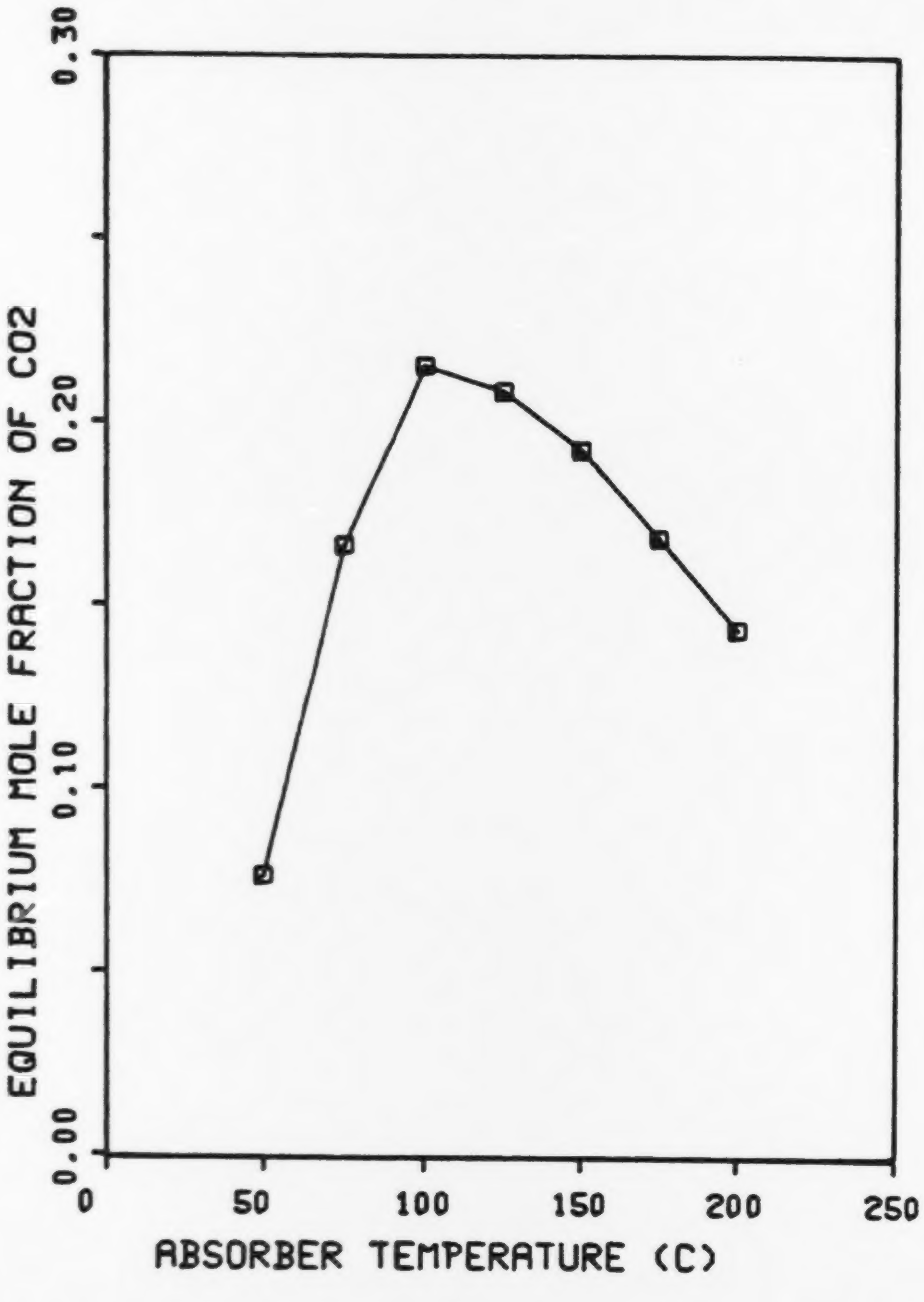

Figure 37 Effect of Absorber Temperature on Equilibrium Gas Phase Mole Fraction of CO2

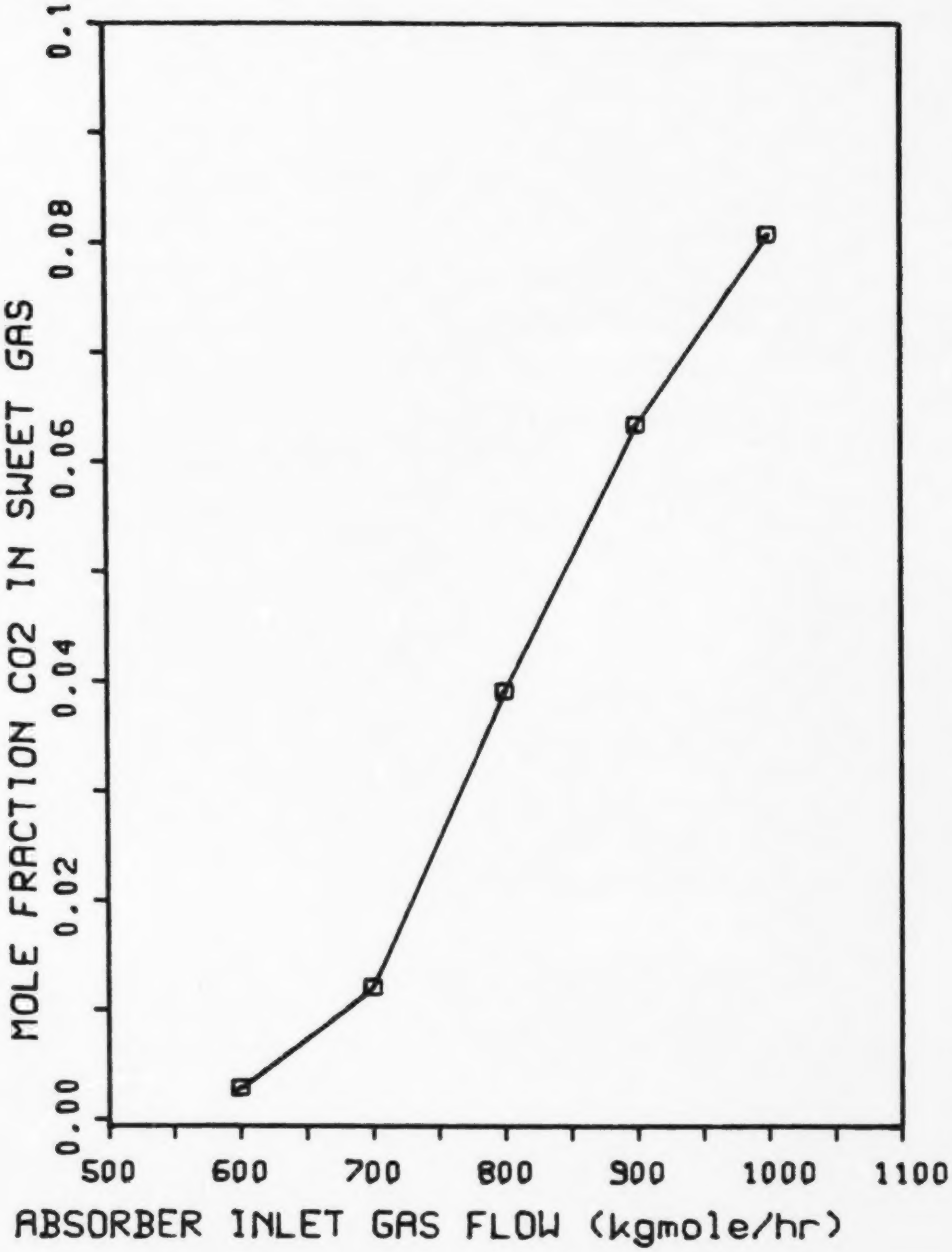

Figure 38 Effect of Absorber Gas Flow Rate on Absorption of CO2

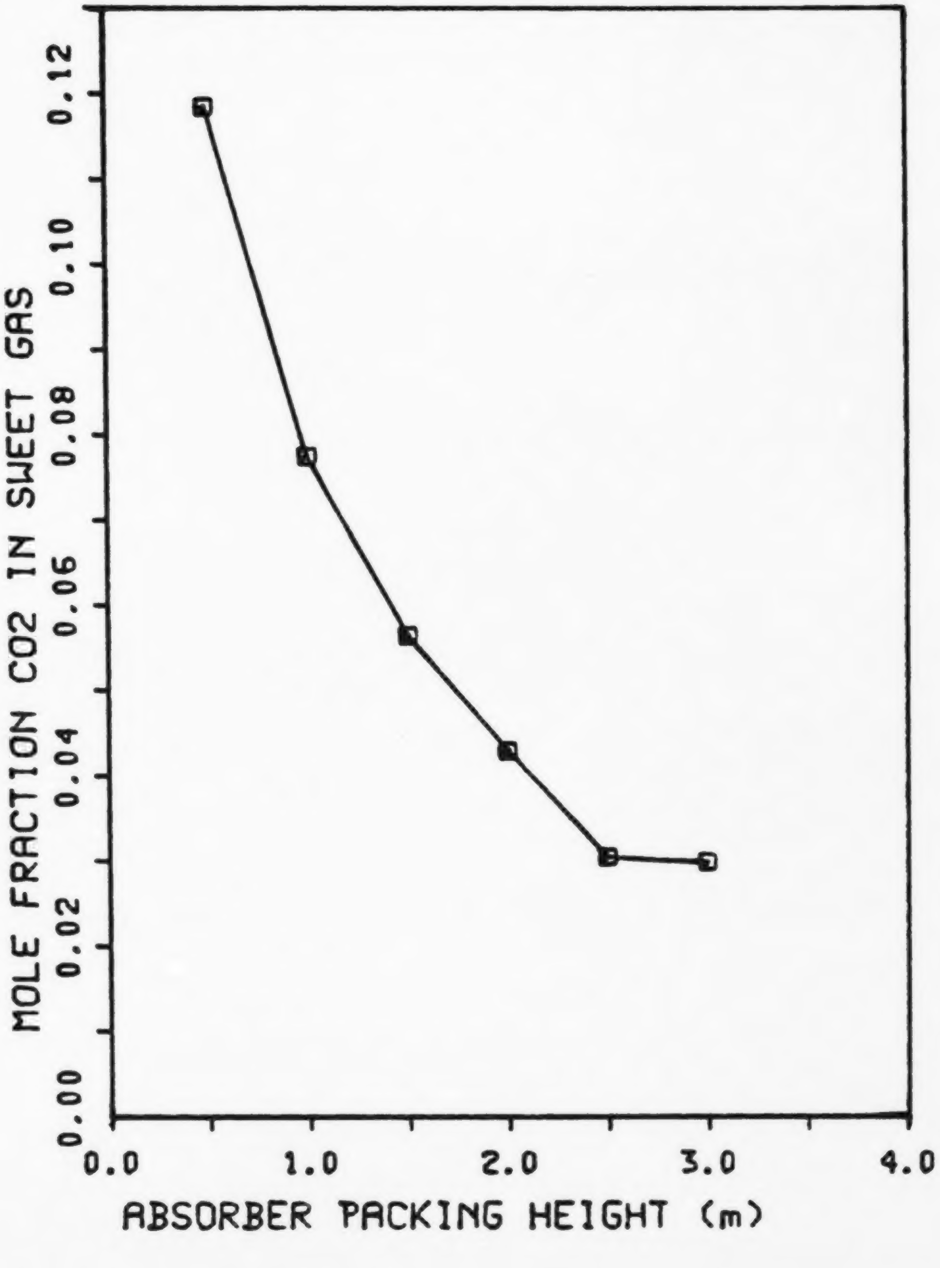

Figure 39 Effect of Absorber Packing Height on Absorption of CO2

condition. At a pinched condition the absorption of CO_2 is controlled by equilibrium, and further increases in the packing height do not increase absorption. It is interesting to note the shape of the plot in Figure 39. As the packing height approached that sufficient for a pinched condition, the effect of additional packing became less.

In some situations, acid gas removal is governed primarily by the composition of the liquid stream returned to the absorber from regeneration operations. Model predictions and pilot plant experimental results indicate that the regeneration of CO_2 accomplished by flashing is not significant with this solvent. Hence, changing flash tank operating conditions does not have a significant effect on the absorption of CO_2 and is not examined in this section.

Stripping column operating conditions determine regeneration efficiency. When a stripping column is operated with a reboiler, the stripping column temperature is set by the boiling point of the solvent at the reboiler pressure. As a consequence, stripping column temperature and pressure can not be varied independently. In addition, the boiling point of the solvent determines the absorber temperature.

Figure 40 illustrates the effect of stripper packing height on the mole fraction of CO_2 in the absorber exit gas. As shown, the absorption of CO_2 is highly dependent on stripper height at the conditions of Run ACIL-29. At a height of approximately 10 meters, the stripper packing was sufficient to cause a pinched condition, and further increases in the packing height had no effect on the absorption of CO_2. This is in agreement with the results of Run ACIN-2 that indicated the desorption of CO_2 was not controlled by a pinched condition when 6.48 meters of packing were used in the stripping column. It is interesting to note that at the conditions of Run ACIL-29, 10 meters of packing were required for a pinched condition in stripping, while only 2.5 meters were required in absorption. Due to the shape of the equilibrium curve, the driving force for mass transfer of CO_2 is greater in absorption than in stripping. Since increases in packing height have a smaller effect at lower mass transfer rates, this difference in packing required for a pinch would be expected.

Figure 41 gives predicted mole fractions of CO_2 in the absorber exit gas as a function of reboiler steam flow rate. Since this variable determines the flow rate of vapor generated in the reboiler, increasing this flow rate corresponds to decreasing the liquid-to-gas ratio in the stripping column. As shown, this decrease also had a large effect on the absorption of CO_2 at the conditions of Run ACIL-29.

In most acid gas removal systems, regeneration sets process energy requirements and the distribution of recovered acid gases. These results illustrate that regeneration may also govern absorber performance.

Figure 42 shows the effect of K_2CO_3 concentration on the mole fraction of CO_2 in

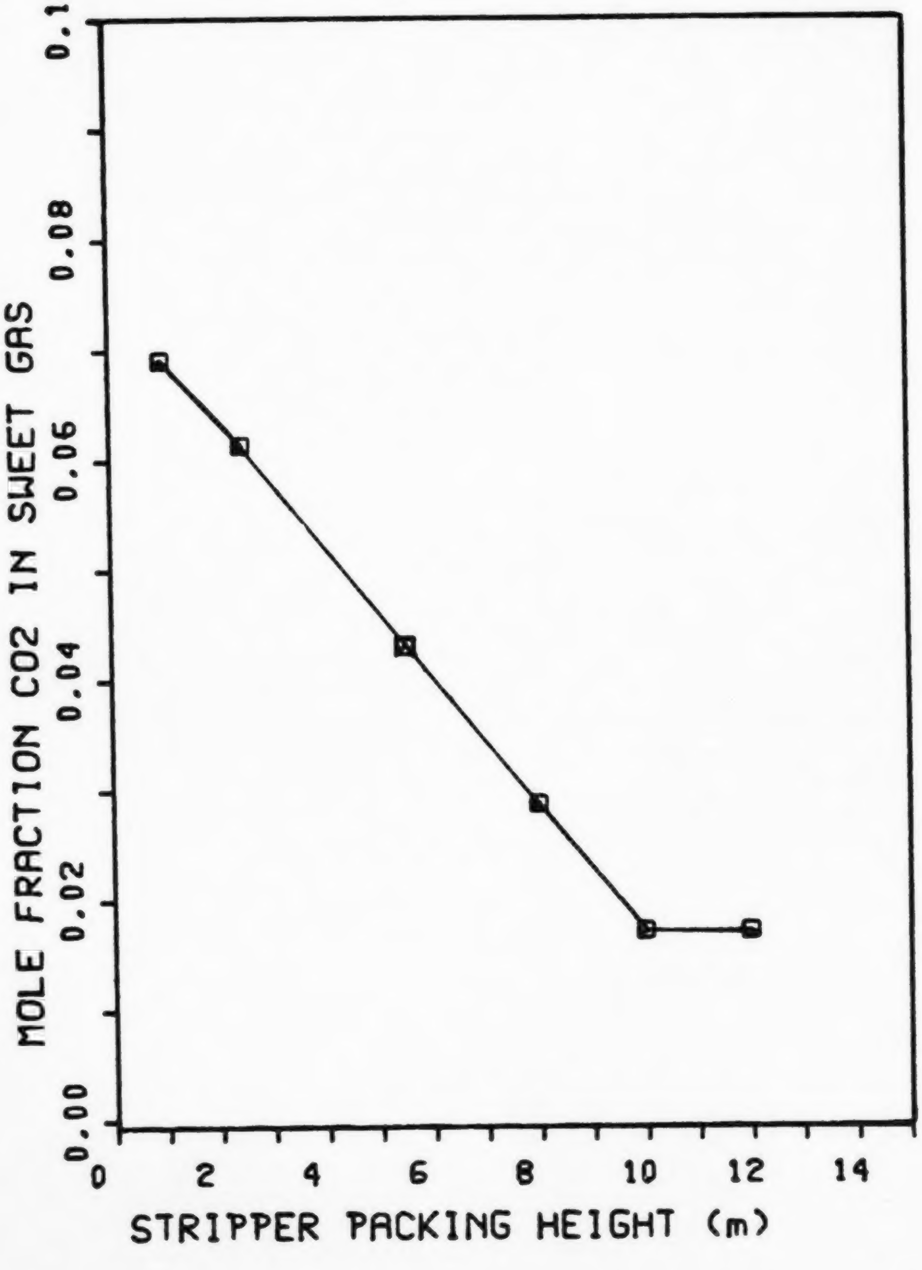

Figure 40 Effect of Stripper Packing Height on Absorption of CO2

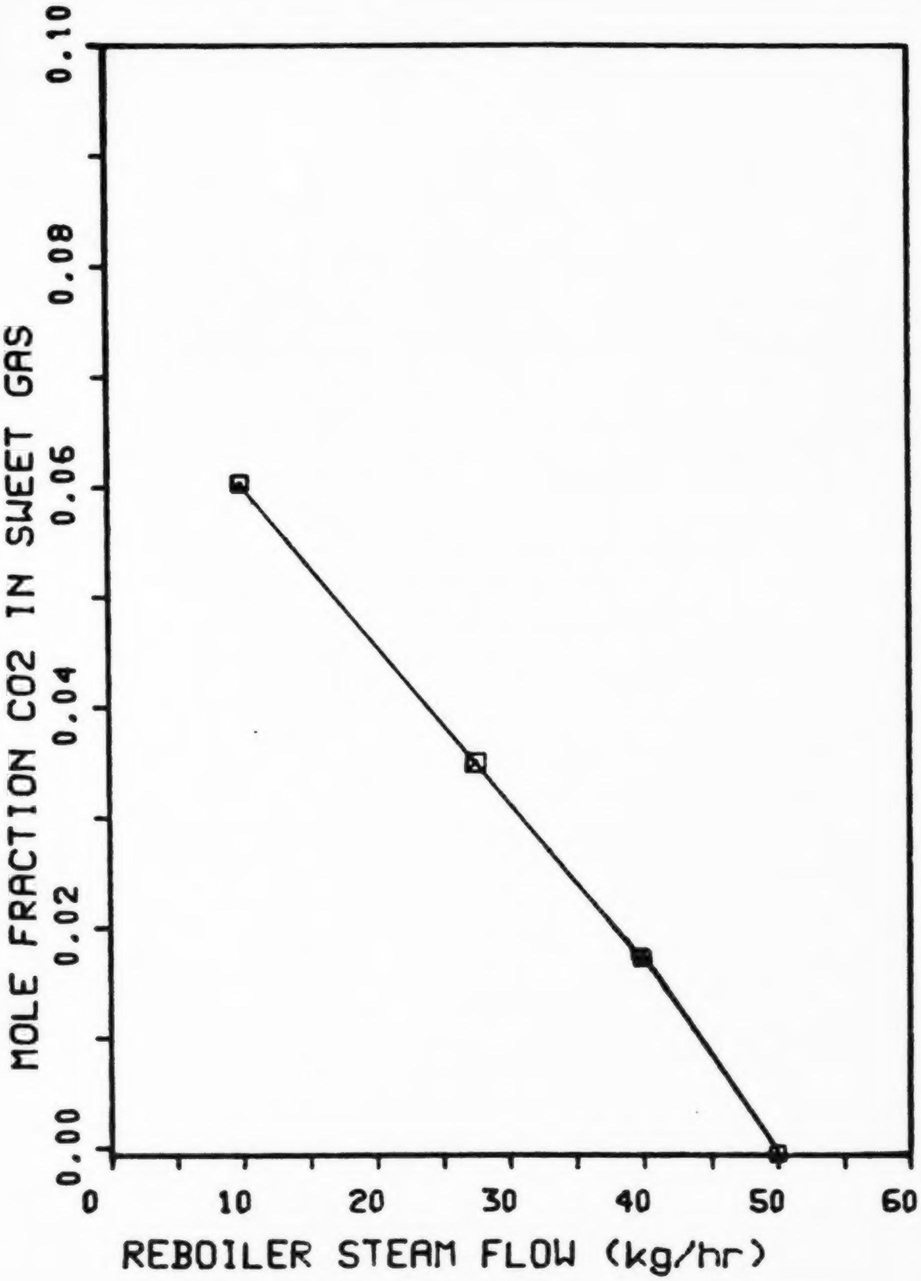

Figure 41 Effect of Reboiler Steam Flow Rate on Absorption of CO2

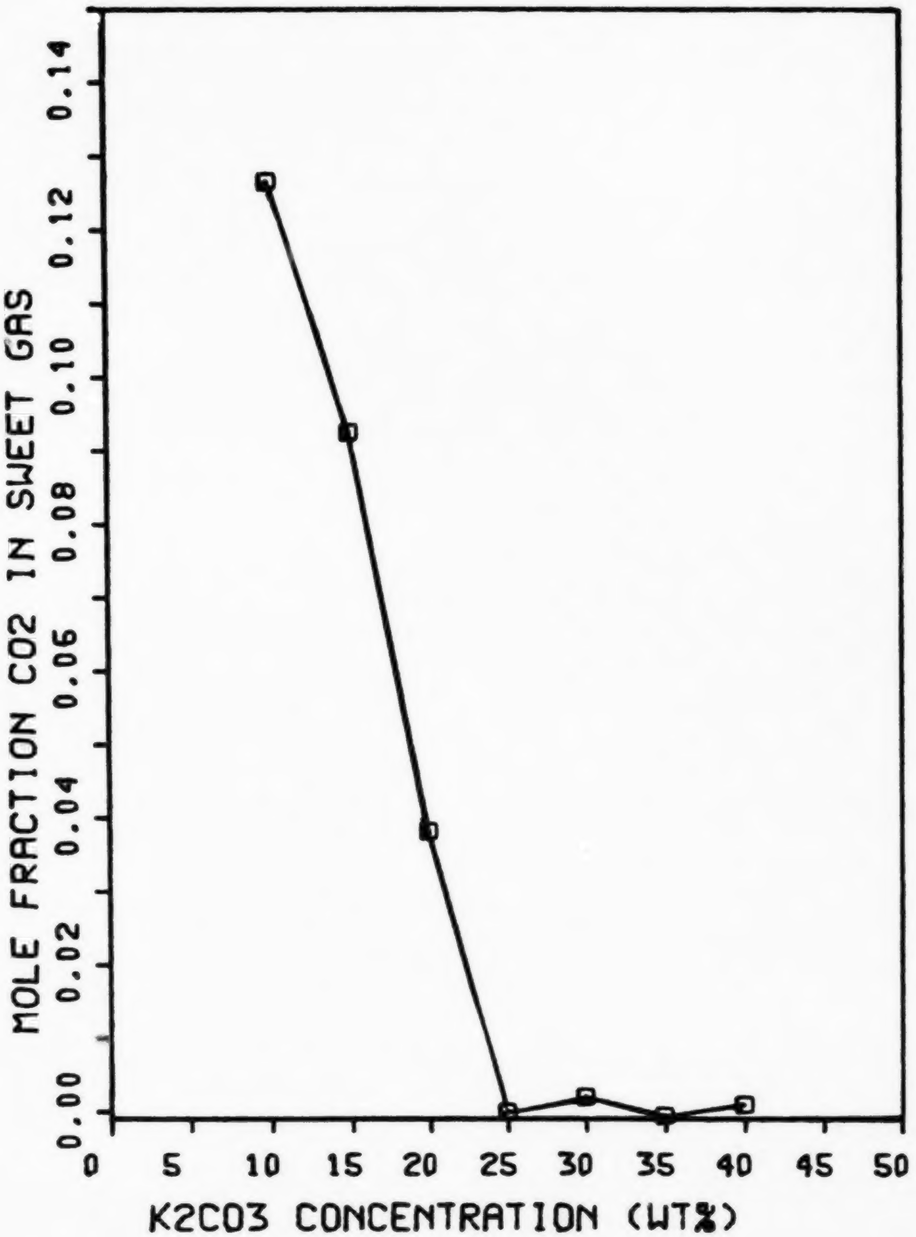

Figure 42 Effect of Solvent Composition on Absorption of CO2

the absorber exit gas. At the conditions of Run ACIL-29, increasing the concentration of K_2CO_3 from 10% to 25% had a large effect on the absorption of CO_2. Further increases, however, had no significant effect. Similar results were obtained with the pilot plant. Such behavior is a result of the equilibrium of CO_2 in K_2CO_3 solutions and is explained in the following paragraphs.

Consider the equilibrium relationships and operating lines of Figure 43. Operating lines with slope Lm/G represent mass balances, where L is the liquid flow rate, m is the solvent molarity, and G is the gas flow rate. In Figure 43 there is an intersection between operating lines and equilibrium relationship at the top of the diagram. This represents a pinched condition at the bottom of the absorber, and fixes the position of the corresponding operating line and the exit liquid composition. The intersection of the operating line and y_{in} (fractional saturation of the entering liquid) gives the partial pressure of CO_2 in the absorber exit gas. As can be seen in Figure 43, the partial pressures of CO_2 in the absorber exit gas corresponding to the three operating lines are significantly different. Hence, increasing the K_2CO_3 concentration, when absorption is controlled by a pinched condition at the bottom of the absorber, significantly reduces the partial pressure of CO_2 in the absorber exit gas.

Now consider Figure 44 which shows intersections between operating lines and equilibrium relationships at the bottom of the diagram, and represents a pinched condition at the top of the absorber. As can be seen, the partial pressures of CO_2 in the absorber exit gas corresponding to the three operating lines are not significantly different. Hence, when absorption is controlled by a pinched condition at the top of the absorber, the effect of increasing the concentration of K_2CO_3 on the partial pressure of CO_2 in the absorber exit gas is small.

The slope of the operating lines of Figure 44 is greater than that of the operating lines of Figure 43. Recalling that the slope of an operating line on this type of diagram is the ratio Lm/G, it is clear that increasing the concentration of K_2CO_3 in the solvent increases the probability that an intersection will occur as in Figure 44. The simulations of Figure 42 agree with this analysis. At low K_2CO_3 concentrations, the model indicates that the absorption of CO_2 is controlled by a pinched condition at the bottom of the absorber. At a K_2CO_3 concentration of 20%, the model indicated no pinch occured and at K_2CO_3 concentrations of 25% and higher, that absorption of CO_2 was controlled by a pinched condition at the top of the absorber column.

Figure 45 shows predicted mole fractions of CO_2 in the absorber exit gas as a function of solvent circulation rate. Increasing the solvent circulation rate from 100 L/h to 300 L/h significantly reduced the mole fraction of CO_2 in the absorber exit gas. Further increases in this flow rate, however, resulted in a slight decrease in the absorption of CO_2. This may be explained by recognizing that as the solvent circulation rate is increased, the liquid-to-gas ratio in the stripping column as well as the absorption

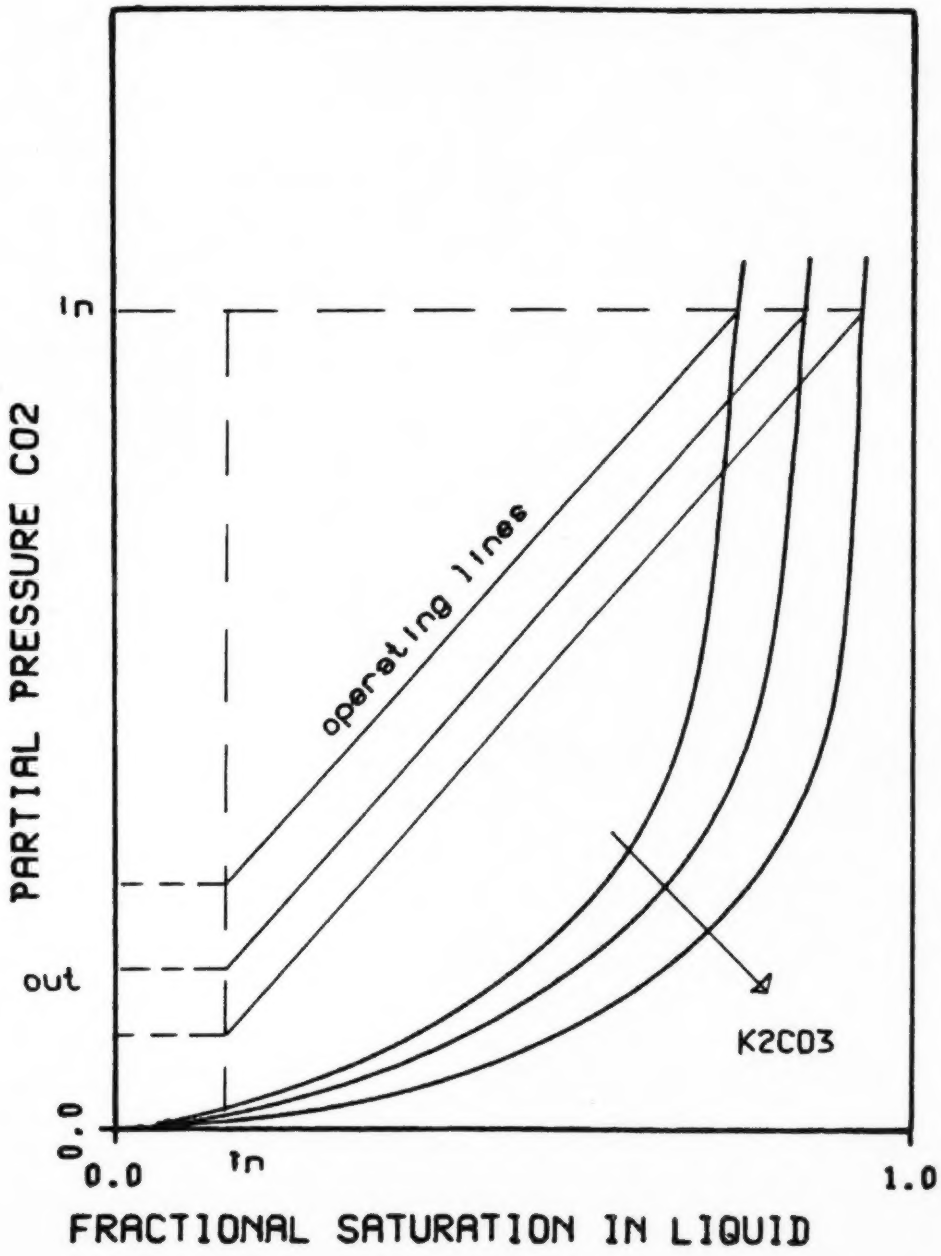

Figure 43 Absorption of CO2 with Bottom Pinch

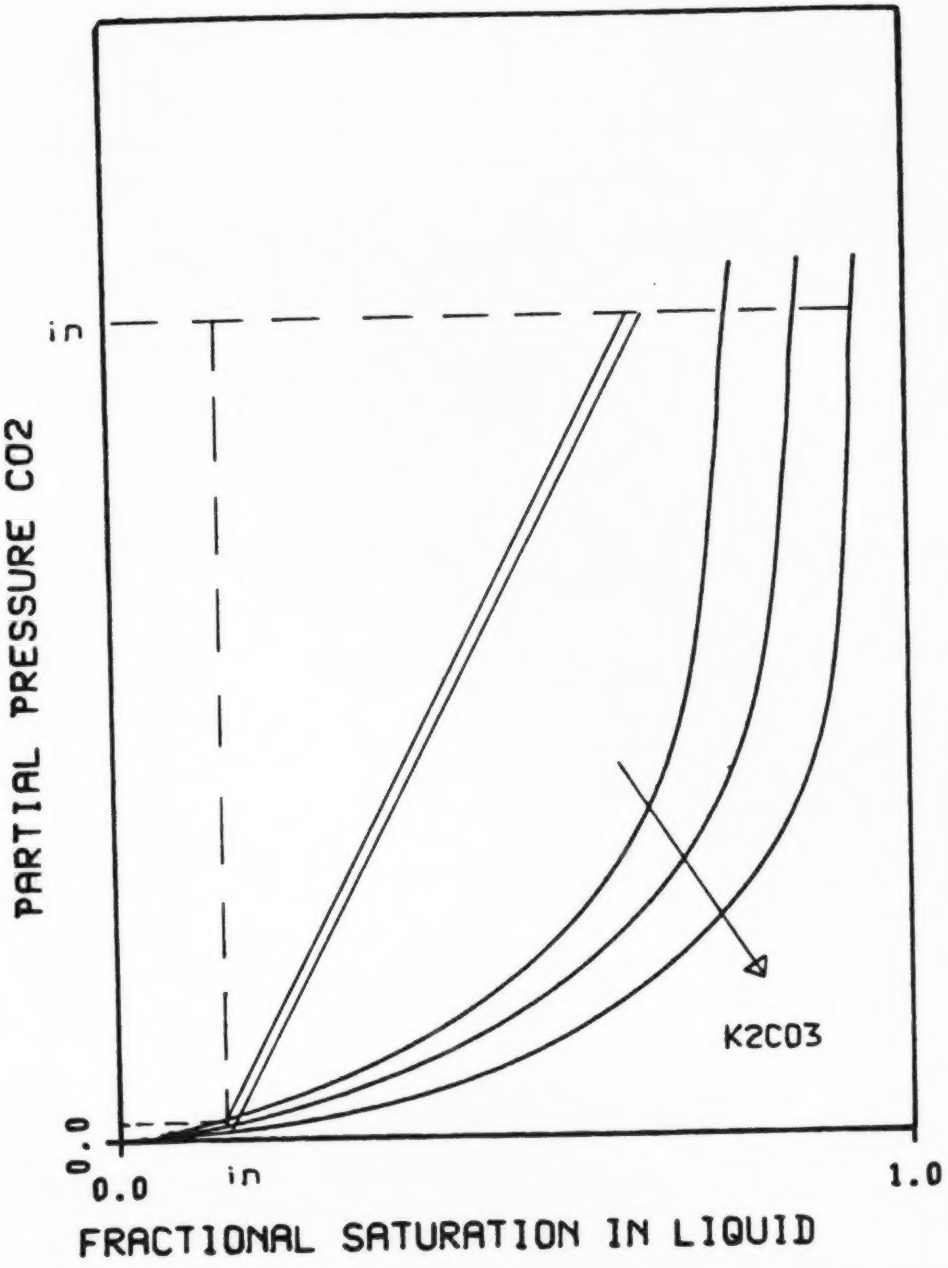

Figure 44 Absorption of CO2 with Top Pinch

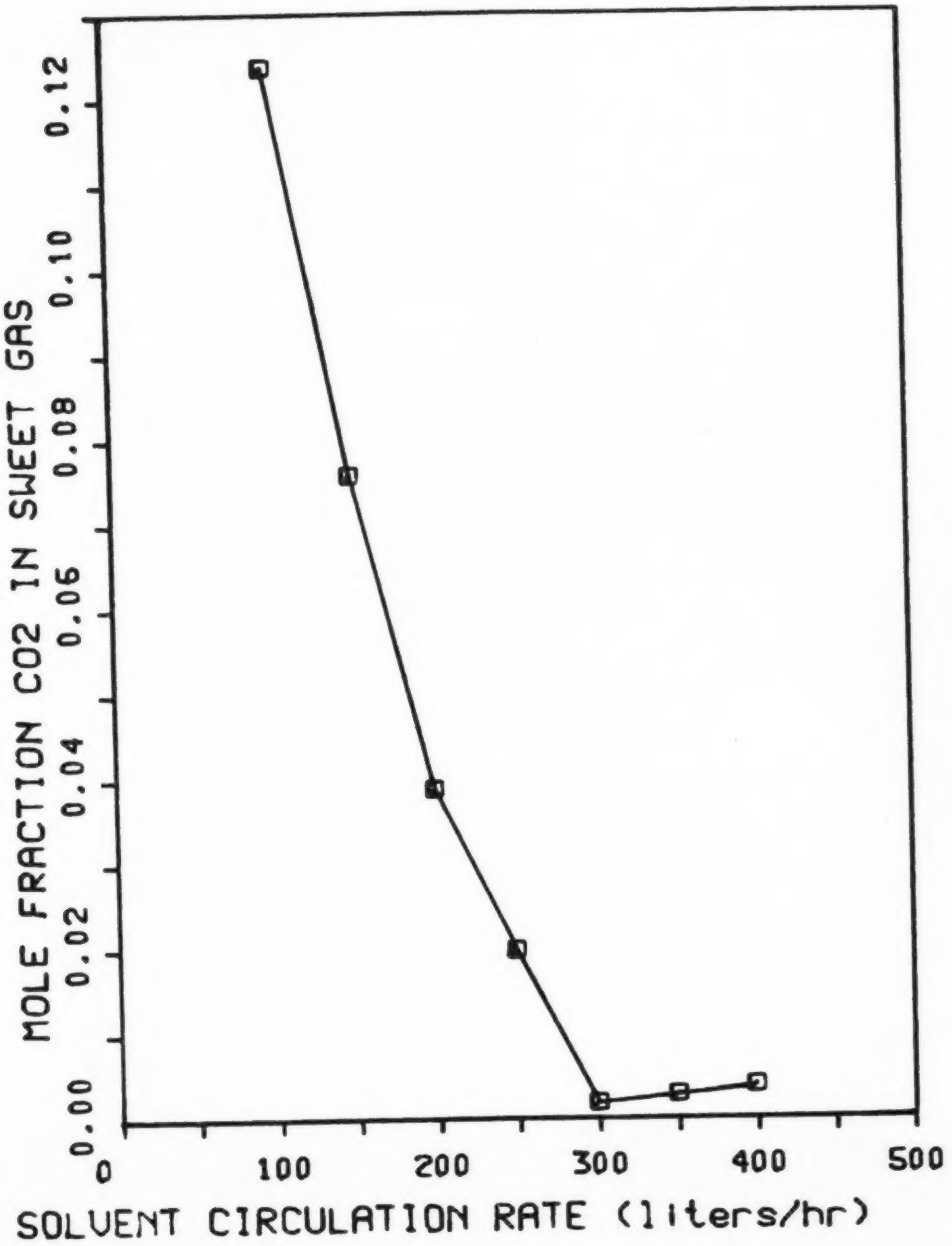

Figure 45 Effect of Solvent Circulation Rate on Absorption of CO2

column is increased. In other words, increasing this flow rate improves absorption conditions but hinders stripping. At a solvent circulation rate under 300 L/h, the predominant effect of increasing this flow rate was in absorption. At higher flow rates, the predominant effect was in stripping. These results futher illustrate the importance of regeneration in system operation and absorber performance.

SELECTIVITY

The system model developed in this study may also be used to determine AGRS operating conditions that result in selective absorption of certain species. In many situations, the selective absorption of sulfur compounds such as H_2S and COS is required.

In the pilot plant operation and model simulations, measured and predicted H_2S removals were greater than 98% at all AGRS operating conditions examined. Hence, AGRS operating conditions that cause selective removal of H_2S are those that minimize the absorption of CO_2. As was shown by the experimental results given in Figure 11, these conditions include low K_2CO_3 concentrations and low absorber pressure. Parametric studies such as those illustrated in the previous section may be used to locate optimal operating conditions for the selective removal of H_2S in a given acid gas removal system.

Regeneration is also important if the selective absorption of H_2S is required. Since the absorption of H_2S was found to be controlled by equilibrium between the gas and liquid phases at the top of the absorber, the concentration of H_2S in the absorber exit gas is highly sensitive to regeneration. This was illustrated in Run ACIL-27 when operation of the reboiler with a reduced steam flow rate resulted in an increasing H_2S concentration in the sweet gas (Figure 7). If, as in Run ACIL-26, the absorption of CO_2 is controlled by a pinched condition at the bottom of the absorber and is insensitive to regeneration, lower regeneration efficiency will result in lower selectivity.

H_2S may also be removed selectively by taking advantage of the difference in the rates of reaction of CO_2 and H_2S in K_2CO_3 solutions. If the selective removal of H_2S is required, an additive that increases the mass transfer rate of CO_2 should obviously not be used. Also to be avoided in this case is the overdesign of absorber height.

As noted previously, the model developed in this study assumes the absorption of COS is a function only of absorber temperature. Model predictions agree well with data presented in literature and experimental data obtained in the pilot plant facility. AGRS operating conditions that result in the selective removal of COS, as well as H_2S should include high absorber temperatures with other conditions selected to minimize CO_2 absorption.

CONCLUSIONS

The present work had two primary objectives: (1) to evaluate the performance of aqueous solutions of hot potassium carbonate in conditioning gases produced from coal, and (2) to develop a model that could be used in the design or simulation of packed adiabatic absorbers and strippers that use hot potassium carbonate to condition gases produced from coal. An experimental program was conceived and executed to satisfy the first objective directly and to assist with the second. Several operational variables were purposefully manipulated to examine the effect on removal of carbon dioxide, hydrogen sulfide, and carbonyl sulfide from the gas exiting the absorber. The model developed to describe adiabatic absorption and stripping was incorporated into a system model that consisted of an absorber, a flash tank, and a stripper, and a computational procedure was developed to predict system performance. As a result of the experimental and modeling efforts several conclusions regarding the use of potassium carbonate can be drawn. These are as follows:

1. The model developed in this study predicted gas flow rates and compositions that were in close agreement with measured values.
2. Heat effects with the hot potassium carbonate process are less than with most other acid gas removal solvents. Calculations assuming isothermal operation in the absorber, flash tank, and stripper give accurate results.
3. CO_2 removal ranged from 38.1% to 98.4% at the conditions examined, and was, in general, highly sensitive to AGRS operating conditions and solvent composition. The effect of H_2S and other coal gas species on the mass transfer rate of CO_2 appeared to be small.
4. The absorption of CO_2 was found to be insensitive to solvent composition when the absorption of CO_2 was controlled by equilibrium between the gas and liquid phases at the top of the absorber column.
5. The absorption of CO_2 was found to be highly dependent on the degree of solvent regeneration.
6. The regeneration of CO_2 accomplished by flashing was negligible at the conditions examined.
7. H_2S removal ranged from 97.3% to 100% at the conditions examined and was found to be insensitive to solvent composition. The absorption of H_2S was found to be controlled primarily by equilibrium between the gas and liquid phases at the top of the absorption column.

8. COS removal ranged from 20.0% to 95.8% at the conditions examined and appeared to be primarily a function of absorber temperature.

9. Selective removal of H_2S and COS may be obtained with AGRS operating conditions that include low K_2CO_3 concentrations, low absorber pressures, and high absorber temperatures.

10 The absorption of coal gas species that do not participate in a reaction in the solvent was found to be insensitive to solvent composition at the conditions examined. The absorption of these species was found to be controlled by equilibrium between the gas and liquid phases at the bottom of the absorber column.

11. An amine additive, commonly used to increase the mass transfer rate of CO_2, appeared to have no significant effect on the fates of other coal gas species. This additive appeared to increase the absorption of CO_2 slightly when such absorption was controlled by equilibrium between the gas and liquid phases in the absorption column.

REFERENCES

Alexander, J. H., T. R. Blanke, D. H. Brownell, W. D. Henline and D. E. Wilkins, "Dynamic Simulation of Sulfur Removal Systems," E.P.R.I. Report No. AP-2187, Palo Alto, California, 1982.

Alper, E., M. Lohse and W. D. Deckwer, "On the Mechanism of Enzyme-Catalysed Gas-Liquid Reactions: Absorption of CO_2 into Buffer Solutions Containing Carbonic Anhydrase," *Chem. Eng. Sci.*, **35**, 2147 (1980).

Astarita, G., *Mass Transfer With Chemical Reaction*, Elsevier Publishing Company, Amsterdam, 1967.

Astarita, G., D. W. Savage and J. M. Longo, "Promotion of CO_2 Mass Transfer in Carbonate Solutions," *Chem. Eng. Sci.*, **36**, 581 (1981).

Astarita, G. and D. W. Savage, "Simultaneous Absorption with Reversible Chemical Reaction," *Chem. Eng. Sci.*, **37**, 677 (1982).

Astarita, G., D. W. Savage and A. Bisio, *Gas Treating with Chemical Solvents*, John Wiley and Sons, New York, 1983.

Auyang, L., Y. C. Liu, M. Petrik and L. Siwajek, "Trace Contaminants Challenge Synfuels Acid Gas Removal," *Acid and Sour Gas Treating Processes*, S. A. Newman, Ed., Gulf Publishing Co., Houston, 1985.

Barreto, G. F. and I. H. Farina, "An Approximate Solution to the Simultaneous Chemical Absorption of Two Gases. One Gas Reacts Instantaneously," *Chem. Eng. Journal*, **24**, 81 (1982).

Bartoo, R. K., "Benfield Process for Acid Gas Removal," presented at the AIChE Winter National Meeting, March 11-14, Atlanta, Georgia, 1984.

Benson, H. E., J. H. Field and R. M. Jimeson, "CO_2 Absorption Employing Hot

Potassium Carbonate Solutions," *Chem. Eng. Prog.*, **50**, 356 (1954).

Berkowitz, N., *An Introduction to Coal Technology,* Academic Press, Inc., New York, 1979.

Bocard, J. P. and B. J. Mayland, "New Charts for Hot Carbonate Process," *Hydro. Proc.* Pet. Ref., **41**(4), 128 (1962).

Bradley, A. A., "Analysis and Fate of Aromatic Hydrocarbons in the Condensed Phases Associated with a Coal Gasification Pilot Plant," M. S. Thesis, North Carolina State University, Raleigh, 1983.

Carnes, K. J., "Fate of Trace Components in Treating Gas Produced from Coal," M.S. Thesis, North Carolina State University, Raleigh, 1985.

Cornelisee, R., A. A. Beenackers and W. P. Van Swaaij, "Simultaneous Absorption of Two Gases in a Reactive Liquid, One Gas Reacting Instantaneously," *Chem. Eng. Sci.*, **32**, 1532 (1977).

Danckwerts, P. V., *Gas-Liquid Reactions,* McGraw-Hill Book Company, New York, 1970.

Dean, J. A., *Lang's Handbook of Chemistry,* 12th ed., McGraw-Hill Book Co., New York, 1979.

DeCoursey, W. J., "Enhancement Factors for Gas Absorption with Reversible Reaction," *Chem. Eng. Sci.*, **37**, 1483 (1974).

Dunlop, M. K., "Physical Solvents in Cleaning Gases Produced from Coal and Other Fossil Sources," presented at the Conference on Gas Cleaning in the Production of Synfuels, North Carolina State University, Raleigh, 1982.

Eickmeyer, A. G. and H. A. Gangriwala, "Acid Gas Removal in Synfuels Production," *Energy Prog.*, **1**, 9 1981.

Feintuch, H. M. and R. E. Treybal, "The Design of Adiabatic Packed Towers for Gas Absorption and Stripping," *Ind. Eng. Chem. Proc. Des. Dev.*, **17**, 505 (1978).

Felder, R. M. and R. W. Rousseau, *Elementary Principles of Chemical Processes,* 2nd ed., John Wiley, 1986.

Ferm, R. J., "The Chemistry of Carbonyl Sulfide," *Chem. Rev.*, **57**, 621 (1957).

Ferrell, J. K., R. M. Felder, R. W. Rousseau, J. C. McCue, R. M. Kelly and W. E. Willis, "Coal Gasification/Gas Cleanup Test Facility; Volume I Description and Operation," Report No. EPA-600/7-80-046a, NTIS No. PB80-188378, 1980.

Field, J. H., E. G. Johnson, H. E. Benson and J. S. Tosh, *U. S. Bureau of Mines, Rep. Invest., No. 5660,* 1960.

Fleming, D. K. and H. S. Primack, "Purification Processes for Coal Gasification," presented at the AIChE Eighty-First National Meeting, Kansas City, Missouri, 1976.

Forman, J. C., "News and Notes of AIChE," *Chem. Eng. Prog.,* **80**, 124 (1984).

Frances, W., *Coal, Its Formation and Composition,* Edward Arlond LTD, 1954.

Gavalas, G., P. H. Cheong and R. Jain, "Model of Coal Pyrolysis," *Ind. Eng. Chem. Fund.,* **20**, 113 (1981).

Ghassemi, D., D. Strehler, K. Crawford and S. Quinlivan, "Applicability of Petroleum Refinery Control Technologies to Coal Conversion," Report No. EPA-600/7-78-190, NTIS No. PB 288630, Research Triangle Park, N. C., 1978.

Giavarini, G. and M. Moresi, "Development of a New Product for Carbon Dioxide Absorption," *Chem. & Ind.,* **21**, 601 (1982).

Goar, B. G., "Guidelines Set for Handling Sour Gas," *Oil & Gas Journal,* June 26, 160 (1978).

Goar, B. G., "Packed Selectox Units, A New Approach to Sulfur Recovery from Dilute Acid Gas Streams," presented at the Conference on Gas Cleaning in the Production of Synfuels, North Carolina State University, Raleigh, 1982.

Goettler, L. A. and R. L. Pigford, "Computational Studies of the Simultaneous Chemical Absorption of Two Gases," *AIChE Journal,* **17**, 793 (1971).

Hikita, H., S. Asai and H. Ishikawa, "Simultaneous Absorption of Two Gases in a Reactive Liquid, One Gas Reacting Instantaneously," *Chem. Eng. Journal,* **18**, 169 (1979).

Jeffreys, G. V. and A. F. Bull, "The Effect of Glycine Addition on the Rate of Absorption of Carbon Doxide in Sodium Carbonate Solutions," *Trans. Inst. Chem. Engrs.,* **42**, 118 (1964).

Joshi, S., "Mass Transfer Processes Coupled with Kinetic Phenomena," Ph.D. Thesis, University of Delaware, 1980.

Joshi, S., G. Astarita and D. W. Savage, "Prediction of Pilot Plant Performance for a Chemical Gas Absorption Process," *AIChE Symposium Series,* **202**, 66 (1981).

Kelly, R. M., "Use of Methanol as a Solvent in an Acid Gas Removal System Coupled with a Coal Gasifier I. Operation II. Simulation," Ph.D. Thesis, North Carolina State University, Raleigh, 1981.

Kelly, R. M., R. W. Rousseau and J. K. Ferrell, "Design of Packed, Adiabatic Absorbers: Physical Absorption of Acid Gases in Methanol," *Ind. & Eng. Chem. Proc. Des. & Dev.,* **23**, 102 (1983).

Killeffer, D. H., "Absorption of Carbon Dioxide," *Ind. & Eng. Chem.,* **29**, 1293 (1937).

King, C. J., *Separation Processes,* McGraw-Hill Book Company, New York, 1980.

Kohl, A. L. and F. C. Riesenfeld, *Gas Purification,* Gulf Publishing Company, Houston, 1979.

Lom, W. L. and A. F. Williams, *Substitute Natural Gas,* John Wiley and Sons, Inc., New York, 1976.

Nelson, P. A., "Countercurrent Equilibrium Stage Separation with Reaction," *AIChE J.,* **17**, 1043 (1971).

Onda, K., H. Takeuchi and Y. Okumoto, "Mass Transfer Coefficients Between Gas and Liquid Phases in Packed Columns," *J. Chem. Eng. Japan,* **1**, 56 (1968).

Onda, K., E. Sada and H. Takeuchi, "Gas Absorption with Chemical Reaction in Packed Columns," *J. Chem. Eng. Japan,* **1**, 62 (1968).

Orbon, J. J., "Effects of Non-Ideal Behavior on the Units of a Refrigerated Methanol Acid Gas Removal System," M.S. Thesis, North Carolina State University, Raleigh, 1984.

Pandya, J. D., "Adiabatic Gas Absorption and Stripping with Chemical Reaction in Packed Towers," *Chem. Eng. Comm.,* **19**, 343 (1983).

Parrish, R. W. and H. B. Neilson, "Synthesis Gas Purification Including Removal of Trace Contaminants by the Benfield Process," presented at the 167th National Meeting of the

American Chemical Society, I. & E. C. Division, Los Angeles, 1974.

Perry, R. H. and C. H. Chilton, *Chemical Engineers' Handbook,* 5th Ed., McGraw-Hill Book Company, New York, 1973.

Probstein, R. F. and R. E. Hicks, *Synthetic Fuels,* McGraw-Hill Book Company, New York, 1982.

Purdy, M. J., "Operation and Modeling of a Fluidized Bed Coal Gasifier," Ph.D. Thesis, North Carolina State University, Raleigh, 1983.

Ramachandran, P. A. and M. M. Sharma, "Simultaneous Absorption of Two Gases," *Trans. Inst. Chem. Engrs.,* **49**, 253 (1971).

Ratcliff, G. A. and J. G. Holdcroft, "Diffusivities of Gases in Aqueous Electrolyte Solutions," *Trans. Inst. Chem. Engrs.,* **41**, 315 (1963).

Reid, R. C., J. M. Prausnitz and T. K. Sherwood, *The Properties of Gases and Liquids,* 3rd ed., McGraw-Hill, 1977.

Reklaitis, G. V., A. Ravindran and K. M. Ragsdell, *Engineering Optimization: Methods & Applications,* Wiley-Interscience, New York, 1983.

Rib, D. M., S. G. Kimura and D. P. Smith, "Coal-Gas Cleanup Facility," *Env. Prog.,* **2**, 86 (1983).

Roughton, F. J. and V. H. Booth, "The Catalytic Effect of Buffers on the Reaction $CO_2+H_2O \rightarrow H_2CO_3$," *Biochem. Journal,* **32**, 2049 (1938).

Savage, D. W., G. Astarita and S. Joshi, "Chemical Absorption and Desorption of Carbon Dioxide from Hot Carbonate Solutions," *Chem. Eng. Sci.,* **35**, 1513 (1980).

Say, G. R., F. J. Heinzelman, J. N. Iyengar, D. W. Savage, A. Bisio and G. Sartori, "Development of a New Hindered Amine-Promoted Hot Carbonate Scrubbing Solution for Simultaneous CO_2 and H_2S Removal from Gases," in *Acid and Sour Gas Treating Processes,* S. E. Newman, Ed., Gulf Publishing Co., Houston, 1985.

Secor, R. M. and R. W. Southworth, "Absorption with an Infinitely Rapid Chemical Reaction in Packed Towers," *AIChE J.,* **7**, 705 (1961).

Sherwood, T. K., R. L. Pigford and C. R. Wilke, *Mass Transfer,* McGraw-Hill Book Company, New York, 1975.

Shier, A. L. and P. V. Danckwerts, "Carbon Dioxide Absorption into Amine-Promoted Potash Solutions," *Ind. & Eng. Chem. Fund.*, **8**,415 (1969).

Srivastava, R. K. and B. Joseph, "Simulation of Packed-Bed Separation Processes Using Orthogonal Collocation," *Comp. & Chem. Eng.*, **8**, 43 (1984).

Staton, J. S., "Modeling of an Adiabatic Stripping Column in a Coal Gasification Plant Acid Gas Removal System," M.S. Thesis, North Carolina State University, Raleigh, 1983.

Staton, J. S., "Performance and Modeling of a Hot Potassium Carbonate Acid Gas Removal System in Treating Coal Gas," Ph. D. Thesis, North Carolina State University, Raleigh, NC, 1985.

Staton, J. S., R. W. Rousseau and J. K. Ferrell, "Solvent Regeneration in Conditioning Gases form Coal," in *Acid and Sour Gas Treating Processes,* S. E. Newman, Ed., Gulf Publishing Co., Houston, 1985.

Tosh, J. S., J. H. Field, H. E. Benson and W. P. Haynes, "Equilibrium Study of the System Potassium Carbonate, Potassium Bicarbonate, Carbon Dioxide, and Water," Report No. 5484, U. S. Dept. of Interior Bureau of Mines, Pittsburgh, 1959.

Treybal, R. E., *Mass-Transfer Operations,* McGraw-Hill Book Company, New York, 1980.

Van Krevelen, D. W. and P. J. Hoftijzer, Chimie et Industrie, Numero Speciale du XXI e Congres International de Chimie Industrielle, Bruxelles, 168 (1948).

von Stockar, U. and C. R. Wilke, "Rigorous and Short-Cut Design Calculations for gas Absorption Involving Large Heat Effects. 1. A New Computational Method for Packed Gas Absorbers," *Ind. & Eng. Chem. Fund.*, **16**, 88 (1977).

Wall, H. H., M.S. Thesis, University of Delaware, 1966.

Wall, J. D., "Gas Processing Handbook," *Hydro. Proc.*, **61**, 85 (1982).

Walpole, R. E. and R. H. Myers, *Probability and Statistics for Engineers and Scientists,* 2nd ed., Macmillan Publishing Co., New York, 1978.

Wender, I., "Catalytic Synthesis of Chemicals form Coal," *Cat. Rev. Sci. & Eng.*, **14**, 101 (1976).

Wilhelm, E., R. Battino and R. J. Wilcock, "Low-Pressure Solubility of Gases in Liquid Water," *Chem. Rev.*, **77**, 219 (1977).

Willis, W. E., "A Data Acquisition System for a Coal Gasification Pilot Plant," Ph.D. Thesis, North Carolina State University, Raleigh 1981.

LIST OF SYMBOLS

a – surface area per unit volume of packing, area/volume

$[A]$ – local liquid phase concentration of component A, moles/volume

$[A]_o$ – bulk liquid phase concentration of component A, moles/volume

$[A]_t$ – total concentration of both physically dissolved and chemically combined component A, moles/volume

$[A]_i$ – liquid phase concentration of component A at the gas-liquid interface, moles/volume

$[A']$ – defined in Equation 64

C_i – concentration of species i in the liquid phase, moles/volume

D – diffusivity, area/time

E – rate-promotion factor, dimensionless

f – defined in Equation 60

f_i – molar flow rate of component i in feed, moles/time

F – molar flow rate of feed, moles/time

F_j – defined in Equation 97

F_j^* – defined in Equation 96

g – defined in Equation 60

g_i – defined in Equation 81

g_o – defined in Equation 67

G – gas molar flow rate, moles/time-area

G' – molar flow rate of inert gas, moles/time-area

h – defined in Equation 44

H – Henry's law constant, pressure-volume/mole

H^o – Henry's law constant in water, pressure-volume/mole

I – rate-enhancement factor, dimensionless

I_i – ionic contribution defined in Equation 45, dimensionless

I_F – rate-enhancement factor from fast reaction regime asymptotic solution, dimensionless

I_I – rate-enhancement factor from instantaneous reaction regime asymptotic solution, dimensionless

I_S – rate-enhancement factor from slow reaction regime asymptotic solution, dimensionless

J_A – diffusive flux of component A, moles/time-area

k – reaction rate constant, time^{-1}

k_{OH} – reaction rate constant for Equation 3, time^{-1}

k_G – gas phase mass transfer coefficient, mole/time-area-pressure

k_L – liquid phase mass transfer coefficient, distance/time

k_L^* – liquid phase mass transfer coefficient with chemical reaction, distance/time

K – reaction equilibrium constant, dimensionless

K_{oG} – overall mass transfer coefficient based on gas side driving force, mole/time-area-pressure

K_{oG}^* – overall mass transfer coefficient with chemical reaction based on gas side driving force, mole/time-area-pressure

l – liquid hold-up, volume/volume packing

L – flow rate of liquid, volume/time

m – molarity of the solvent, moles/volume

M – defined in Equation 132

n – adjustable parameter in Equation 103, dimensionless

N_A – flux of component A, mole/time-area

P – pressure

P^* – vapor pressure, pressure

P_A – partial pressure of A, pressure

q_j – defined in Equation 90

q'_j – defined in Equation 9

Q – defined in Equation 102

r – net rate of reaction of species A, mole/time-volume

r_F – rate of forward reaction of species A, mole/time-volume

r_R – rate of reverse reaction of species A, mole/time-volume

R – defined in Equation 128

S – defined in Equation 84

v_j – stoichiometric coefficient of component j, dimensionless

V – molar flow rate of vapor, moles/time

u_x – bulk fluid velocity in x direction, length/time

W – defined in Equation 70

x – space coordinate, length

x_A – liquid phase mole fraction of component A, dimensionless

x_{Ai} – liquid phase mole fraction of component A at the gas-liquid interface, dimensionless

X – defined in Equation 102

y – degree of saturation, dimensionless

y_A – gas phase mole fraction of component A, dimensionless

y_{Ai} – gas phase mole fraction of component A at the gas-liquid interface, dimensionless

y_A^* – gas phase mole fraction of component A that would be in equilibrium with the bulk liquid phase mole fraction of component A, dimensionless

Y – gas phase mole fraction of key component, dimensionless

Y_i – vapor phase mole fraction of component i, dimensionless

Z – height of packing, length

Z_i – charge of ion i, dimensionless

Z_j – defined in Equation 10

Z_k – extent of reaction k, dimensionless

δ – thickness of film in the film theory, distance

λ_v – latent heat of vaporization, energy/mass

μ – viscosity, mass/length-time

ρ – density, mass/volume

ρ_m – molar density, moles/volume

ξ – fractional conversion of COS, dimensionless